Hochschule für Angewandte
Wissenschaften Hamburg
Hamburg University of Applied Sciences

Hochschule für Angewandte Wissenschaften Hamburg

Fakultät Life Sciences

CFD Investigations of Vertical Axis Wind Turbine

Master Thesis

Renewable Energy Systems – Environmental and Process Engineering

submitted by

Prince Deep

Matr. No: [redacted]

Hamburg

21.10.2019

Advisor: Prof. Dr.-Ing. Rainer Stank (HAW Hamburg)

Advisor: Prof. Dr.-Ing. Holger Schwarze (HAW Hamburg)

Contents

1. INTRODUCTION 1
1.1 How do Wind Turbines work? 1
1.2 Wind Energy- Power in Wind 1
1.3 Classification of Wind Turbines 3
1.4 Comparison of VAWT to HAWT 4
1.5 Vertical Axis Wind Turbines-History 5
1.6 Motivation for Research & Development of VAWT 6
2. OBJECTIVES OF THE THESIS 8
3. THEORY OF VERTICAL AXIS WIND TURBINES 9
3.1 Aerodynamic Forces Diagram 9
3.2 Tip Speed Ratio (λ) 14
3.3 Angle of Attack (α) 15
3.4 Blade Pitch Angle (β) 15
3.5 Rotor Power Coefficient (Cpr) 16
4. CHOSEN APPROACH TO SOLVE THE OBJECTIVES 17
4.1 Approach about the Geometry 17
4.1.1 Airfoil Type 17
4.1.2 Number of Blades (Nb) 18
4.1.3 Radius of Rotor 18
4.1.4 Chord Length 19
4.1.5 Center of Airfoil 19
4.1.6 Wind Speed and Tip Speed Ratio 19
4.2 Approach about Meshing 20
4.3 Approach about Analysis type 21
5. METHODOLOGY AND NUMERICAL SETUP 22
5.1 Verification of formula for Local AOA 22
5.2 Transient State Analysis with Quasi-2D Mesh Approach for Single Bladed Rotor 24
5.2.1 Geometry of the Setup 24
5.2.2 Blocking and Meshing 27
5.2.3 Setting Up Boundary Conditions 33

5.2.4 Calculating Timestep 34
5.2.5 Turbulence Modelling 35
5.2.6 Transforming mesh to implement Pitching 38
5.2.7 Main Processing and Data Extraction 39
5.2.8 Post Processing 41
5.3 Transient State Analysis with Quasi-2D Coarse Mesh Approach for 1 Bladed Rotor 42
5.4 Transient State Analysis with Quasi-2D Mesh Approach for Two Bladed Rotor 43
6. RESULTS AND DISCUSSIONS 44
6.1 Angle of Attack 44
6.2 Lift Force for NACA 0012 Airfoil 45
6.3 Torque/Cpr from Unpitched Transient Analysis of 1 Bladed System 45
6.4 Single Blade Constant Pitch 46
6.5 Single Blade Optimized Pitch 50
6.6 Two Blades Optimized Pitching 52
6.7 Quality of Mesh 57
6.8 Steady State Analysis and Transient State Analysis 58
7. COMPARISON OF RESULTS WITH LITERATURE 59
7.1 Localized Angle of Attack 59
7.2 Coefficient of Lift Force vs Angle of Attack 60
7.3 Torque of Single Blade vs Azimuthal angle 61
7.4 Constant Pitching angle vs Torque 62
7.5 Quality of Mesh 64
8. SUMMARY AND FUTURE SCOPE 65
9. CITATIONS 67
APPENDICES 69
APPENDIX 1: Figures of Initial 3-D Mesh Study with Tetrahedral mesh elements 69
APPENDIX 2: Additional figures of AGILE VAWT with Pitching Mechanism 70
APPENDIX 3: Excel Worksheets of Selected Data 71
APPENDIX 4: Figures depicting the manual Design Approach 72
APPENDIX 5: Forces acting on Airfoil in X and Y direction in Solver Monitors 74

List of Figures

Figure 1 Power Extraction from flowing Wind [1] 1
Figure 2 Rotor Power Coefficients of various Wind Turbines [1] 2
Figure 3 Typical 3 Bladed HAWT [1] 3
Figure 4 Different designs of VAWTs [1] 4
Figure 5 VAWT for milling grains [1] 6
Figure 6 Agile VAWT with Pitching Mechanism [3] 7
Figure 7 Aerodynamic Forces on a VAWT (obtained from Literature) [4] 9
Figure 8 Aerodynamic Forces at Azimuthal angle 0deg 10
Figure 9 Aerodynamic Forces at Azimuthal angle 30deg 10
Figure 10 Aerodynamic Forces at Azimuthal angle 60deg 11
Figure 11 Aerodynamic Forces at Azimuthal angle 90deg 11
Figure 12 Aerodynamic Forces at Azimuthal angle 120deg 12
Figure 13 Aerodynamic Forces at Azimuthal angle 180deg 12
Figure 14 Aerodynamic Forces at Azimuthal angle 240deg 13
Figure 15 Aerodynamic Forces at Azimuthal angle 270deg 13
Figure 16 Aerodynamic Forces at Azimuthal angle 330deg 14
Figure 17 Airfoil with various Aerodynamic Angles [1] 15
Figure 18 Resultant Velocity of a VAWT 16
Figure 19 NACA 0012 Airfoil [8] 17
Figure 20 Single and Two Bladed Rotors 18
Figure 21 Preliminary design Parameters 18
Figure 22 Monthly Average Wind Speed in Hamburg [10] 19
Figure 23 3D Mesh with Tetrahedral Elements 20
Figure 24 2D Mesh Approach 20
Figure 25 Verification of AOA Formula by CAD Model 23
Figure 26 Verification of AOA at Azimuthal Angle 30deg 23
Figure 27 Imported data points for Airfoil generation 24
Figure 28 Scaling and Translation of Geometry 25
Figure 29 Generation of Outer Domains around Airfoil 26
Figure 30 Dimensions of Domains according to Literature 27
Figure 31 Settings for Edge Association in Blocking 28
Figure 32 Settings for Splitting the Block 28
Figure 33 Generating the O-Block around the Airfoil Geometry 29
Figure 34 Settings for Pre-Mesh Parameters to determine the Quality of Mesh elements 30
Figure 35 Pre-Mesh Structure 30
Figure 36 Settings for Mesh Extrusion to generate Quasi-2D mesh 31
Figure 37 Unstructured Extruded Mesh 32
Figure 38 Final Mesh Elements Visualization to observe the Quality of mesh 32
Figure 39 Zoomed and Focused view of mesh 33
Figure 40 Angular Velocity of Rotating Domain containing Airfoil 34
Figure 41 Settings for Rotating domains and Turbulence Modelling 36

Figure 42 Settings for Domain Interfaces 37
Figure 43 Settings for defining the Expressions and Setting up Monitors 38
Figure 44 Mesh Rotation to acquire -6deg and 15deg Blade Pitch Angles 39
Figure 45 Main Processing displaying Convergence of Solution 40
Figure 46 Torque Curve for Single Blade observed by Torque Monitor in Main Processing 40
Figure 47 Flow Visualization around the Airfoil 41
Figure 48 Pressure Chart around the Airfoil 41
Figure 49 Visualization of a Coarse mesh around the Airfoil and other Domains 42
Figure 50 Geometry of a Two Bladed Rotor 43
Figure 51 Torque Curves of two Blades visualized from Solver Window 43
Figure 52 Angle of Attack and sinθ for Unpitched Rotor 44
Figure 53 Lift Coefficient vs Angle of Attack 45
Figure 54 Torque and Rotor Power Coefficient vs Azimuthal Angle 46
Figure 55 Torque curves for Constant Pitch angles from -6.477deg to -1deg 47
Figure 56 Torque curves for Constant Pitch angles from 0deg to 6deg 47
Figure 57 Torque curves for Constant Pitch angles from 7deg to 14deg 48
Figure 58 Torque curves for Constant Pitch angles from 16deg to 22.477deg 48
Figure 59 Torque Comparison for Best Constant Pitch angle(-3deg) and Unpitched Rotor 50
Figure 60 Angle of Attack (Unpitched) vs Optimized Angle of Attack (by Optimized Blade Pitching) 51
Figure 61 Comparison of Torque for Unpitched and Optimized Variable Pitching Approach 51
Figure 62 Rotor Power Coefficient along with Blade Pitch visualization for Optimized Variable Pitching 52
Figure 63 Torque Curves of Individual Blades and Combined Torque for 2-Bladed Rotor 53
Figure 64 Torque Curves for Unpitched 2-Bladed Rotor vs Optimized Blade Pitch 2-Bladed Rotor 55
Figure 65 Turbulence due to Wake effects and Visualization at Azimuthal Positions 56
Figure 66 Small streak of flow disturbance at Mesh Interface 57
Figure 67 Torque Curves for Fine and Coarse mesh 57
Figure 68 Torque Curves for Transient State and Steady State Analysis Type 58
Figure 69 Angle of Attack vs Azimuthal Angle (Literature) [18] 59
Figure 70 Angle of Attack vs Azimuthal Angle (Result of Study) 60
Figure 71 Lift Coefficient for NACA 0012 (Literature) [8] 60
Figure 72 Lift Coefficient for NACA 0012 (Result of Study) 61
Figure 73 Torque Curve of Unpitched Single Blade Rotor (Literature) [14] 62
Figure 74 Torque Curve of Unpitched Single Blade Rotor (Result of Study) 62
Figure 75 Torque curves for different Constant Pitch Angles (Literature) [6] 63
Figure 76 Torque curves for different Constant Pitch Angles (Result of Study) 63
Figure 77 Torque Curves for different Qualities of Meshes (Literature) [12] 64
Figure 78 Torque Curves for different Qualities of Meshes (Result of Study) 64

Abbreviations, Symbols and Constants

CFD	Computational Fluid Dynamics
K.E	Kinetic Energy
HAWT	Horizontal Axis Wind Turbine
VAWT	Vertical Axis Wind Turbine
AOA	Angle of Attack
CPA	Constant Pitch Angle
OPA	Optimized Pitch Angle
CAD	Computer Aided Design
CSV	Comma Separated Values
TSR	Tip Speed Ratio
m	Mass of Air
v_w	Undisturbed Wind Velocity
P_{wind}	Available Power in Wind
A	Area of Cross section
F_D	Drag Force
F_L	Lift Force
F_t	Resultant Force causing Torque
ρ	Density of Air
λ	Tip Speed Ratio
β	Blade Pitch Angle
α	Angle of Attack
ω	Angular Speed
u	Tangential Velocity of Rotor
V_r	Resultant Wind Velocity
θ	Azimuthal Angle
C_{pr}	Rotor Power Coefficient
C_L	Lift Coefficient
P_{act}	Actual Power generated by Rotor
N_b	Number of Blades

R	Radius of Rotor
c	Chord Length
σ_{max}	Solidity at max C_{pr}
Δt	Timestep

Chapter 1

1. INTRODUCTION

1.1 How do Wind Turbines work?

Wind turbines are power generators that utilize the power available in flowing wind and convert it into usable electrical energy by converting the mechanical motion of Rotor into electricity. These are placed ideally in areas of high wind speeds. The principle of power extraction from wind can either be based on Drag force or Lift force. When the flowing wind is encountered by the Rotor blades of the wind turbine, a part of the available energy is extracted from it, into mechanical energy in the form of rotation of the rotor system. This mechanical energy is converted into electricity by an electrical generator.

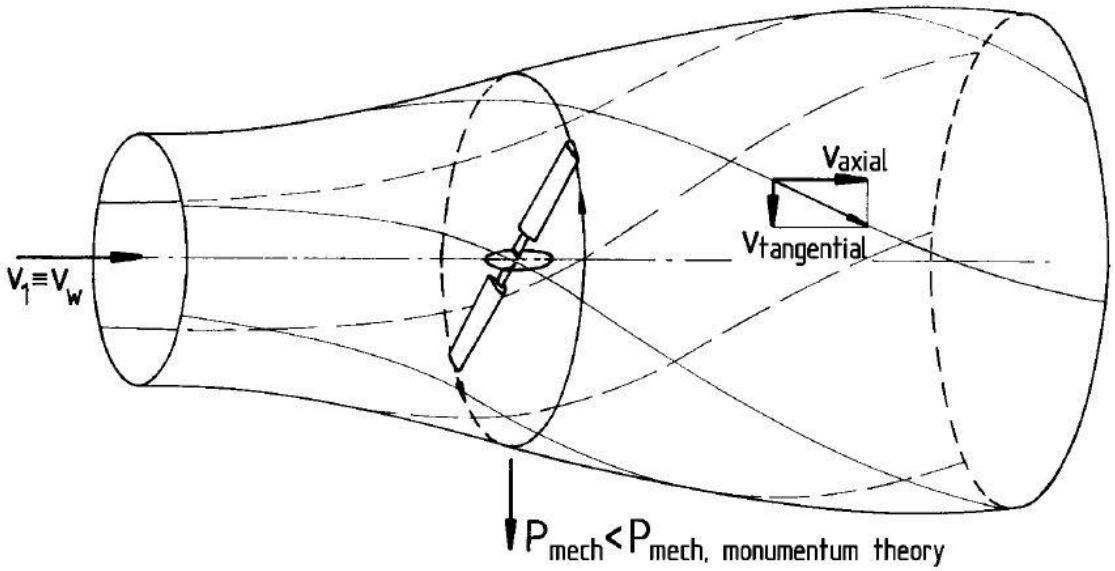

Figure 1 Power Extraction from flowing Wind [1]

1.2 Wind Energy- Power in Wind

The underlying power source behind any Wind turbine is the Kinetic energy present in the flowing wind. The kinetic energy is in turn dependent on the mass of the air (m) and square of velocity of the wind (v) of the stated mass of air. The dependence of Wind Power on velocity is a major factor in the design of Wind turbines [1].

$$K.E. = \frac{1}{2} m {v_w}^2$$

The power available in the so-called air-mass can be defined by the formula expressed below, where the terms P_{wind} means the Power available in the Wind, ρ means the density of air, A means Area of cross section of Air-mass and v_w is the velocity of the flowing wind [1].

$$P_{wind} = \frac{1}{2}\rho A {v_w}^3$$

From the formula, it is clear that the Power available in flowing wind is dependent strongly on the velocity of the wind. In fact, it is dependent as a cubic function of the velocity of the wind. Therefore, large amounts of data and preliminary wind speed measurements are necessary before proceeding with any design studies.

P_{wind} is only the theoretical amount of power possessed by the wind. As is the case with any power generator, it can extract only a percentage of the available power. In case of Aerodynamic power generators, of which VAWTs and HAWTs are part of, a maximum of 59.3% is the extractable amount of power. This limit is called as the Betz Limit and all the practical Aerodynamic wind turbines have efficiency less than this value [1].

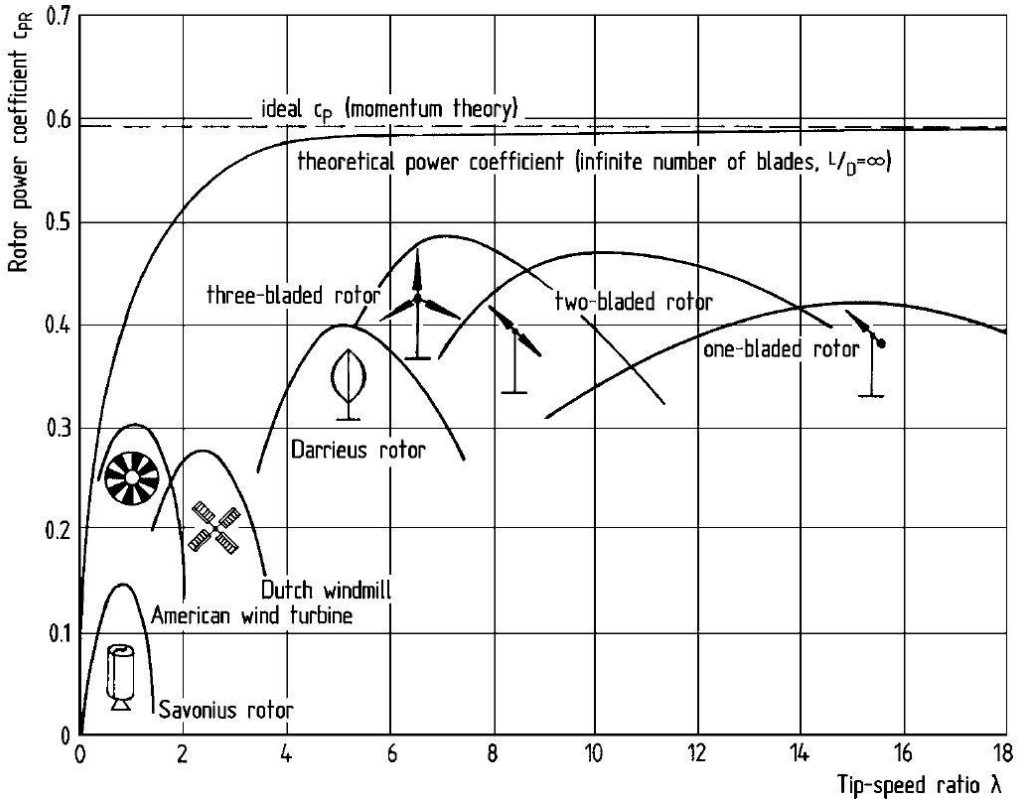

Figure 2 Rotor Power Coefficients of various Wind Turbines [1]

1.3 Classification of Wind Turbines

1. Horizontal Axis Wind Turbines (HAWT)-This design of Wind turbines was originated as European Wind turbines and presently dominate the commercial market share of wind turbines in the world. The principle of power generation is the exploitation of Lift force generated by the Aerodynamic flow over an airfoil. The power output is controlled by varying the pitch angle of the airfoil [1].

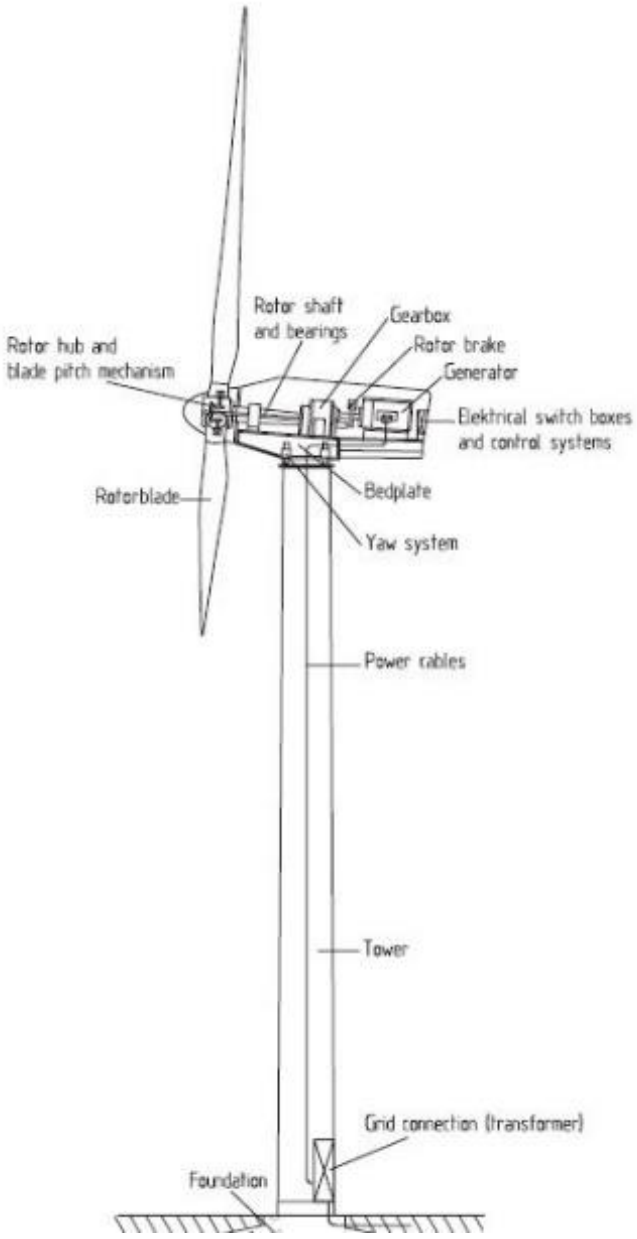

Figure 3 Typical 3 Bladed HAWT [1]

2. Vertical Axis Wind Turbines (VAWT)- This design is the oldest design of wind turbines in existence. There are types of VAWTs which operate on either Drag or Lift Force principle for power generation. The aerodynamic analysis of such Wind Turbines is more complicated due to constant change of AOA during the rotation of rotor [1].

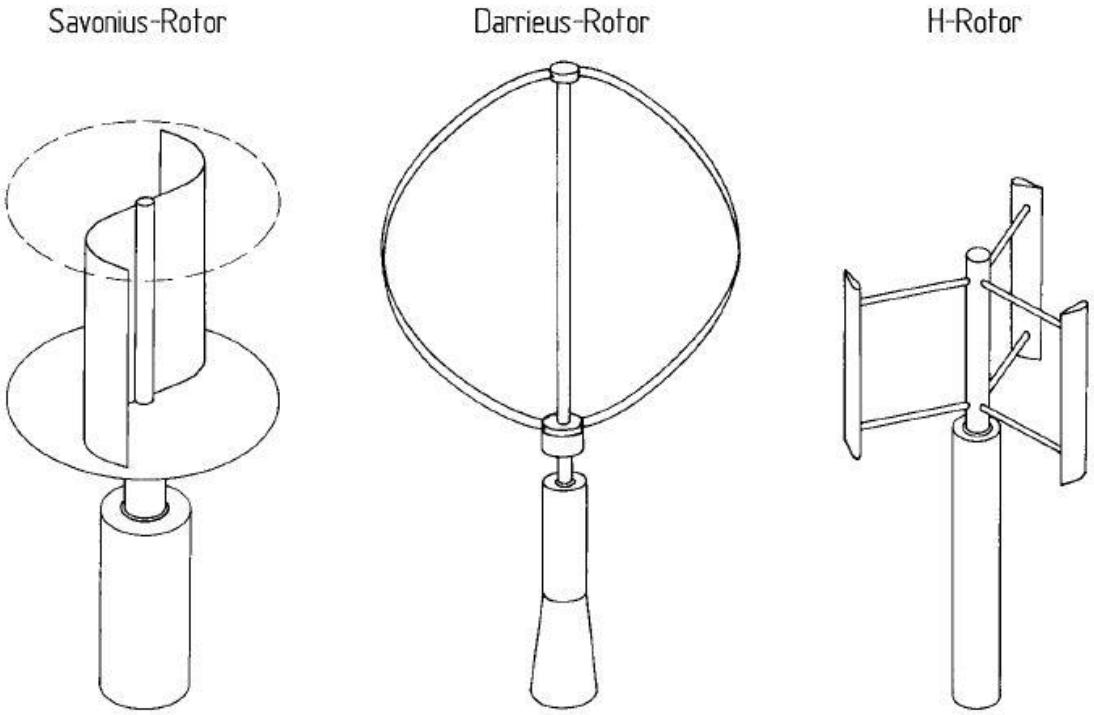

Figure 4 Different designs of VAWTs [1]

1.4 Comparison of VAWT to HAWT

The major and most prominent aspect of difference among the two types of the wind turbines is the physical design. In case of HAWT, the axis of rotor is parallel to the flow of the wind. In case of VAWT, the rotor is placed vertically and hence the axis of rotor is perpendicular to the flow of the oncoming wind. As the Airfoil of the VAWT encounters unique positions at each location during the rotation, the aerodynamic properties such as Angle of Attack (AOA), Drag force (Fd) and Lift forces (Fl)vary constantly and by large extents and thus makes the investigation of VAWTs more complicated [2].

Some of more noticeable advantages and disadvantages of each type of the Wind turbine are summarized in the Table 1.

Table 1 Advantages and Disadvantages of HAWTs and VAWTs [2]

Type	VAWT	HAWT
Advantages	Easy Maintenance	High Stability
	Construction and Repair costs are low	Self-Starting and does not require starting motor
	Self-adjusting to the wind flow direction	High reliability
	Low noise levels	High efficiency
	Operation possible at even low wind speeds	
Disadvantages	Lower efficiency as compared to HAWT	Complex manufacturing and Installment procedures
	Low Torque values, especially during starting	Higher noise level emissions

1.5 Vertical Axis Wind Turbines-History

Whenever the history of Wind turbines comes to mind, people think of European HAWTs used back in 12th century for milling grains and pumping groundwater. But even earlier accounts of VAWT originate from Persia, dating back to 9th century. Surely enough, at that time, these were used as drag devices instead of working on aerodynamic lift principle. The next big ripple in field of VAWT came in 1920s, when first Lift based VAWT was invented by Georges Darrieus in France. This design can be seen even today and is known as ϕ-configuration. Darrieus came up with many prototypes of different configurations for VAWTs in the 1920s and 1930s. However, the first power producing lift based VAWT was built by another Frenchman in 1950s, Jean-Baptiste Morel and it was based on Straight bladed Darrieus model [1], [2].

Figure 5 VAWT for milling grains [1]

Ever since that time, there has been a slow but increasing interest in the revival of VAWTs. There are numerous advantages that the VAWTs have, over their HAWT counterparts. The research has been kind of slow due to HAWTs gaining the major attention and limelight in the Wind turbine industry due to their easy to comprehend aerodynamic responses to wind and higher efficiency as compared to VAWTs.

1.6 Motivation for Research & Development of VAWT

With the Wind industry market already witnessing a saturation in the viable high-wind speed spots for setting up wind farms, at least in Europe and especially in Germany, researchers are looking for new and innovative ways to combat this. At present, a major push is being provided to the research for VAWT, for the reason that, these wind turbines can operate at lower wind speeds and locations where HAWTs cannot exist or thrive. Some of the factors that are promoting the VAWTs are:

1. These are easily scalable and can be modified to suit the requirement. They can be designed to fit the Power output requirements, space constraints or even noise levels [1].
2. These are more robust and less prone to maintenance or repair interventions. Due to these qualities, they have a long lifespan of about 25 years [2].
3. There are a lot of geometrical design options which are at disposal of researchers to investigate, ranging from Savonius, Darrieus and H-Rotor [2].
4. These have inherently low noise generation operation. This attribute alone allows them to infiltrate the urban landscape where HAWTs cannot exist. These can be installed on roofs of buildings and noise levels can still be in permissible limits.
5. These do not have to be yawed to face the direction of the wind, as they are self-adjusting to the direction of the wind [1].
6. The concept of performing the Variable Pitching on a VAWT originated from the prototype seen of an Agile VAWT at Zurich University of Applied Sciences in Winterhur on a visit by Prof. Stank. The prototype includes a rudimentary blade pitching mechanism, which in theory should increase the power [3].

   For different views and additional figures of Agile VAWT, refer Appendix 2.

Figure 6 Agile VAWT with Pitching Mechanism [3]

Chapter 2

2. OBJECTIVES OF THE THESIS

The objectives of this thesis, which were set forth to accomplish, are enumerated below. However, the overall aim is to study, analyze and present the findings of a CFD Simulation conducted to analyze the Operating Procedures of a VAWT and the effects of pitching (constant and Variable) on such a system.

1. Performing a Literature review in order to familiarize with the aerodynamic specifics of a VAWT, studying the already completed studies on pitching and experimental results of similar research methods.

2. Performing and reporting the effects of a Constant Pitch Angle (CPA) on the Torque generation on the geometry so chosen (Single Blade Rotor).

3. Discerning the data and figuring out which Constant Pitch Angle, also called as Optimized Pitch Angle (OPA) should be applied during the whole rotation of the rotor, in order to maximize the Power output of a Single Blade Rotor.

4. Verification of the Optimized Pitch Angle previously figured by applying it on Two Bladed System at each Azimuthal position during one complete rotation of the rotor.

5. Studying the effects of Analysis type on CFD and comparing with present literature and commenting if one of the two options, Steady State Analysis or Transient State Analysis is more fitting for the CFD research of VAWTs.

6. Studying and reporting on the quality of mesh chosen for the study. The outcomes of a CFD analysis is only as good as the quality of mesh. The mesh must be appropriate to capture all the physical phenomenon that are manifested in an experimental setup.

7. Reporting on any improvements if achieved by this study and future scope for further research.

Chapter 3

3. THEORY OF VERTICAL AXIS WIND TURBINES

Before starting to focus on the CFD investigations about the VAWTs, some of the basic concepts about Wind turbines in general, and how they apply to VAWTs, needs some introduction. The major discrepancy between the two types of wind turbines is the interaction with the oncoming wind and how this interaction results in difference in Aerodynamic forces among the two types.

3.1 Aerodynamic Forces Diagram- One of the most important and underlying concept while designing a wind turbine is the investigation and analysis of the Aerodynamic forces which are acting on the Airfoil. Figuring about these forces and diagrams can help in analysis of future results and what to expect from the Simulation results. The aerodynamic forces act completely different in case of VAWTs as compared to the HAWTs. Therefore, it is of importance to present here, how the forces and different aerodynamic variables play a role in case of a VAWT. A diagram depicting the different forces at play in a VAWT, from the literature is presented in figure 7.

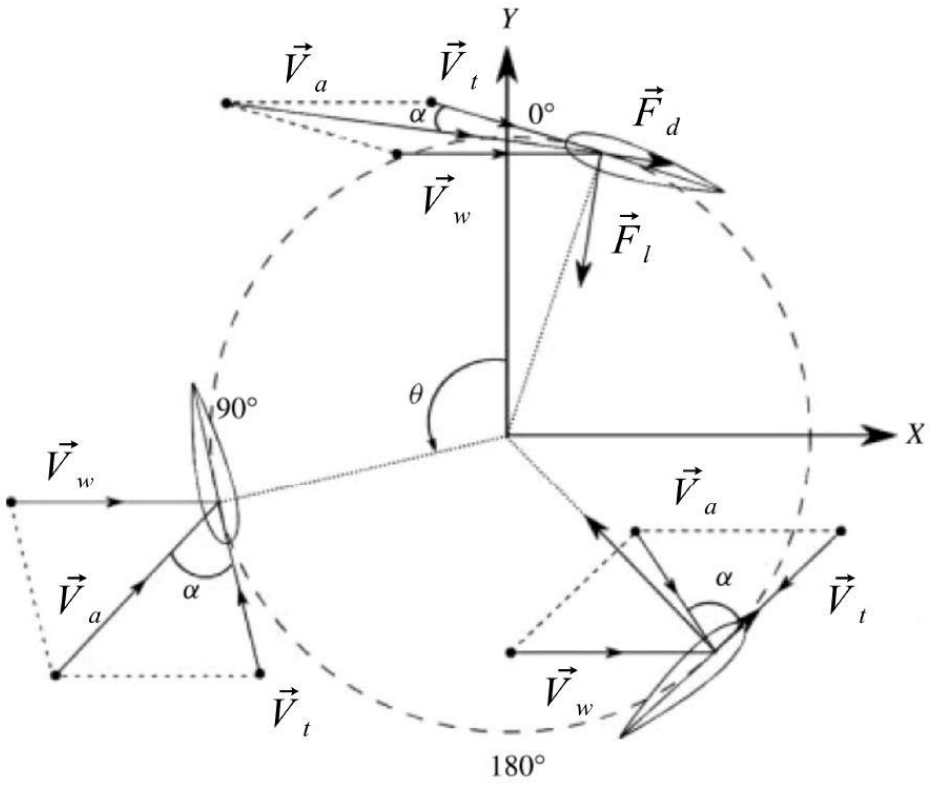

Figure 7 Aerodynamic Forces on a VAWT (obtained from Literature) [4]

In order to understand how these different variables, interact with one another and what the effect of different assumed values for these variables will be considering this study, the study of the forces and angles was completed by hand on paper and was corroborated by the CAD software as well. The following figures 8 to 16 are the result of the preliminary force analysis.

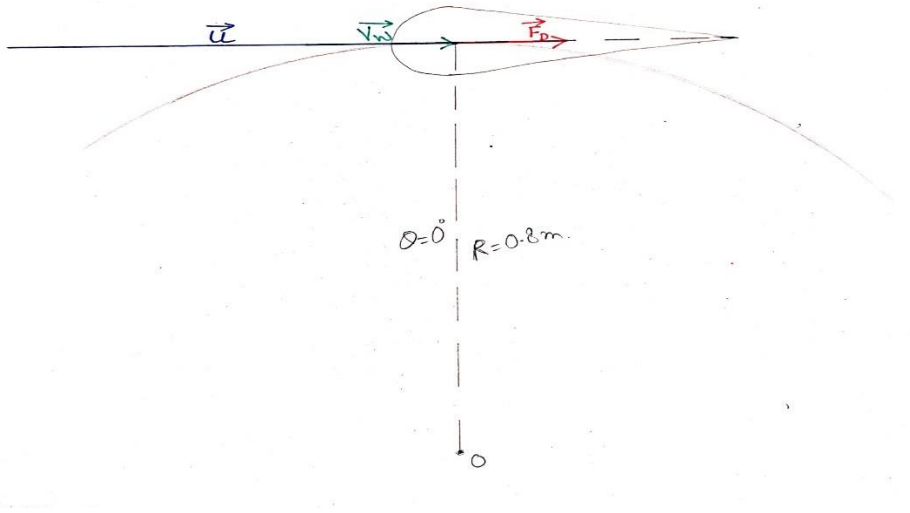

Figure 8 Aerodynamic Forces at Azimuthal angle 0deg

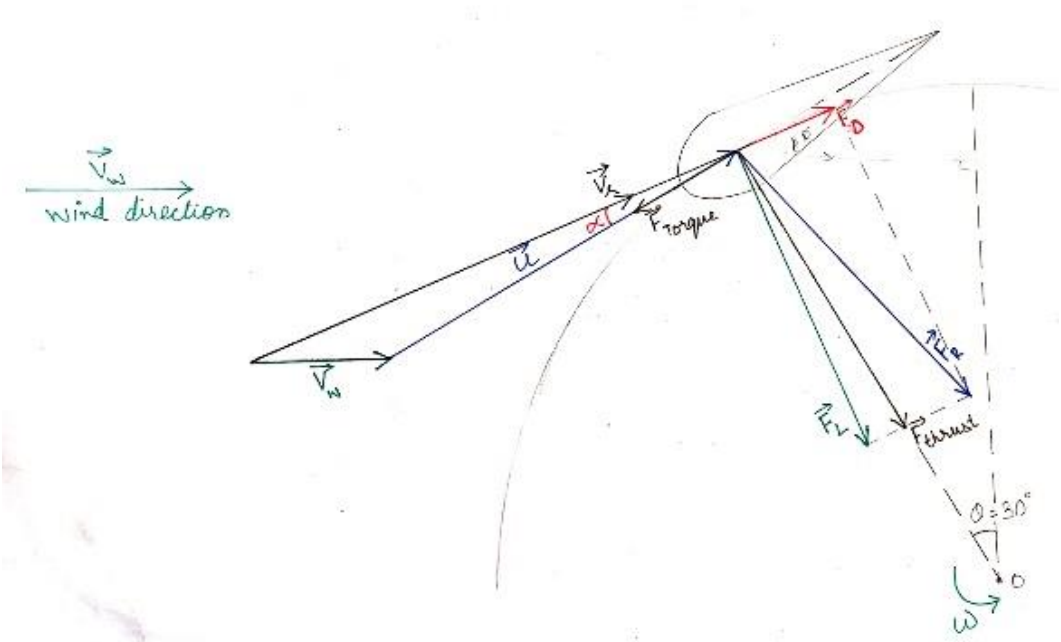

Figure 9 Aerodynamic Forces at Azimuthal angle 30deg

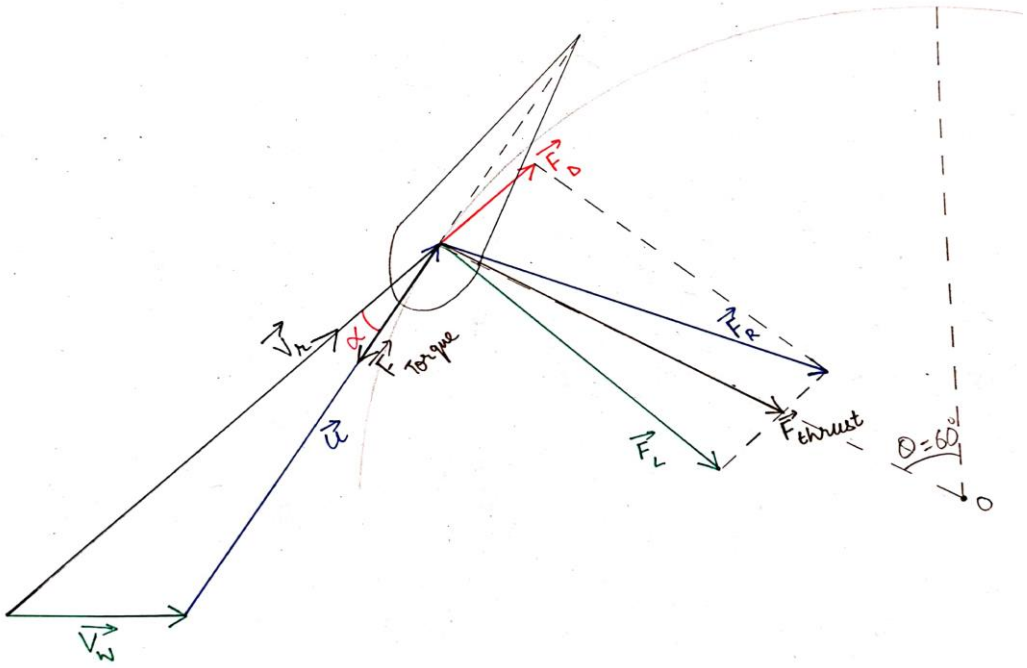

Figure 10 Aerodynamic Forces at Azimuthal angle 60deg

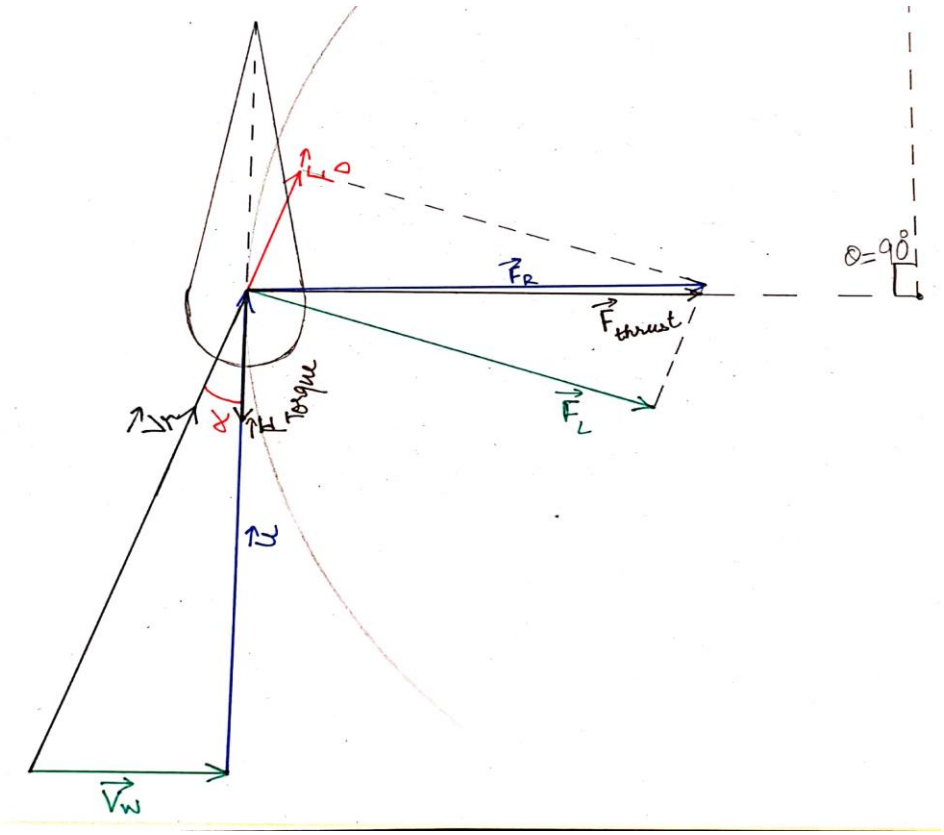

Figure 11 Aerodynamic Forces at Azimuthal angle 90deg

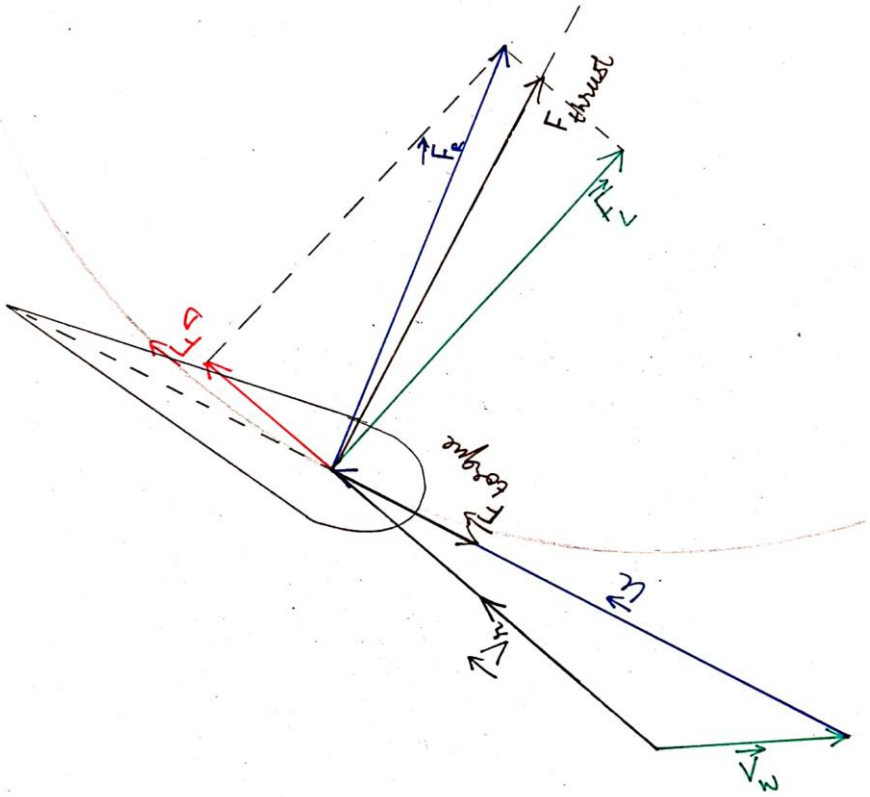

Figure 12 Aerodynamic Forces at Azimuthal angle 120deg

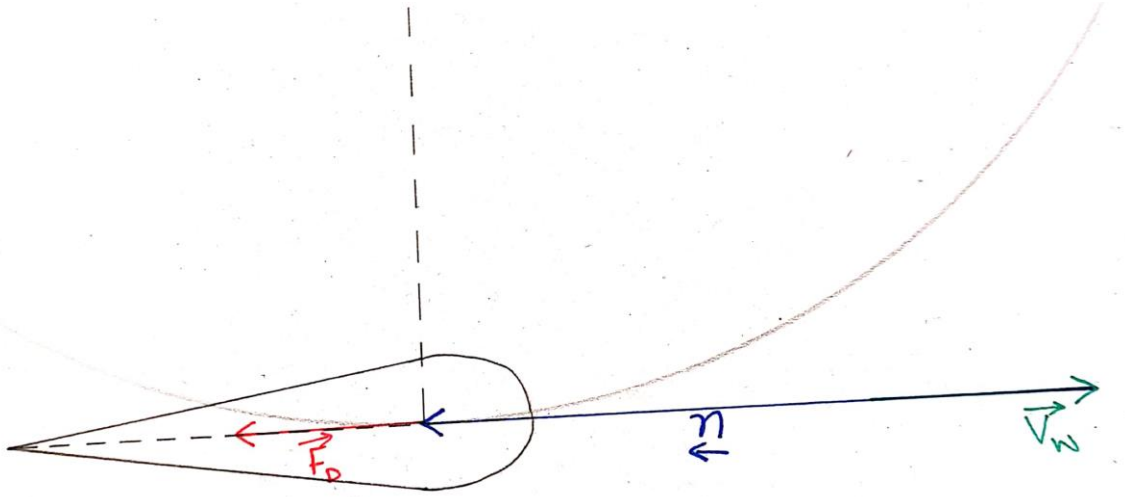

Figure 13 Aerodynamic Forces at Azimuthal angle 180deg

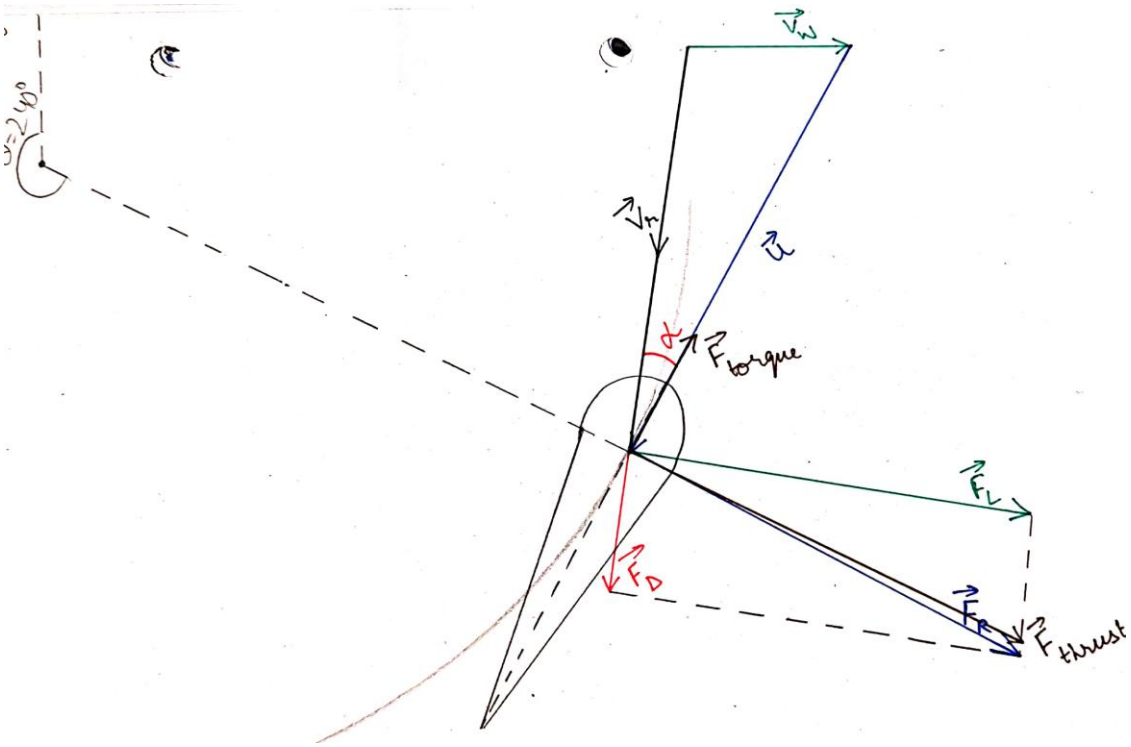

Figure 14 Aerodynamic Forces at Azimuthal angle 240deg

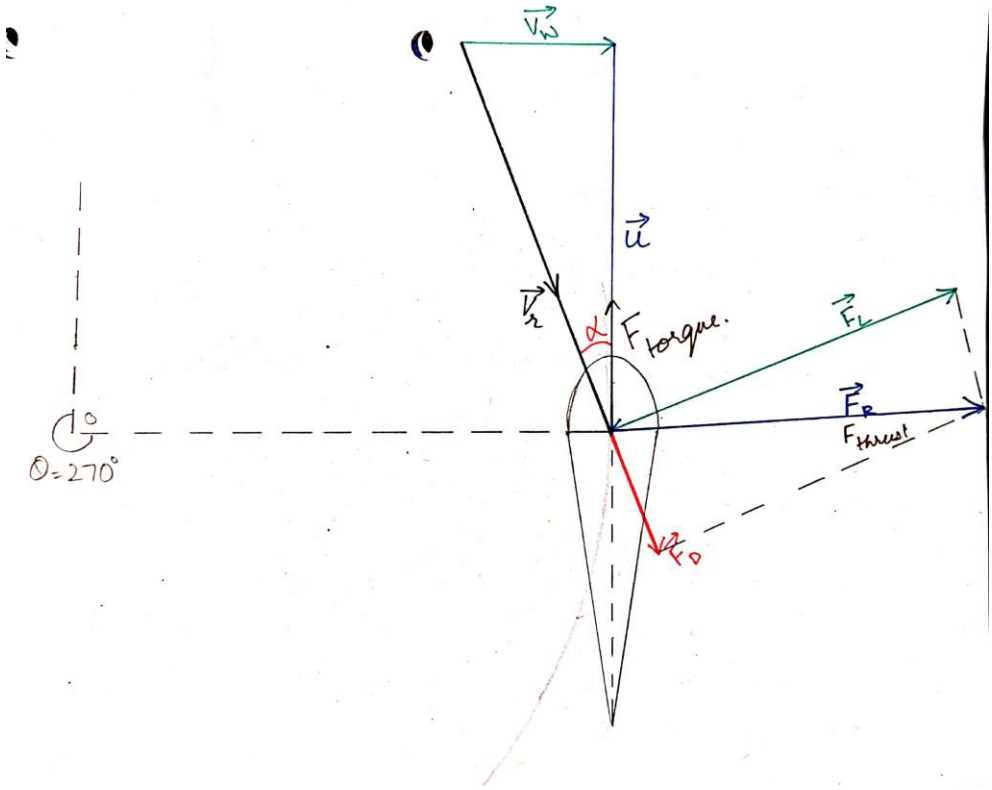

Figure 15 Aerodynamic Forces at Azimuthal angle 270deg

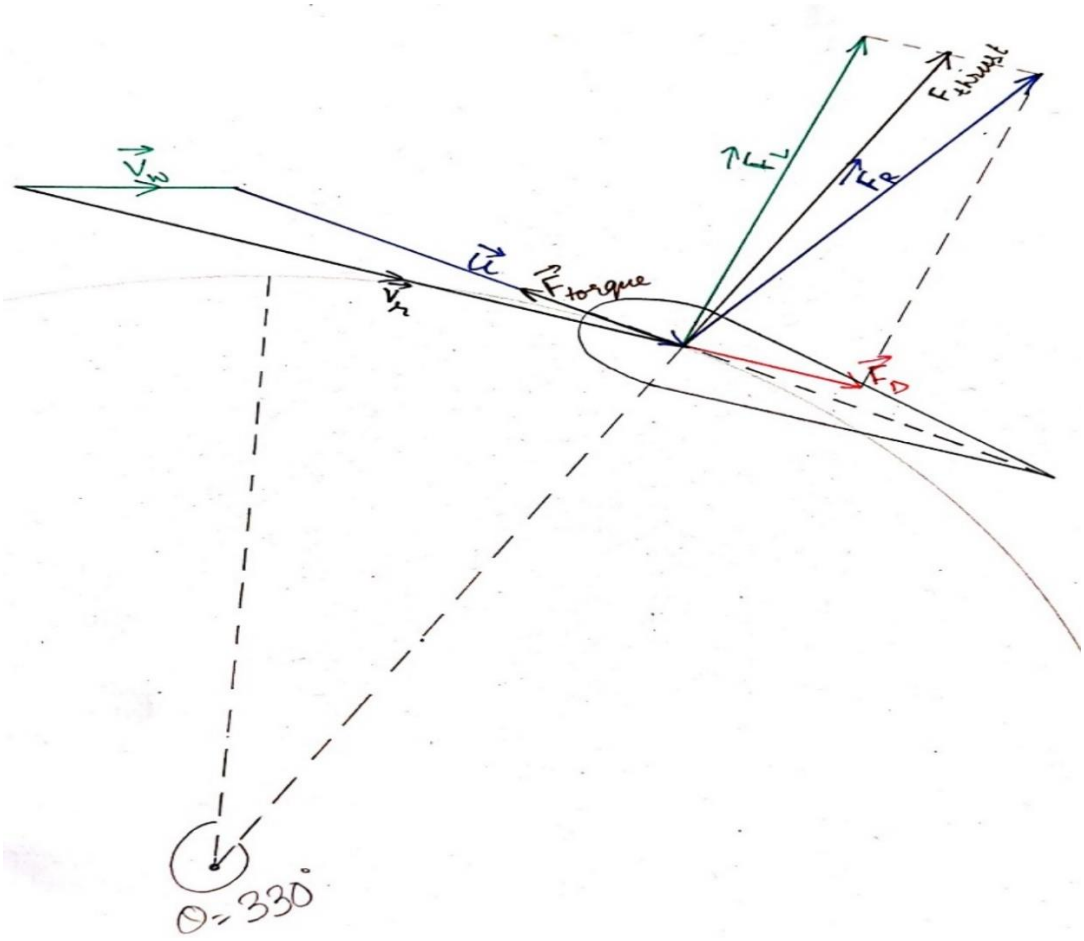

Figure 16 Aerodynamic Forces at Azimuthal angle 330deg

The objective of the manual investigation at the early stage of thesis was to get acquanted with different terminologies and how these variables interacts with one another. The main objective of the study is to make sure that the Airfoil is alligned in such a position so that the overall effect of all the forces and angles give us maximum Net Ft. For more Manual design figures, refer Appendix 4.

3.2 Tip Speed Ratio (λ)- The ratio between the tangential velocity of the Rotor blade to the velocity of the undisturbed wind is termed as Tip Speed Ratio (TSR) and is expressed as λ. This variable is very important to establish at the beginning of the Simulation as the Rotor Power Coefficient (Cpr) is dependent on the TSR. So, to have comparison of results where the variable to be tested and altered is Pitching angle (β), all other variables that can change the Cpr must be kept constant [1].

$$Tip\ Speed\ Ratio(TSR)\lambda = \frac{Tangential\ Velocity\ of\ the\ Rotor(u)}{Undisturbed\ Wind\ Speed(v_w)}$$

3.3 Angle of Attack (α)- The velocity of the wind witnessed by the Leading edge of the Airfoil is not the same wind speed or direction that is the actual undisturbed wind speed. The oncoming wind gets changed due to the fact that the Rotor blade is moving with certain Tangential velocity. So, the resultant velocity (Vr), which is actually witnessed by the Airfoil is equal to the vector combination of the u and v_w [1].

The angle between the Vr and the Chord line of the Airfoil is known as Angle of Attack (AOA) and is represented as α. In case of VAWTs, the AOA varies continuously as going through a complete rotation. The AOA is a function of the Azimuthal Angle (θ) and TSR. The angle follows a sinusoidal pattern but not exactly. The equation which governs the value of AOA is expressed as: [5]

$$\alpha = \tan^{-1}\left(\frac{\sin\theta}{\lambda + \cos\theta}\right)$$

The equation states that the AOA is dependent on TSR. So, this is also the reason to come up with a constant value for TSR at the beginning of the Design phase.

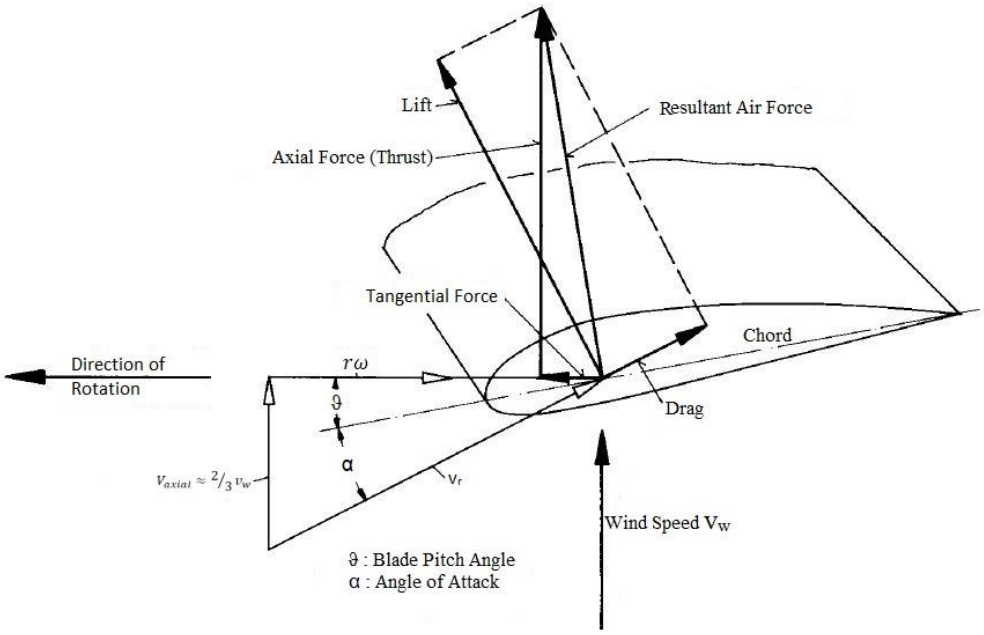

Figure 17 Airfoil with various Aerodynamic Angles [1]

3.4 Blade Pitch Angle (β)- This is the angle, which is made, when the Airfoil is made to rotate about its axis and made to face a direction that would ideally not be present, if the rotor is left undisturbed. This is denoted by β. This parameter is very important because the Power output of the Wind turbine is changed

by altering Pitch angle. If left undisturbed, the VAWT will have AOA which is addressed by the equation addressed above [5].

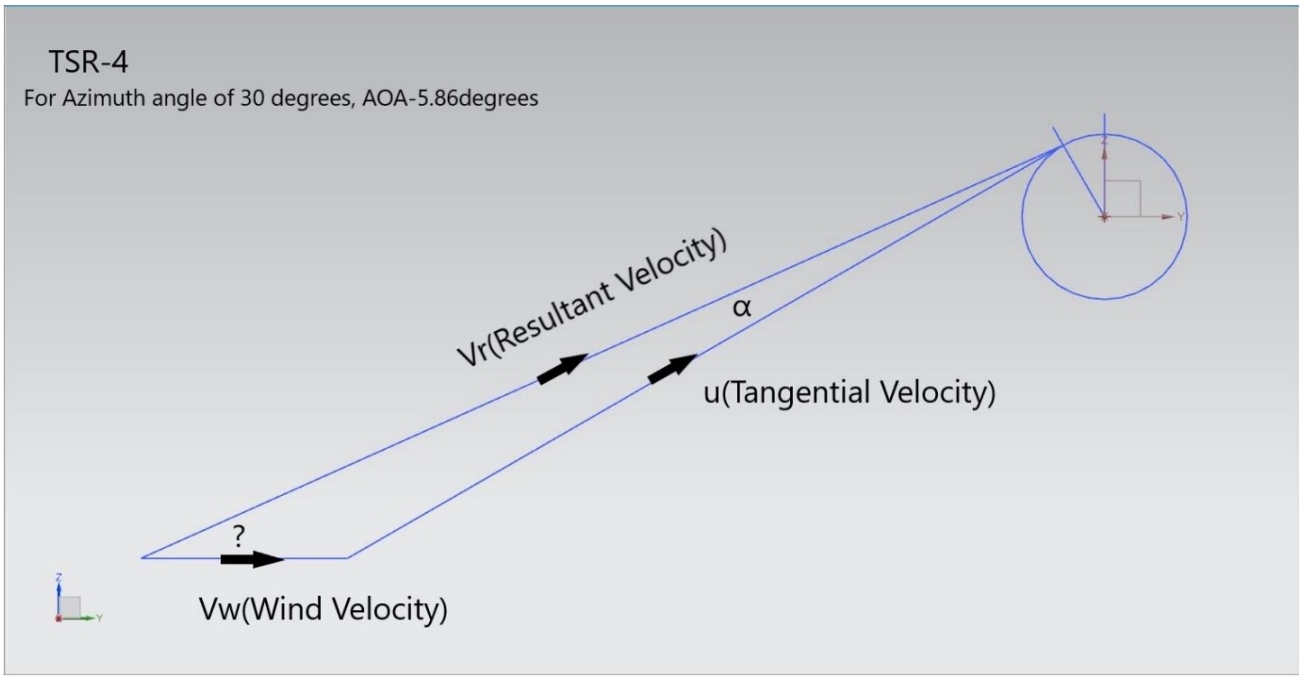

Figure 18 Resultant Velocity of a VAWT

But in this research, the objective is to observe how the desired parameters (Torque and Cpr) varies by changing the β. There can be different approaches employed for pitching, in order to improve the power Coefficient. It can be Constant pitching, where the blade pitch angle takes a constant value throughout the whole rotation of the airfoil [6]. Or it can be Variable Pitching, in which, the pitching is varied during different Azimuthal positions throughout the complete rotation. In this research, the effect of both of such approaches are reported.

3.5 Rotor Power Coefficient (Cpr)- This coefficient is essentially the depiction of efficiency of the rotor system. It states that what percentage of the Power that is available in the wind, is converted to usable mechanical Power by the Rotor system of the Wind turbine. It is the ratio of the mechanical Power actually developed by the rotor to Power available in the flowing Wind (P_{wind}).

This is utilized in order to compare the results from different studies as this Coefficient takes the power output from the system and makes it independent of the geometry and turns it to a dimensionless quantity [1].

$$C_{pr} = \frac{P_{act}}{P_{wind}}$$

Chapter 4

4. CHOSEN APPROACH TO SOLVE THE OBJECTIVES

As there are quite a many objective of the research, there had to be a set of different approaches that were employed to obtain the results. There exist numerous design approaches for Wind Turbine and after confirming those, different Simulation approaches that can be or should be employed in order to complete the objectives set forth at the beginning of the research. So, in this chapter, discussion about different approaches employed at each stage of Simulation are reported and reasoning behind those choices.

4.1 Approach about the Geometry- The geometry is the most important part of any Simulation. In order to make comparisons about Pitching angles, all other parameters, including the shape and size of the Airfoil needs to be constant during all the different Simulation scenarios. The geometry should be of such nature, that enough Literature exists about it from different sources in order to make inferences and comparisons of the results to the Literature.

4.1.1 Airfoil Type- The Airfoil used in the investigation is the NACA 0012. The reason behind choosing this Airfoil is the abundance of Simulation and Experimental data at disposal for this Airfoil from many credible sources. Also, this Airfoil is symmetrical which helps in distinguishing the unequal forces occurring on the two sides as a result of AOA. Opposed to the innate geometry of Asymmetrical Airfoils, which causes the inequal forces on the two sides of the airfoil even at 0deg AOA [7].

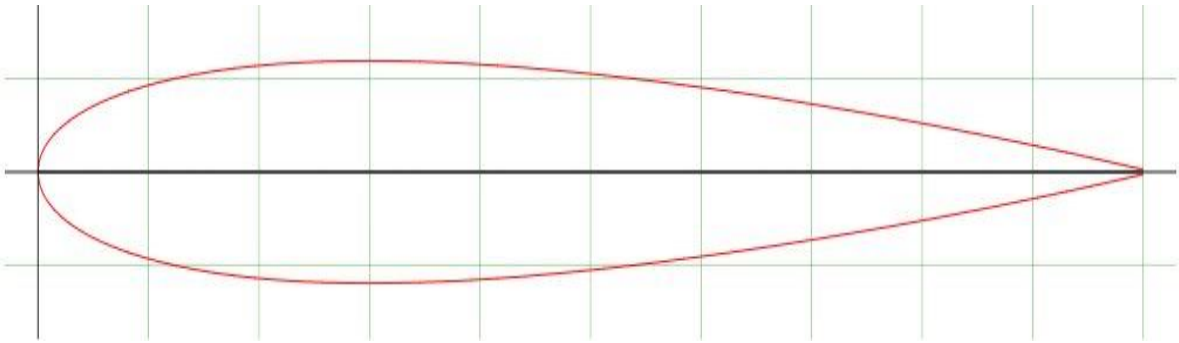

Figure 19 NACA 0012 Airfoil [8]

4.1.2 Number of Blades (Nb)- The amount of Power produced, and the efficiency of the wind turbine depends on the number of blades used in the rotor. As one of the objectives of the research is to make a comparison of how the variable pitching affects the Single bladed system and Multiblade System (Two Blades in this case), two geometry options are made and tested for this purpose.

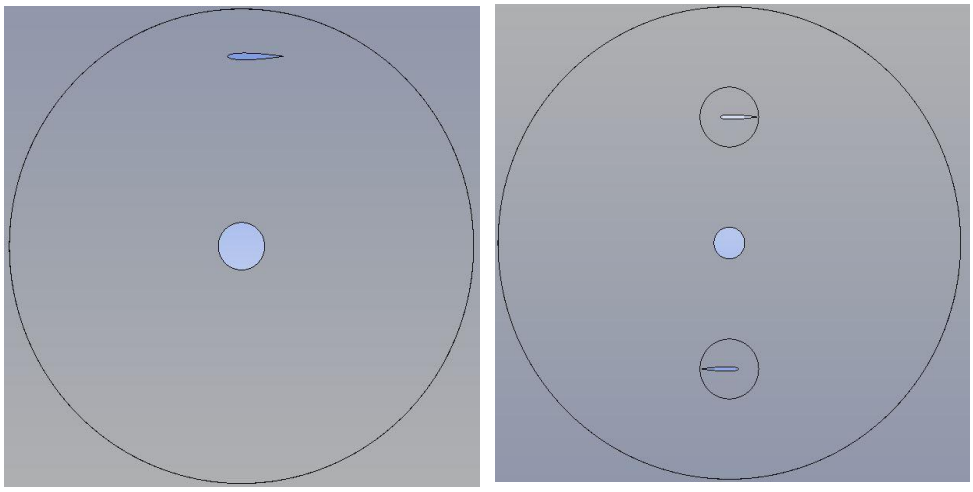

Figure 20 Single and Two Bladed Rotors

4.1.3 Radius of Rotor- The Radius (R) of the VAWT is the centroid point of the Rotor Blade. This was chosen a value of 0.8m following the example of the Agile prototype VAWT which Prof. Stank had seen and observed from where the idea of variable pitching on such a system originated [3].

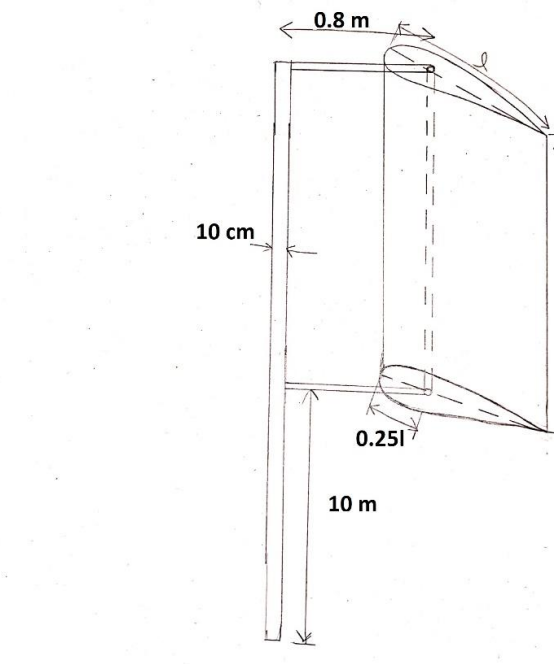

Figure 21 Preliminary design Parameters

4.1.4 Chord Length- The chord length (c), of any Airfoil is the length of a straight line joining the Leading edge to the Trailing edge. In case of VAWT, the chord length is a function of different parameters such as number of blades, Radius of rotor and Solidity (σ). From literature, the formula acquired for determining the chord length for VAWT is: [9]

$$Chord\ length\ (c) = \frac{\sigma_{max} R}{N_b}$$

Where σ_{max} is the solidity where the maximum Cp exists. Its value is obtained from the literature and is equal to 0.3 [9]. By this formula, the chord length of the airfoil is adjusted to be equal to 0.24m.

4.1.5 Center of Airfoil- It is already established that the Radius of the Rotor is considered from the center of the Airfoil. The Airfoil can be a long entity and therefore, there exist a need to define a point on the chord length which could be considered as the center of the airfoil. From Wing Section Theory by Abbott, this point exists at the 25% of the chord length from the Leading edge [8]. So, the center of the airfoil lies 6cm away from the Leading edge on the chord line.

4.1.6 Wind Speed and Tip Speed Ratio- The average wind speed in the city of Hamburg is taken as 5m/s. The data is taken from Open Web-source about weather and climate in Hamburg [10].

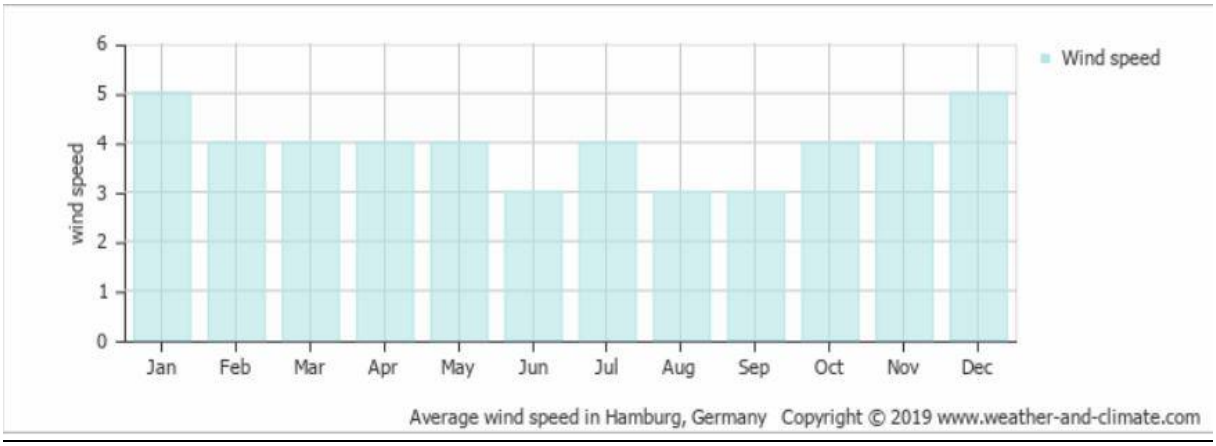

Figure 22 Monthly Average Wind Speed in Hamburg [10]

The TSR is also another parameter that plays a big role in the Simulation study. There are numerous studies where the effects of TSR on the Cpr of the VAWTs are analyzed. For this study, a constant value of TSR is needed. The maximum Cpr, according to different studies, was reported for TSR values between 3 and 4. So the TSR was taken as 4 in this study [11].

4.2 Approach about Meshing- The mesh quality and the type of mesh has a drastic impact on the quality of results obtained from the Simulation. The approach used initially during the research was with 3-D Unstructured mesh, where the mesh elements were tetrahedron. This approach required a lot of computational power and time to achieve the required mesh element size [12]. For additional 3D mesh figures from the Preliminary study, refer Appendix 1.

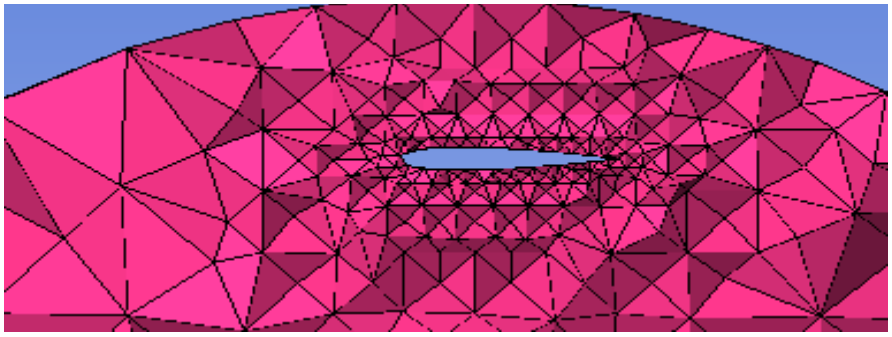

Figure 23 3D Mesh with Tetrahedral Elements

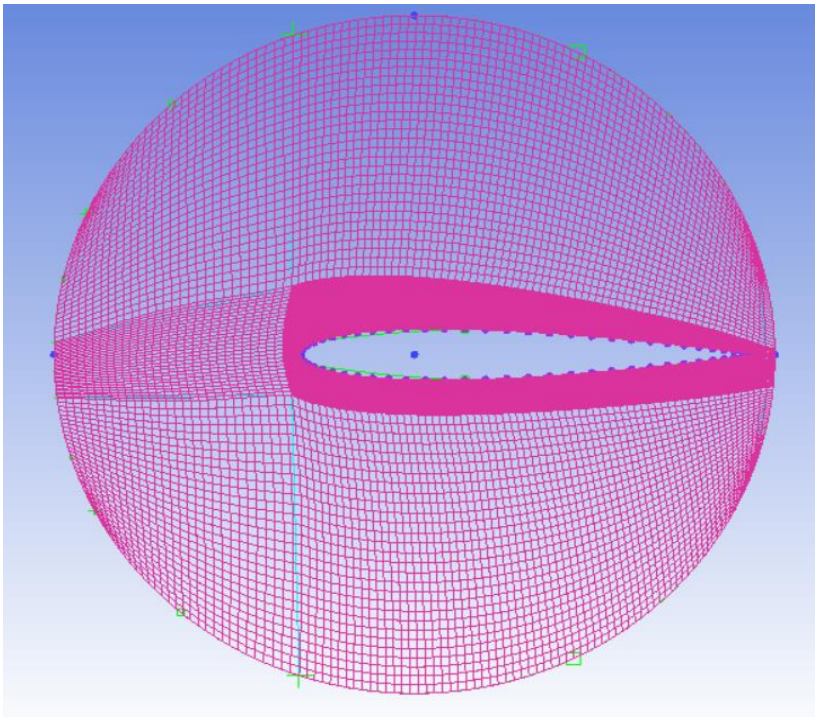

Figure 24 2D Mesh Approach

The mesh option utilized in the end was the Quasi-2D mesh in which the “Openings” of the domain are specified as “Symmetry” in the Pre-Processing. The mesh is defined after Blocking the 2D geometry and then extending the Pre-Mesh into the third dimension by extruding the mesh by one mesh element. This approach was referred after studying a Literature paper about similar technique. This technique helped a lot in saving the time and faster Main Processing [12].

Another aspect of the Objectives was studying the effects of mesh size and how it will affect the Outputs of the simulation. To achieve that, that element size of the mesh was increased significantly to obtain a Coarse mesh as compared with the mesh of all the normal studies.

4.3 Approach about Analysis type

- There are two Analysis options that are opted and reported in this research. Both the Steady state analysis and Transient State analysis are performed by keeping the geometry and boundary conditions similar and results on both are reported. Comparison between both of these was also one of the objectives.

Chapter 5

5. METHODOLOGY AND NUMERICAL SETUP

As the scope of this thesis is dealing with numerous topics related to the VAWTs, various Design and Numerical setup approaches were employed to cover each specific objective. In this chapter, description of different methods is reported. It is easier to explain one of the complete techniques in detail with all its different steps in continuity, instead of explaining one procedural step in different setup scenarios. So, this chapter is divided in different sections where each section explains the necessary methodology behind one of the setup scenarios.

5.1 Verification of formula for Local AOA – In this section, the methodology depicting the calculation of AOA from the formula extracted from the literature and verifying the formula using the drafting tools is reported. The formula used was: [5]

$$\alpha = \tan^{-1}\left(\frac{\sin\theta}{\lambda + \cos\theta}\right)$$

According to this formula, the AOA assumes the values as expressed in the Table 2 below

Table 2 Angle of Attack by Formula

Azimuthal Angle (θ)	Angle of Attack (α)
0	0
30	5.866739
60	10.89339
90	14.03624
120	13.89789
150	9.064678
180	0
210	-9.06468
240	-13.8979
270	-14.0362
300	-10.8934
330	-5.86674
360	0

In order to be sure that the results from the formula are accurate and reproducible, similar geometry condition was generated using CAD software and the results from the measurement were exact replicates of the values from the formula. Therefore, the task of verifying the formula is achieved from this exercise.

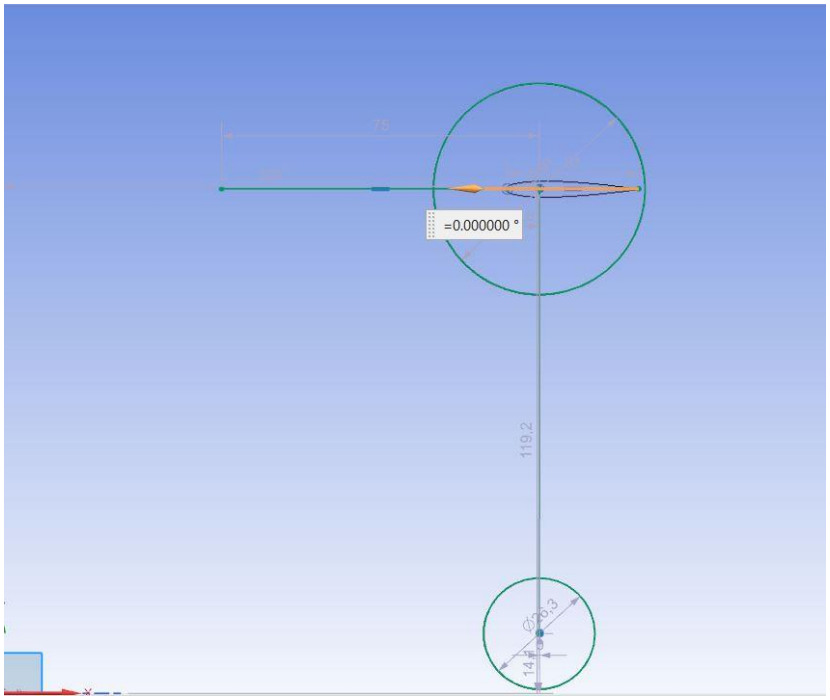

Figure 25 Verification of AOA Formula by CAD Model

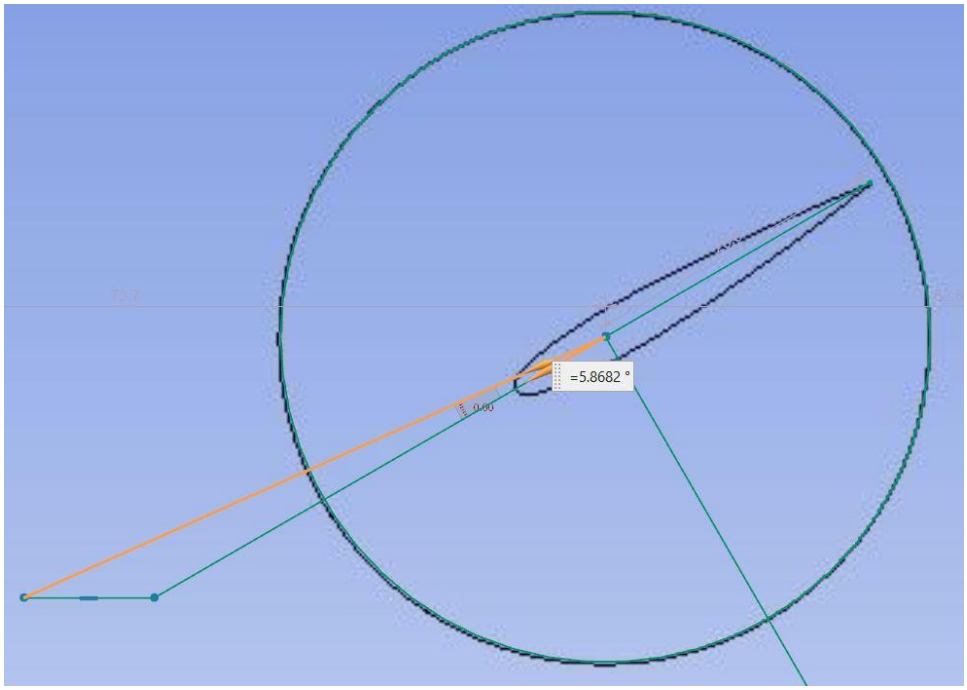

Figure 26 Verification of AOA at Azimuthal Angle 30deg

5.2 Transient State Analysis with Quasi-2D Mesh Approach for Single Bladed Rotor – This study is part of the later stages of the thesis. In this approach, the Geometry consists of only one blade and is utilized to figure out the optimum pitching positions for the blade at each Azimuthal position. The values for Optimal Pitching derived from this approach are applied to two Bladed geometry to validate the findings.

5.2.1 Geometry of the Setup: In order to generate the geometry, one approach available is to import the geometry generated in a CAD software such as Siemens NX, Solidworks or any other. But this approach was not utilized because of some exporting complications which can arise when trying to mesh an imported geometry. So, the choice of developing the geometry in the ANSYS ICEM CFD was better suited and was chosen. In such a case, the geometry is created, and mesh generation is achieved by a single software.

The geometry was established in collaboration by Prof. Stank. The rotor system is chosen to have a single blade and the Rotor diameter is equal to 0.8m. The center of the Airfoil is considered to be present at 25% on the chord length from the leading edge [3].

The data about the NACA 0012 Airfoil is procured from Prof. Stank. The file contains the comma separated values for points necessary for generating the Airfoil [8]. Once the data is loaded as CSV file, the ICEM CFD, converts the values into discrete points which in represent the shape of the Airfoil.

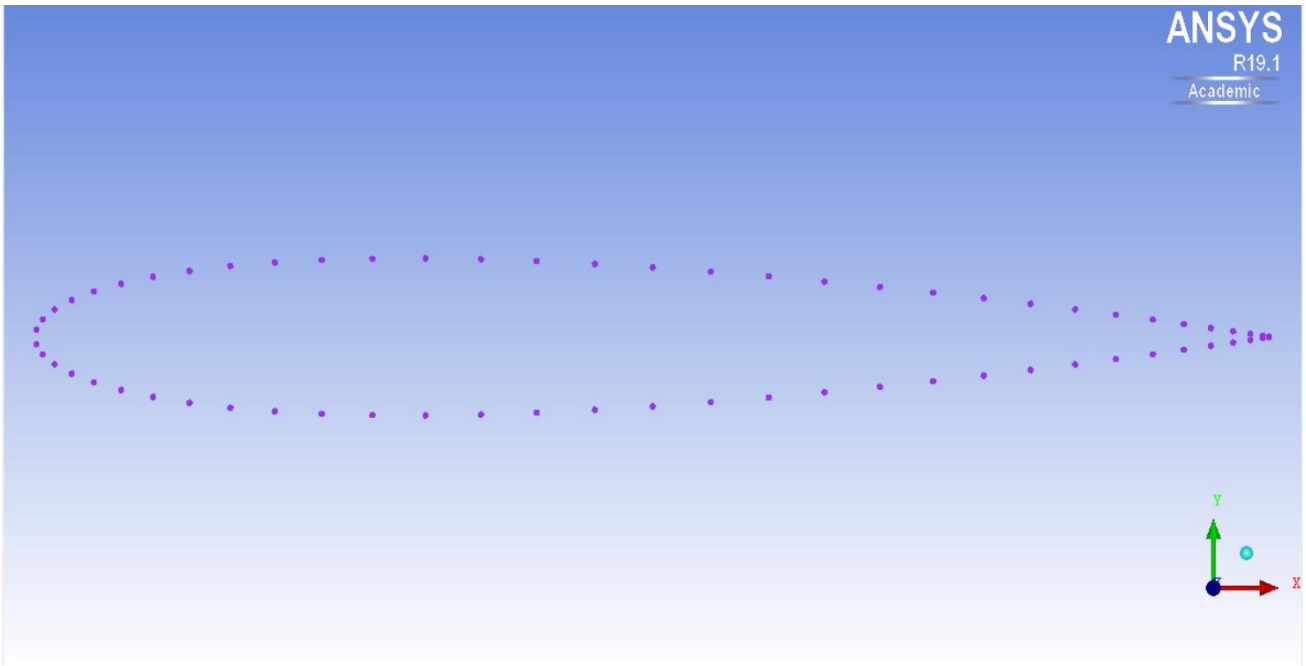

Figure 27 Imported data points for Airfoil generation

After the points are loaded, the next step is to join these points and form curves from these points. It is made sure that the entire airfoil is formed of at least three curves which will later help in accurate Blocking which helps in capturing the Boundary layer phenomena accurately.

Next step is to develop the accompanying geometry such as including the central Pole to which the Rotor is considered to be attached. During this step, the curves forming the airfoil goes through some transformation steps such as Translation and Scaling. The geometry, which is needed, requires the Pole to be located at the origin and thus the Airfoil to translate equal to the rotor radius as explained in an earlier chapter. The size of the Airfoil for a VAWT is depicted by formula: [5]

$$Chord\ length\ (c) = \frac{\sigma_{max} R}{N_b} = 0.24m$$

$\sigma_{max} = 0.3$, R=0.8m and $N_b = 1$

The chord length of the Airfoil from the data is equal to 1m. So, in order to apply it to the case at hand, it has to be scaled down by the factor of 0.24 in X and Y axis.

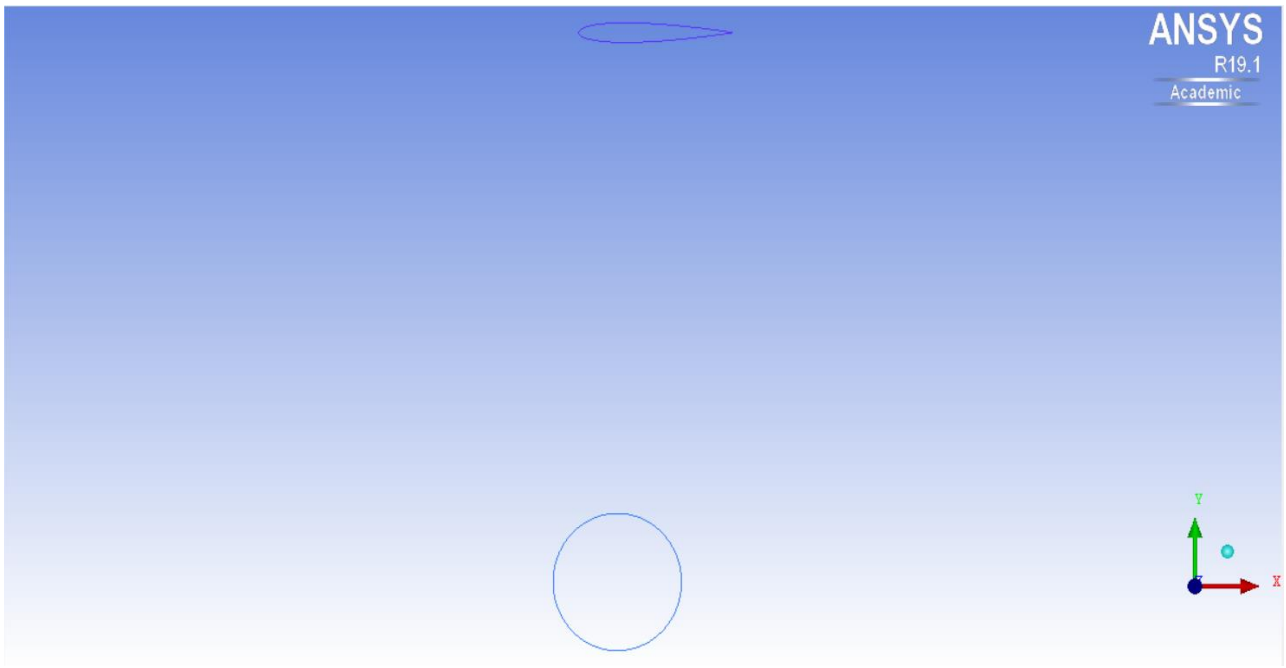

Figure 28 Scaling and Translation of Geometry

After the Airfoil and pole are generated, the next step in Geometry generation is to create the enclosures which will allow to make different domains such that each component of the geometry can act according to the freedom which is desired. So, there are two domains which are generated around the geometry already generated. In the end there is a large enclosure which simulates the wind tunnel.

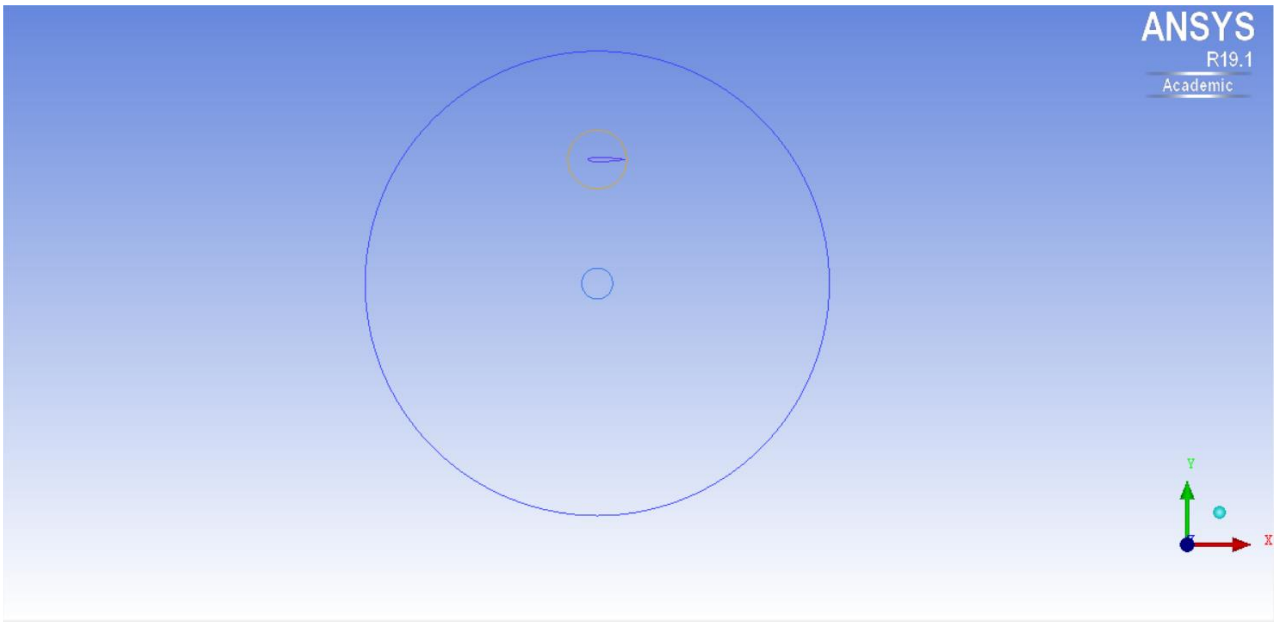

Figure 29 Generation of Outer Domains around Airfoil

Following the specifications from the Literature and in order to simulate the conditions of a Wind tunnel, the dimensions are as a rule of thumb described as:

Standard length from side to side should at least be 15 times the length of Rotor diameter. In this case, it is taken as 30m which is almost 19 times the rotor diameter [13].

The standard length behind the Airfoil should be between 25 times and 40 times the rotor diameter and it should be at least of 15 times before the Airfoil. In this case these values were taken as 50m and 30m respectively [13].

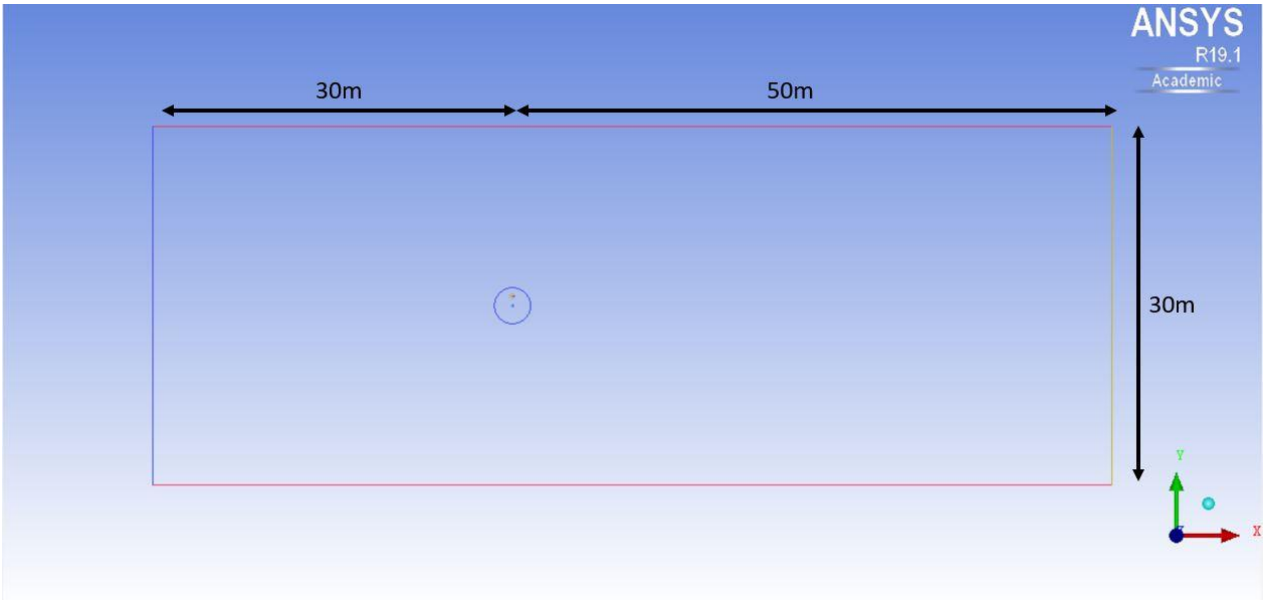

Figure 30 Dimensions of Domains according to Literature

5.2.2 Blocking and Meshing- After the geometry is completed and different domains are created, various Parts are named, and respective curves and surfaces are assigned to the parts named. The next step is to mesh the completed geometry. There are different types of meshing approaches that can be taken, such as Structured meshing, Unstructured meshing or Global meshing [8]. For this particular approach, Unstructured meshing is used because in this geometry, the curves and surfaces prefer an irregular and unstructured meshing system where different element sizes are possible unlike in Structured mesh which cannot complement the dynamic shapes [14].

First of all, the entire 2-D geometry is enclosed by a Planar 2D block which would later turn out to be one of the faces of the geometry. It must be noted that the entire geometry cannot be meshed in one step. Each domain must be meshed separately to make sure that they can interact as needed during Simulation. So, each domain acts as different entity and needs to be meshed differently using the same methods described further. After this step, the edges of the Block must be Associated to the curves of the part of the geometry that is needed to be meshed.

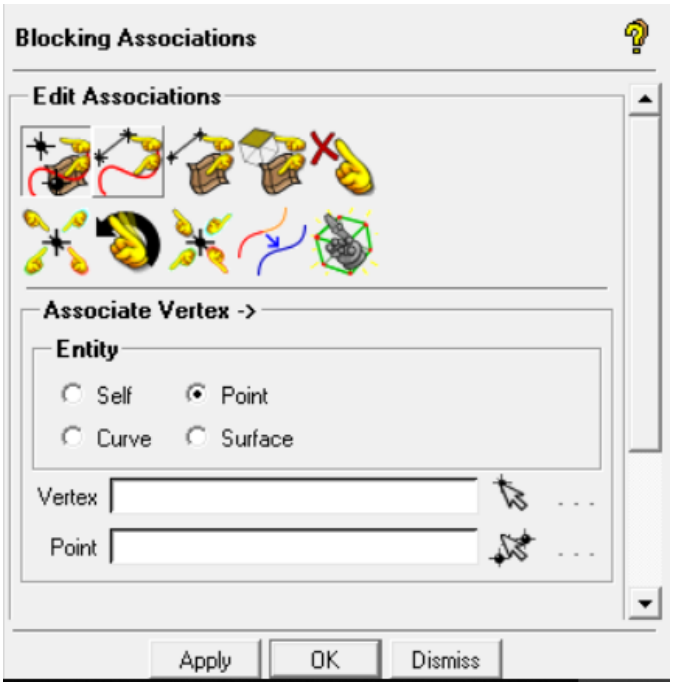

Figure 31 Settings for Edge Association in Blocking

After the initial block is generated around the specific domain, the block needs to be segmented into different parts so that the irregular shapes of the geometry can be captured more accurately. The block is split at as many locations as needed so that each individual part or entity is enclosed in a separate block.

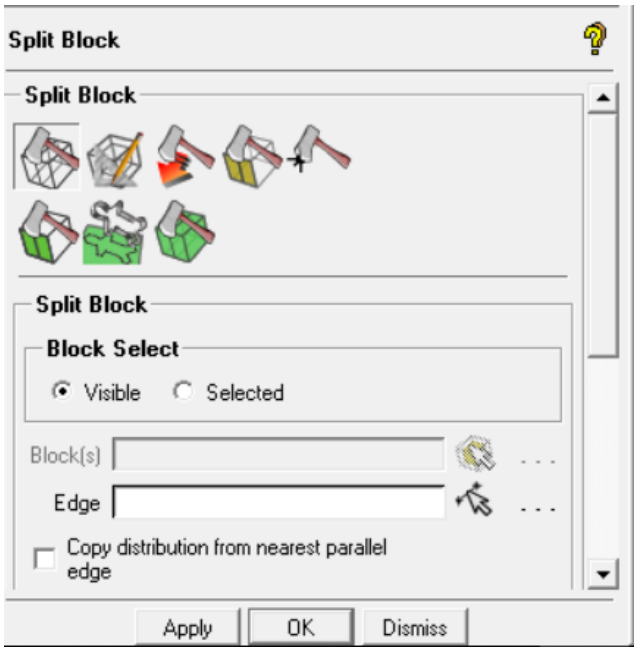

Figure 32 Settings for Splitting the Block

After splitting the initial block into as many as needed blocks, the blocks with entities that need very small mesh elements are split using an O-Grid technique. In this method, the block is divided into two centric Quadrilaterals. The inner block can be associated to the curves of the geometry and the diagonal lines joining the corners of the two quadrilaterals can be divided to specify the height of each mesh element.

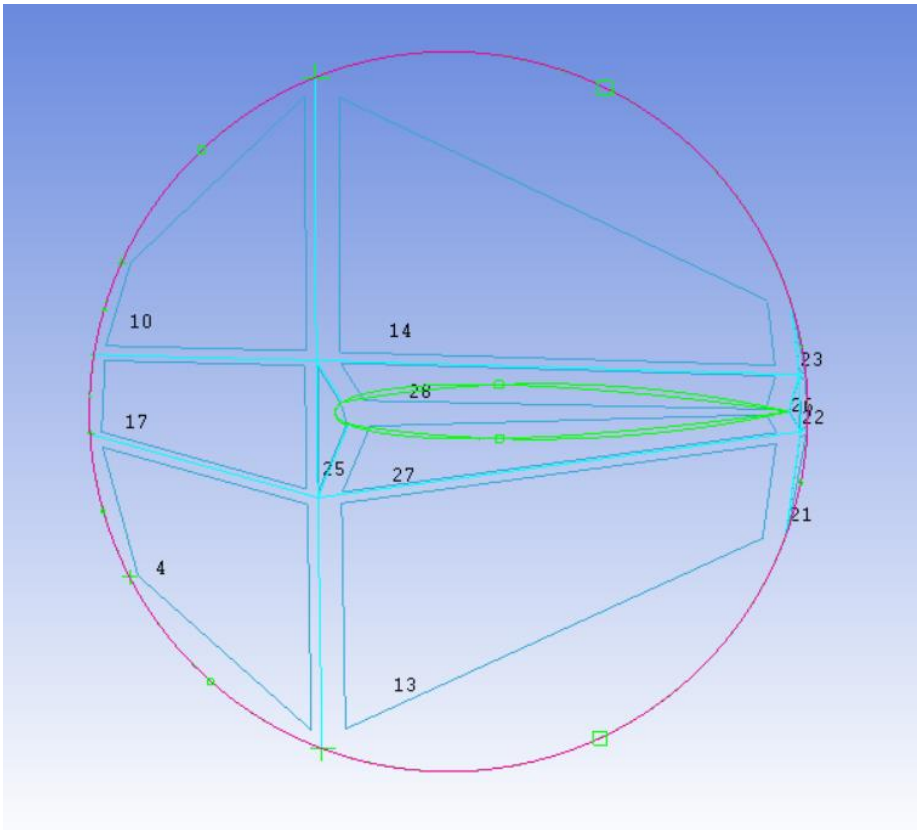

Figure 33 Generating the O-Block around the Airfoil Geometry

After the O-Block has been generated, the block where the physical geometry exists, such as the airfoil or the pole, is deleted so that this block does not get meshed. Because it is either a “Wall” domain or will be meshed as completely separate domain in another mesh run and would ultimately be combined to form one complete setup.

One of the most important steps of meshing section of the Simulation is Pre-Mesh Parameters. These have a direct output on the quality and size of the mesh. As the domain is split up in different blocks in the previous steps, during this step, the number of divisions on the edges of each of these blocks can be specified to attain the degree of the precision which is required from the mesh. The pre-mesh parameters

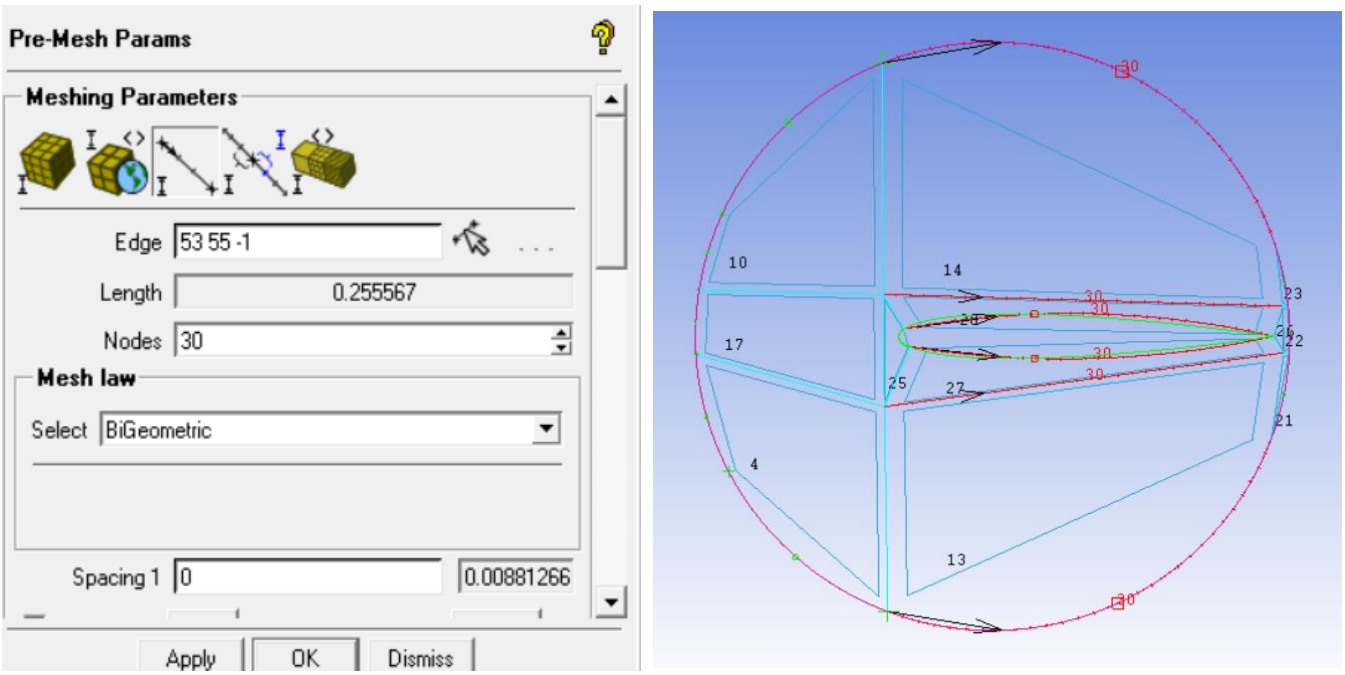

Figure 34 Settings for Pre-Mesh Parameters to determine the Quality of Mesh elements

are specified in such a way that the y+ range can be accurately captured, and effects of boundary layer phenomenon can be seen without being overlooked in the simulation [12].

After all the Pre-Mesh parameters pertaining to different edges are set as required, a preview of the Pre-mesh can be seen which depicts how the final mesh will look like.

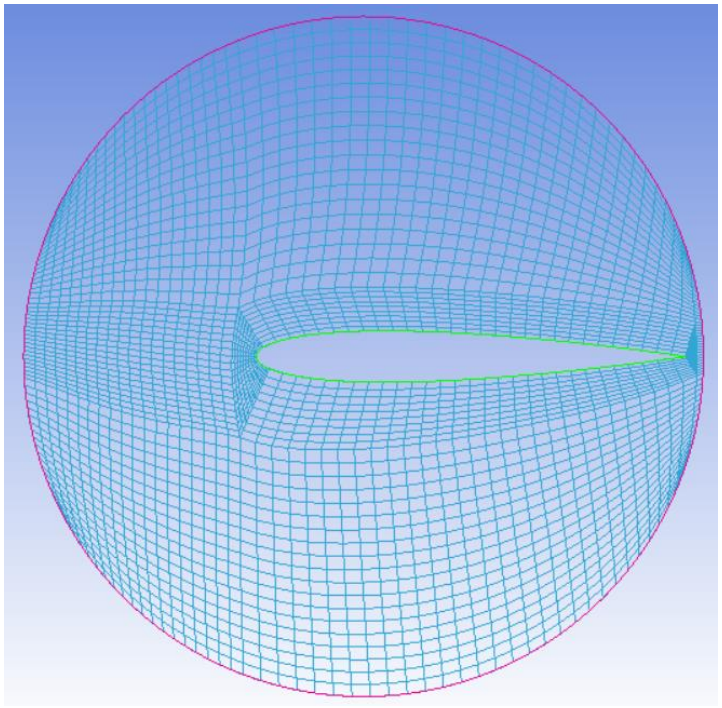

Figure 35 Pre-Mesh Structure

The domain which houses the Airfoil is chosen to be of such specific size, in order to allow the rotation of the mesh containing the Airfoil. The size is limited by the fact that the computational effort increases with increasing number of mesh elements and the limitation of number of nodes available in the Student version of ANSYS. There is an additional domain around the innermost domain so that the effects from the trailing edge are captured precisely.

After a satisfactory Pre-Mesh is generated, an Unstructured Mesh can be generated from this by the press of just one button. Now that an Unstructured mesh has been generated, next step is to convert this 2D mesh into 3D mesh but extruding the Unstructured mesh. This can be achieved from the Edit mesh Tab and selecting “Extrude Mesh” by one element and selecting all visible elements of mesh.
After the 3D mesh is generated by Extrusion, this mesh can be saved by selecting the solver type. The solver type selected for this and also all the runs in this thesis is ANSYS CFX.

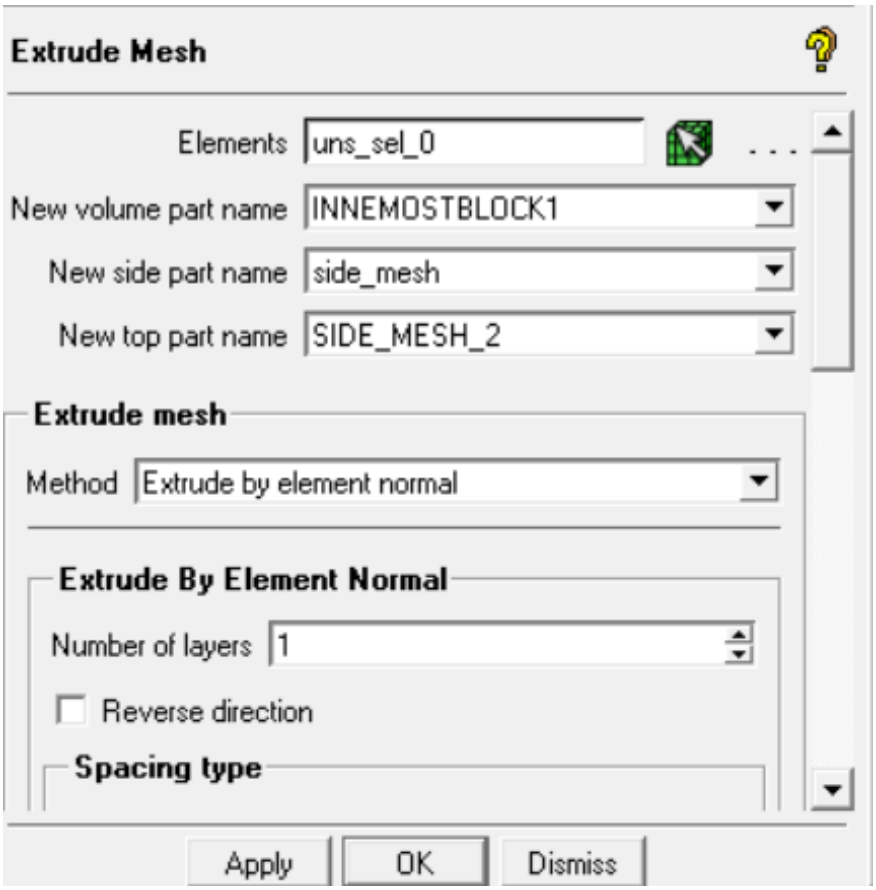

Figure 36 Settings for Mesh Extrusion to generate Quasi-2D mesh

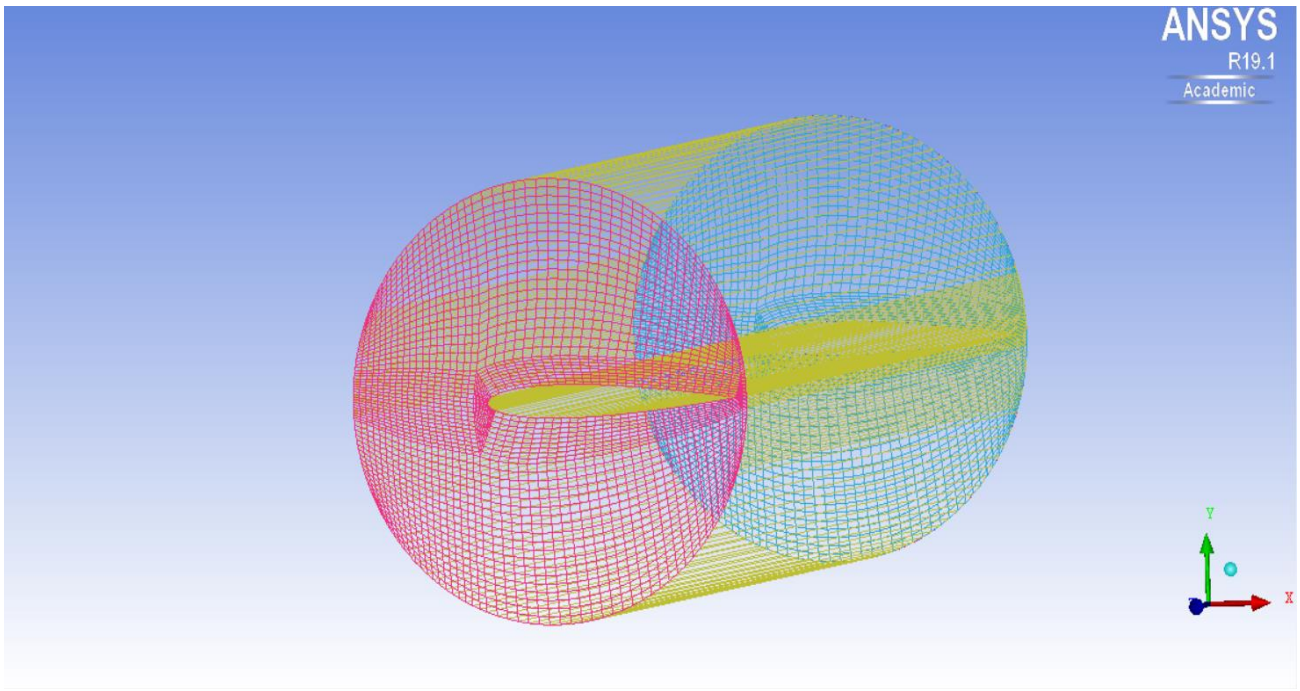

Figure 37 Unstructured Extruded Mesh

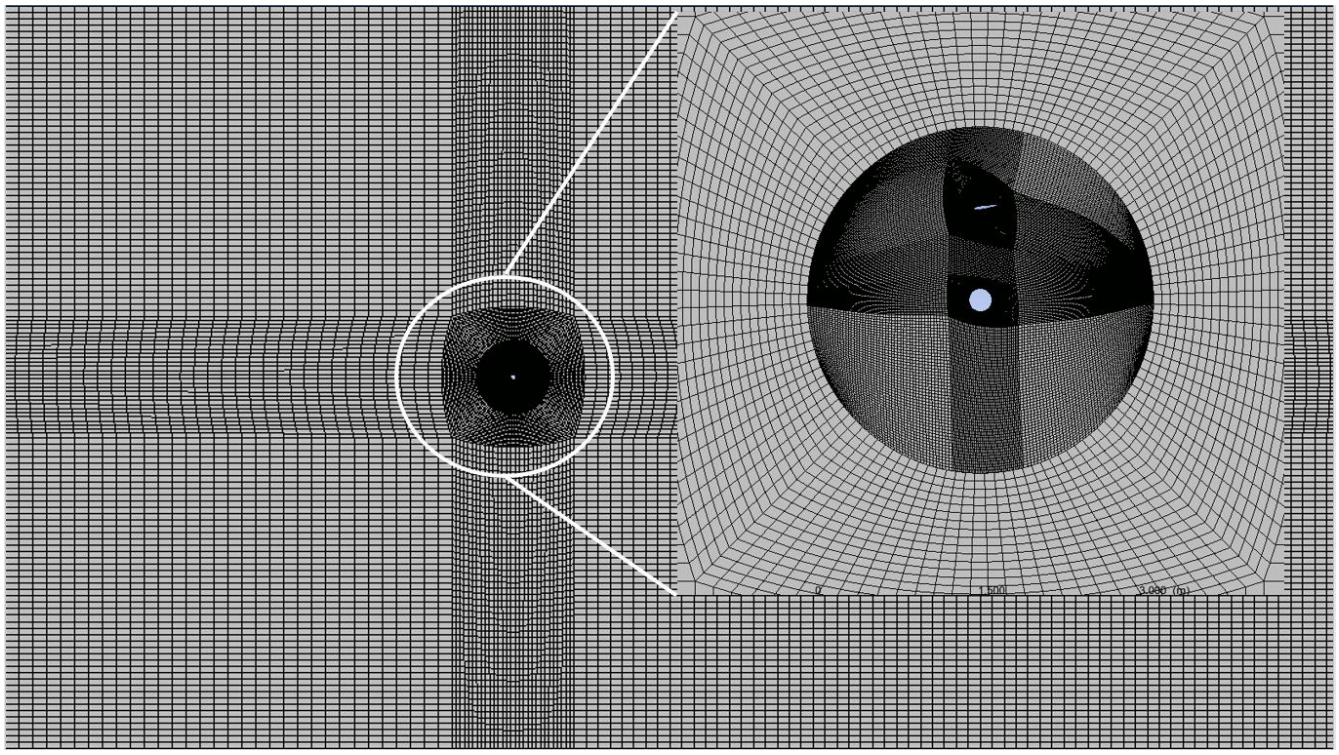

Figure 38 Final Mesh Elements Visualization to observe the Quality of mesh

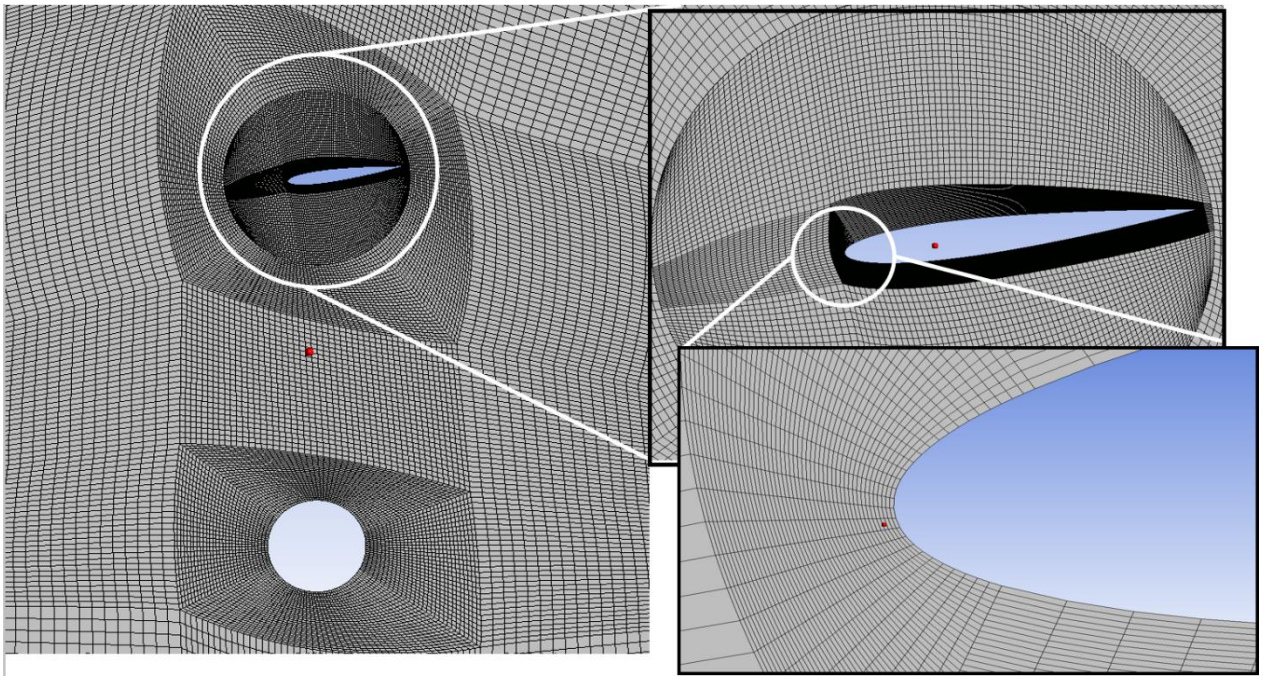

Figure 39 Zoomed and Focused view of mesh

The mesh characteristics after employing this technique of Quasi-2D unstructured mesh generation are appreciated because it allows for the usage of ANSYS student version in which the maximum nodes allowed are 512,000, instead of acquiring a Research License of ANSYS. In this approach, the total number of nodes achieved by combining all the different domains with very high mesh quality is equal to 149,584. This attribute helps a lot in quicker Main Processing runs and makes the process faster and more accurate [12].

5.2.3 Setting Up Boundary Conditions- After all the individual domains are generated and meshed, they are imported into the ANSYS CFX Pre module. In this module, the desired boundary conditions are applied to the framework of the Simulation. This step is very crucial because these conditions have to replicate real-life testing conditions, in this case, that of a wind tunnel. After importing all the meshes which form the complete physical setup, attention must be given so that all the adjacent domains have an inter-connection and interacting domains do not have separated meshes [15].

First of all, the analysis type is selected. For this investigation setup, it is chosen as Transient Blade Row with time initiation as 0 sec. After the type of Analysis is chosen, next step is to apply the appropriate Transient Blade Model. In this section, the definition of time step is provided.

Timestep is the time difference between two consecutive investigation positions. As the geometry will be rotated continuously with a certain angular speed ω, the timestep will specify to the solver that at which time, the certain calculations be performed, and results be reported.

The requirement is that the timestep should be selected such that each Transient result after one Timestep represent one degree of Azimuthal rotation. It means that the timestep will ensure that the calculations are performed at one-degree intervals in the complete rotation of Airfoil around the axis. The following calculation helps in achieving that Timestep.

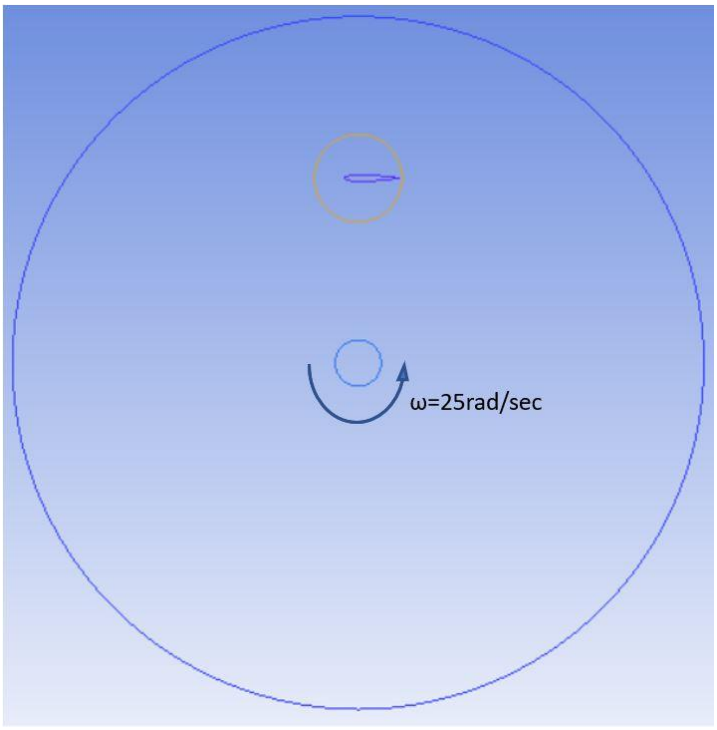

Figure 40 Angular Velocity of Rotating Domain containing Airfoil

5.2.4 Calculating Timestep- Converting Linear velocity to Angular velocity is a step involved in this process. The Wind speed is assumed to be 5m/s which is a linear velocity [10]. The TSR is taken as 4 and consequentially, the linear velocity of the Airfoil becomes 20m/s. The radius of the Rotor is 0.8m.

$$v = r\omega$$

Where v is linear velocity, r is the Radius of rotor and ω is the angular velocity.

So, from this formula, the angular velocity of the rotating domain of which the Airfoil is a part of will be equal to 25rad/sec.

In order to calculate the Timestep, the formula describing the relation between angular position and angular velocity is used. According to it, the angular position of a rotating body can be judged by knowing its angular velocity and time lapsed from the initial position [15].

$$Angular\ position = angular\ velocity \times time\ span$$

$$\Delta\theta = \omega * \Delta t$$

As the angular position desired at new position is separated from the previous one by 1 degree, $\Delta\theta$ is taken as 1 deg or 0.0175 radians.

$$\Delta t = \frac{\Delta\theta}{\omega} = \frac{0.0175\ rad}{25\ rad/sec} = 0.0007 sec$$

So, the Timestep is calculated and this is the time difference between the rotor assumes two consecutive Azimuthal angle positions along the rotation. The total timespan will depend on how many revolutions are required to get the necessary results. In this case, the total time of run is kept at 0.259 sec which compensates for 370 deg revolution of the airfoil.

The next step in Pre-Processing stage is to assign different domains with physical settings. The domains are created, and specific 3D volumes are assigned to each domain. These domains now represent the Outer Fluid which is Stationary, Medium Domain which is Rotating with ω, and Innermost domain which houses the Airfoil and is also rotating with ω. Each of these domains are initialized to provide the Cartesian Velocity at Inlet and Relative pressure at the Outlet [8].

5.2.5 Turbulence Modelling- The challenge in any CFD Simulation is selecting the correct and appropriate Turbulence Model. The type of model chosen is highly dependent on the type of flow considered. The most popular turbulence models, utilized in the CFD community, are Direct Numerical Simulation (DNS), Large Eddy Simulation (LES) and Reynolds-Averaged Navier–Stokes (RANS) [16].

The DNS model requires a very large amount of time and computational power. So, for the sake of this research, it was not opted. LES method is usually applicable when there are large 3D volumes. This model is applicable for Open environmental simulations and not for Wind tunnel studies. The method most suitable for a Quasi 2D simulation study is the RANS method. And the specific type of RANS method opted is k-ε method because this approach provides faster and fairly accurate turbulence modelling [16].

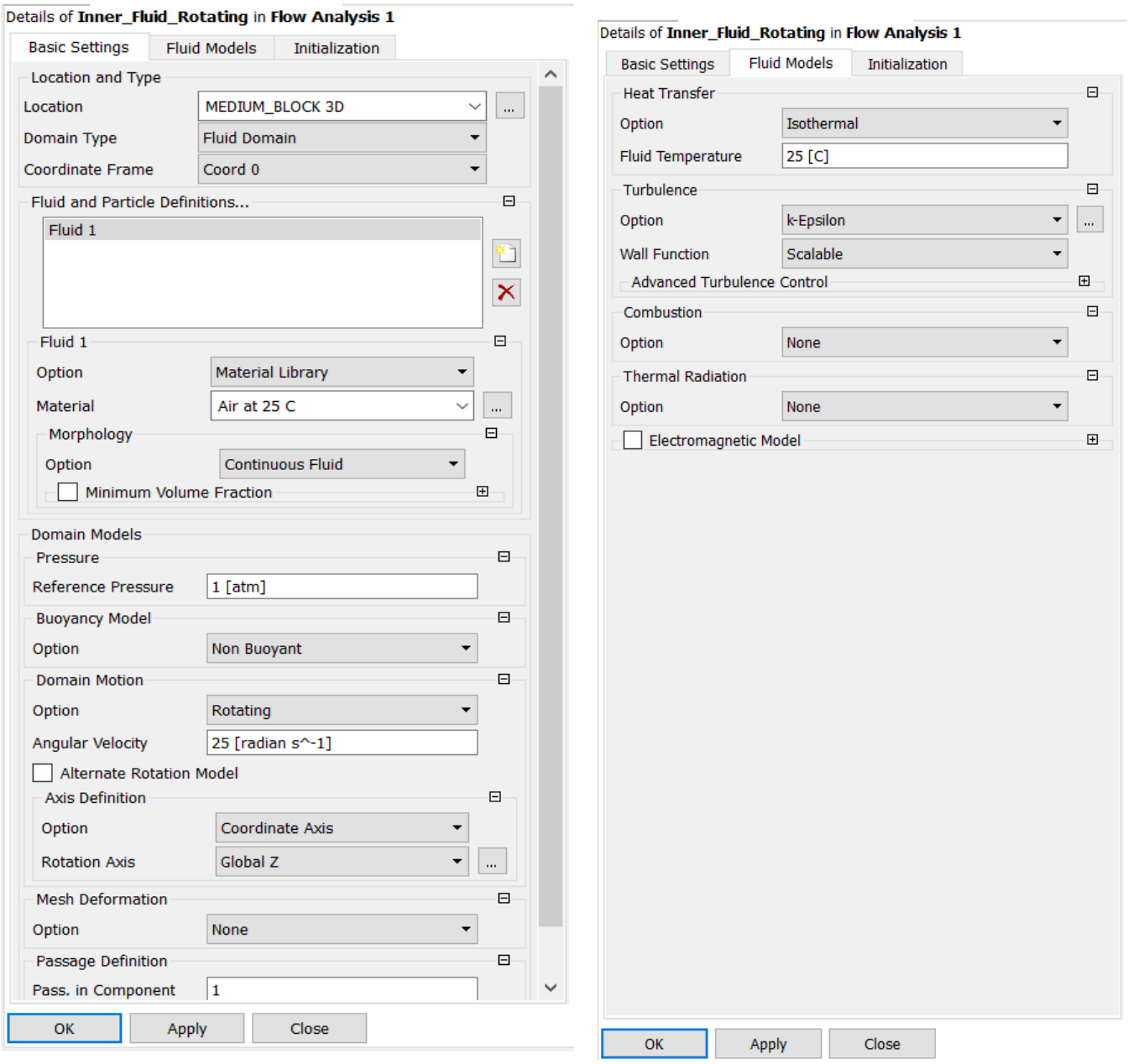

Figure 41 Settings for Rotating domains and Turbulence Modelling

The next step in Pre-Processing is the creation of Domain Interfaces. As it has been stated earlier that the geometry is formed of different meshes and it must be specified how these different meshes interact with one another. The interface must make sure that the similar surface is being selected from both the domains. As the study being performed is Transient in nature, therefore the pitch change is specified to 360 degree for both the meshes.

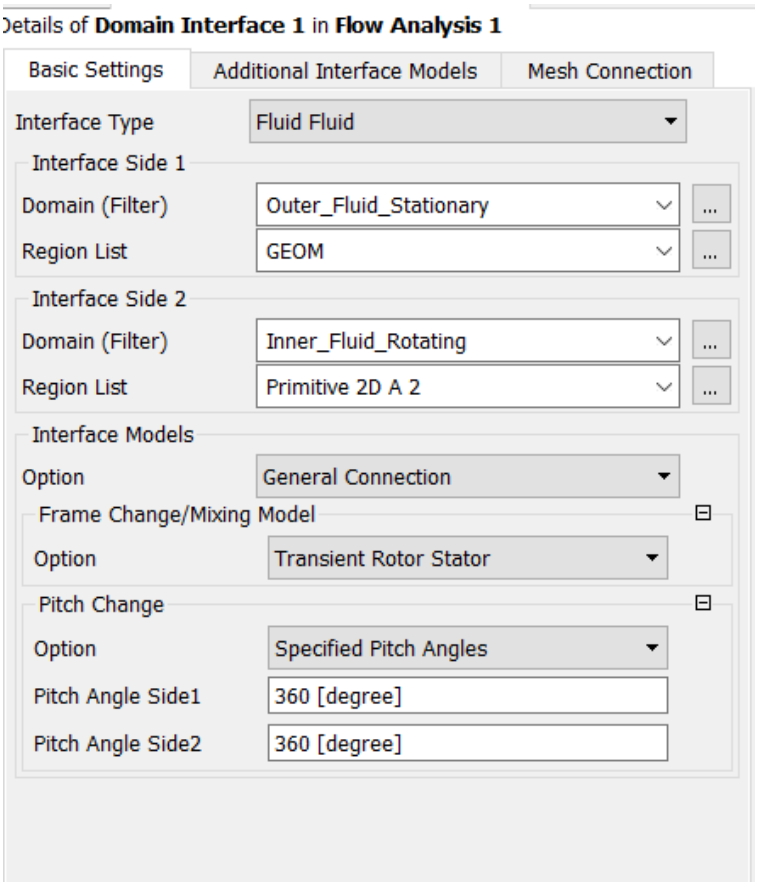

Figure 42 Settings for Domain Interfaces

After the domains and resulting interfaces are specified, next important step is to specify the Solver conditions and implement different monitors to extract data during the Main processing. Solver controls require modifying the convergence criterions and making sure that each result file is saved at individual Timestep progression. The number of iterations required to get convergence for one of the timestep is chosen after different experimental values of 700, 400, 100, 10 and 50. In the end, 50 iterations is chosen as the solution is converged enough after 50 iterations for analysis.

As the analysis based on the Torque results is of major importance to the study, Expressions pertaining to these are defined directly in the Pre-Processing. After the expressions of Forces and Torque are defined, these are added to the Output control so that these expressions can be extracted and can be seen directly in real time during the Main-Processing is in progress.

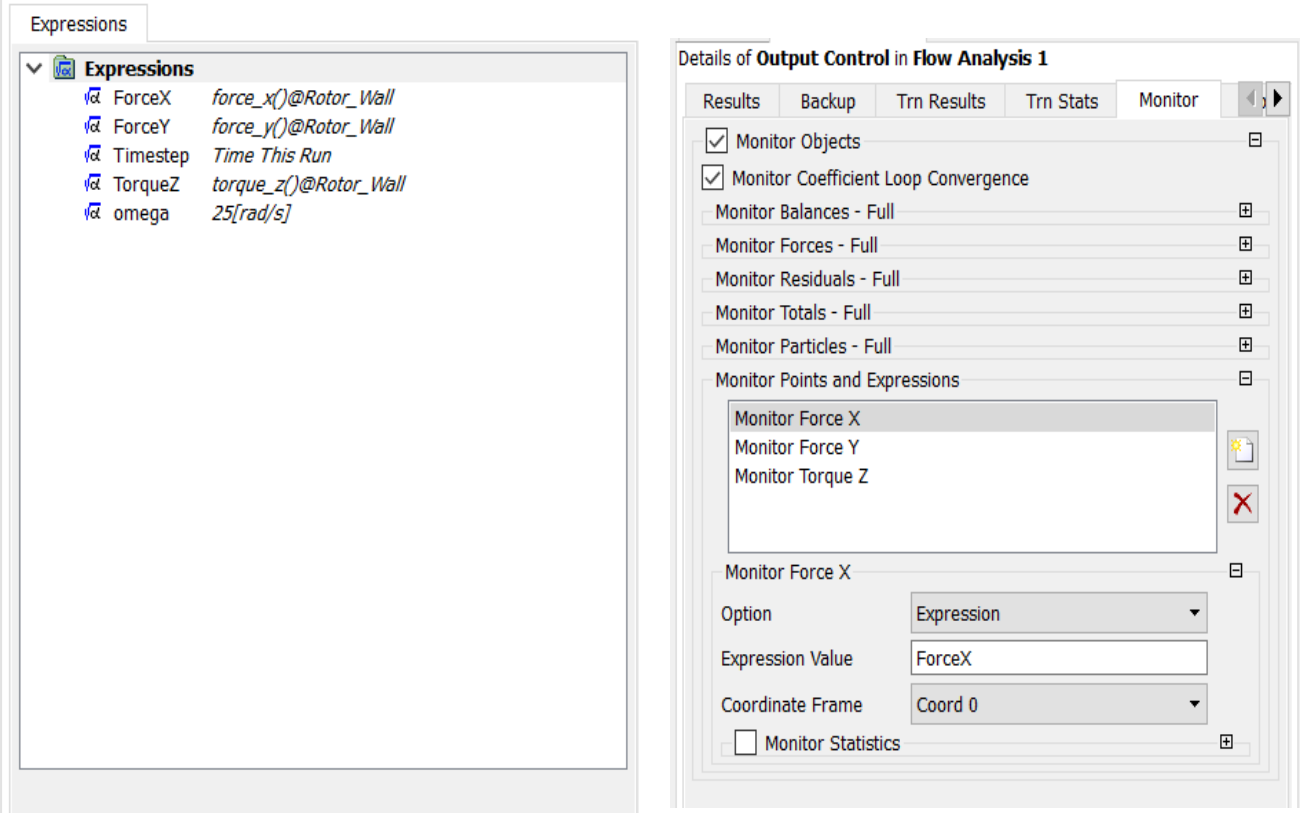

Figure 43 Settings for defining the Expressions and Setting up Monitors

5.2.6 Transforming mesh to implement Pitching- The underlying scope of this research is to investigate the effects of Constant and Variable pitching on the Torque output of the Rotor. In order to achieve that, the mesh containing the Airfoil is needed to transform by rotating it about the center of the airfoil. In this study, the effects of the constant pitch angle on the torque output in comparison to Unpitched rotor are considered [6]. The setup involves the rotation of the mesh by a certain specified amount and then running the Main processing on it. The angles opted for this research are between the range of -6.477deg and 22.477 deg. The effects of such pitch angles are expressed later in this thesis. After the comparison on the values of torque is presented, an analysis to figure out the equation for variable pitching is figured out.

$$-6.477 \leq \beta \leq 22.477$$

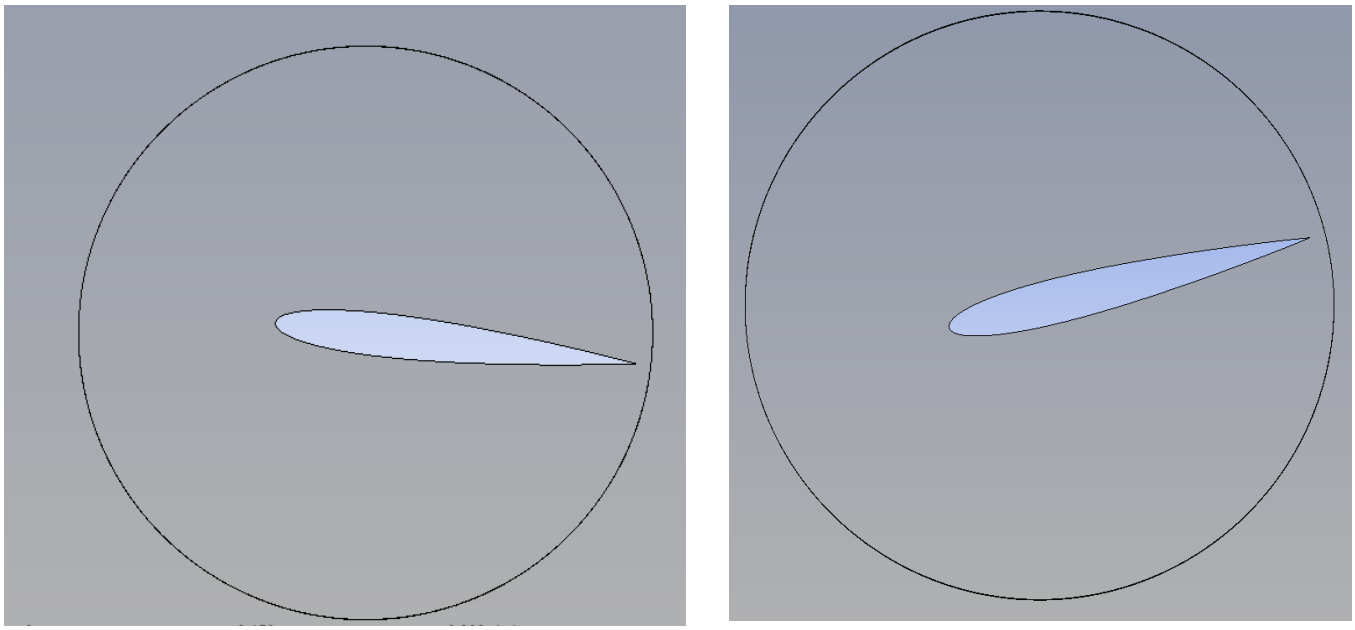

Figure 44 Mesh Rotation to acquire -6deg and 15deg Blade Pitch Angles

After the various Pre-Processing files have been generated, each corresponding to a specific blade pitch angle, Solver definition files are generated, and these can be run by the Main Processor to generate the simulation results.

5.2.7 Main Processing and Data Extraction- As the solutions are being computed by the Main Processor, the Expression monitors which were introduced in the Pre-Processing stage can be enabled and this gives us live progress of the Expressions which are of interest to the study. After the entire computation has been completed successfully, the data pertaining to the Expressions can be extracted directly by exporting the points from the graphs in the monitors from the CFX-Solver. This data can be exported as CSV file and can be analyzed to see the outputs pertaining to different test situations [8]. The analysis of data is performed in Microsoft Excel. A small snippet of Worksheet is attached in Appendix 3. This does not contain the entire Worksheet. These additional files are attached in a CD, the digital Appendix provided with copy of thesis. The curves of Forces acting on Airfoil in X and Y axis can be viewed in Appendix 5.

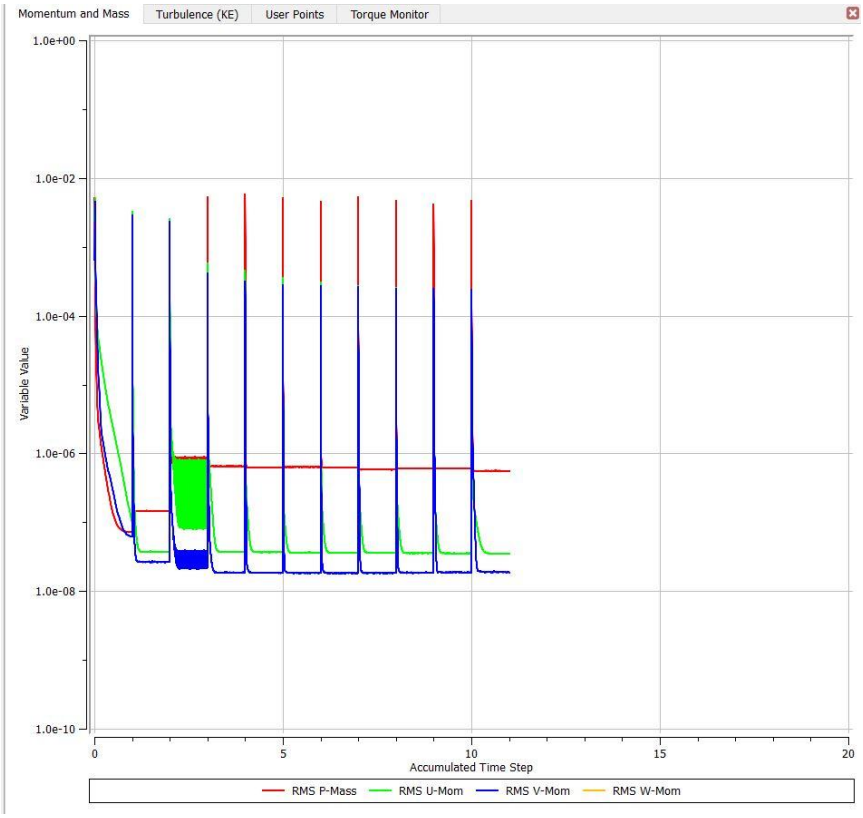

Figure 45 Main Processing displaying Convergence of Solution

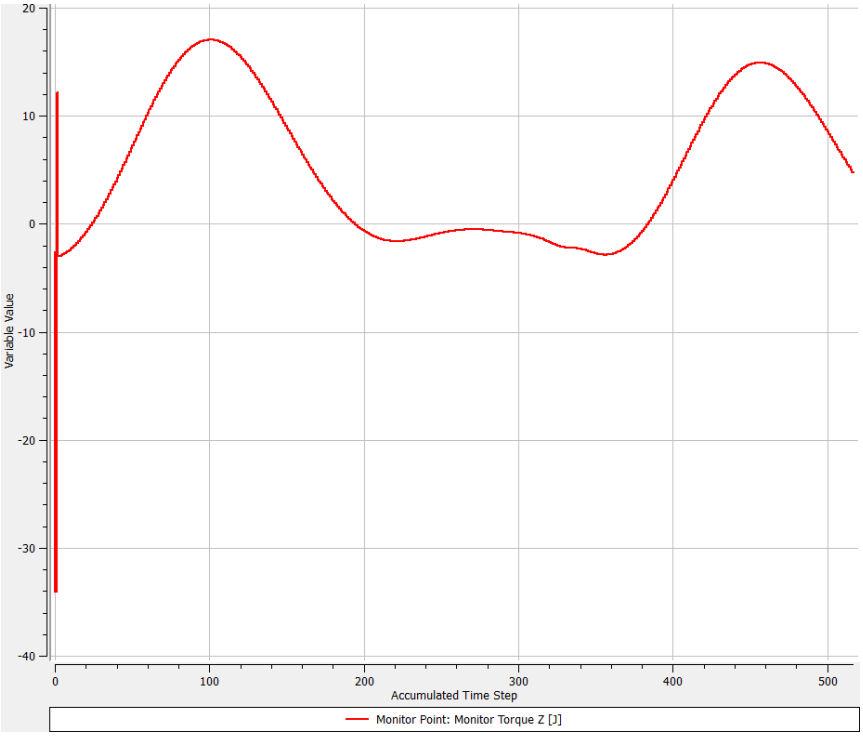

Figure 46 Torque Curve for Single Blade observed by Torque Monitor in Main Processing

5.2.8 Post Processing – Post Processing of Simulation results is also one of the most important steps. In this step, the visual and graphical representation of the results is carried about. Various tools such as Contour Plots, Graphs, Vectors and Simulation Videos can help us understand the results of Simulation in a more comprehensive manner.

In order to implement the Contours Plots of Velocity and Pressure, which are a standard practice in CFD analysis, a plane at the center of the Airfoil is introduced and each Contour is added to this Plane. The effects of flow can be visualized by the contours of Velocity or Pressure around the airfoil and across the different domains [8].

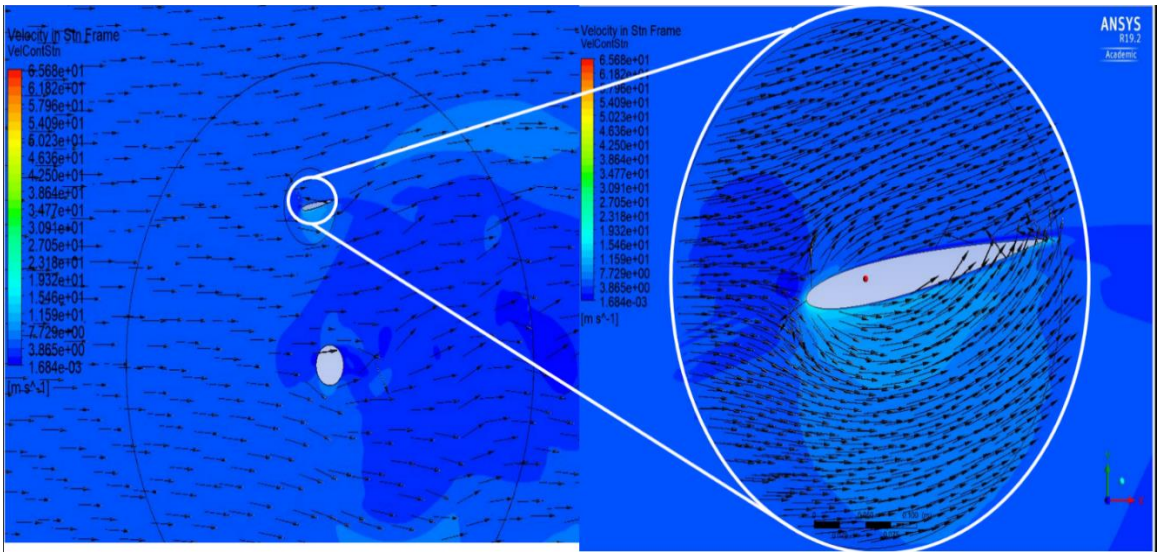

Figure 47 Flow Visualization around the Airfoil

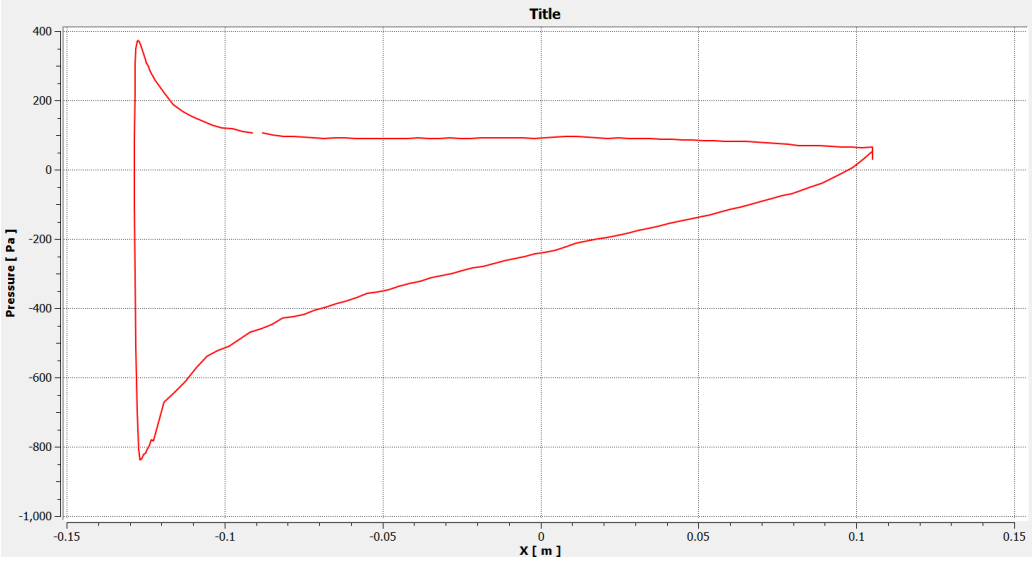

Figure 48 Pressure Chart around the Airfoil

5.3 Transient State Analysis with Quasi-2D Coarse Mesh Approach for 1 Bladed Rotor- This study is completed to elucidate the effects of the quality of the mesh on the Output of the Simulation. All the steps involved in this study are equivalent to the previous study, except the Mesh generation. The Pre-Mesh parameters are tinkered such that, a drastic reduction in the quality and size of mesh cells occurs. The number of divisions of Pre-Mesh edges are cut by half, in most cases. The results and comparisons of this approach can be seen in the Results Section of this thesis [12].

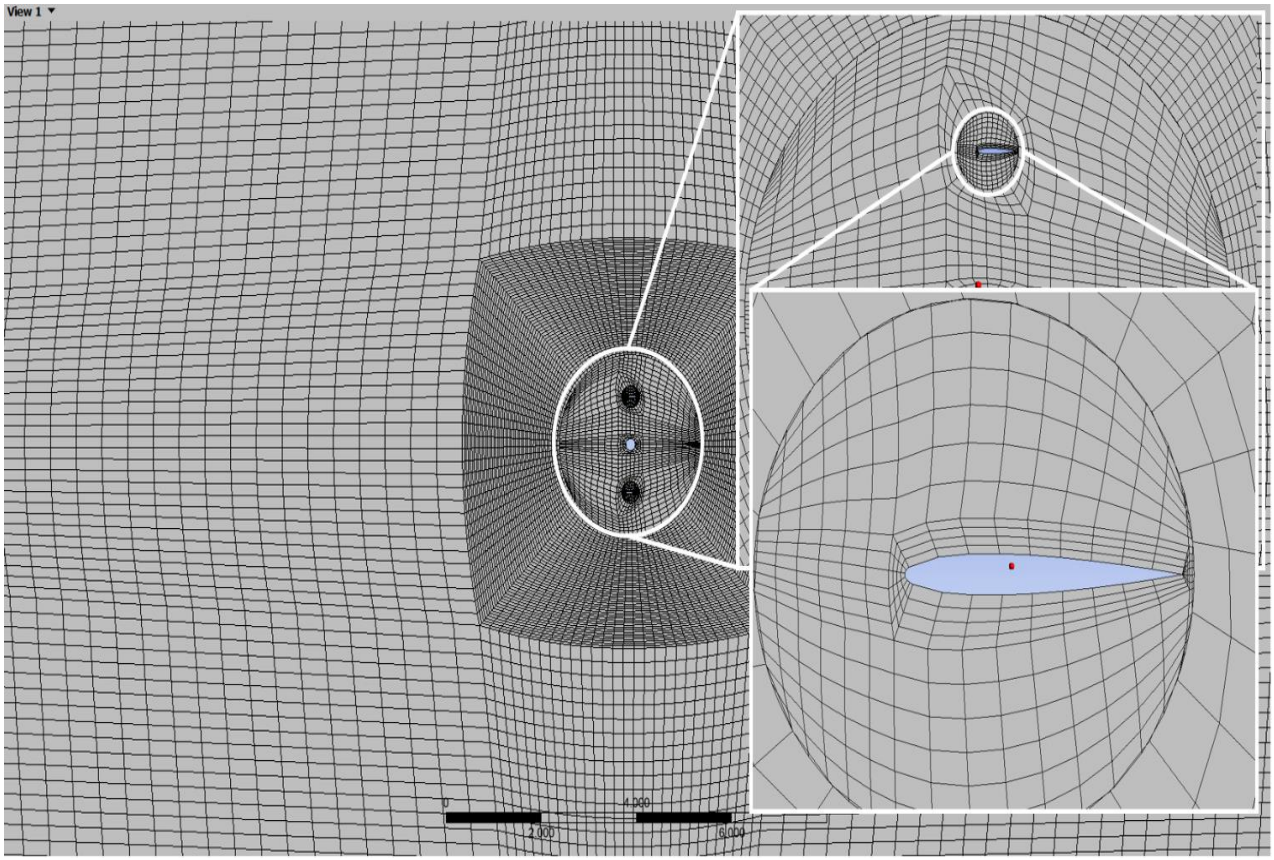

Figure 49 Visualization of a Coarse mesh around the Airfoil and other Domains

The number of mesh nodes in this version of run is only equal to 59,412 as compared to 149,584 nodes in case of Very fine mesh previously used in last study, which is less than half. The expected results would be a reduction in Torque and irregular and aberrant flow patterns around the airfoil.

5.4 Transient State Analysis with Quasi-2D Mesh Approach for Two Bladed Rotor – In this section of the research, the entire process of Simulation with Variable Pitching is performed on a modified rotor with 2 blades instead of one blade. The effects of an Optimized Pitching angle, which is derived from analysis of Single Blade system, is employed and results from this study are reported in upcoming Chapter. In practice, Geometry is modified by copying and transforming the Airfoil and spacing it by 180 degrees about the axis of rotation. The domains are meshed, and Solver runs as normal. The total torque is an addition of Torques from the two Blades.

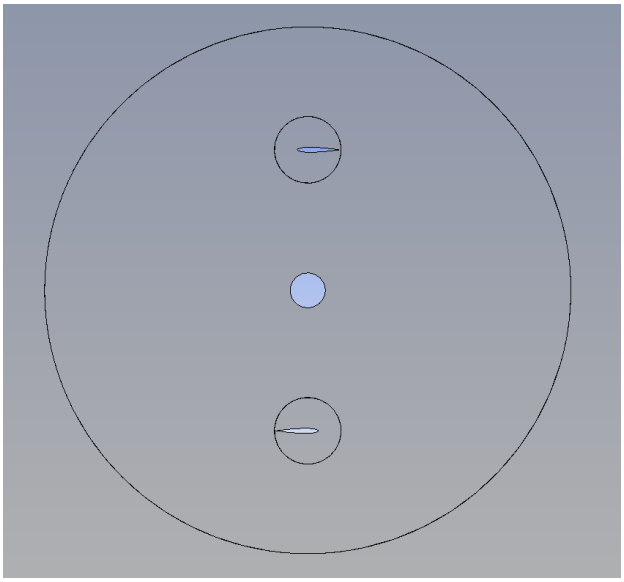

Figure 50 Geometry of a Two Bladed Rotor

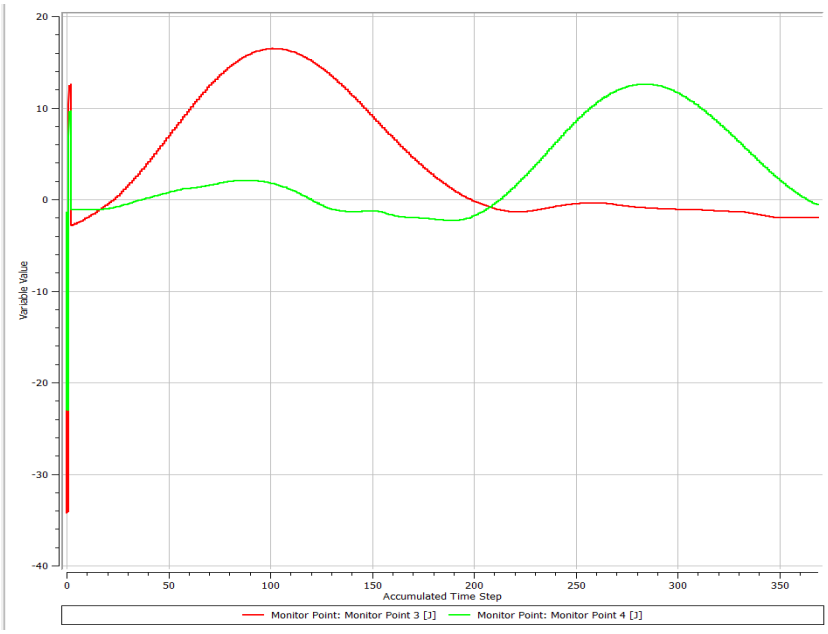

Figure 51 Torque Curves of two Blades visualized from Solver Window

Chapter 6

6. RESULTS AND DISCUSSIONS

The aim of this chapter is to shed light on the outcomes of this study. There were numerous objectives which were stated at the beginning of this thesis. During the course of this research, different studies and runs were performed, each with a specific objective in sight. This chapter is sectioned, keeping each objective as separate point of enquiry. The data has been carefully combed over to make sure that the final results represent the expected outcomes from the Simulations.

6.1 Angle of Attack: As stated in an earlier chapter, the AOA for a VAWT is not constant and it varies as a function of Azimuthal angle θ. The results depicted that the AOA is a close approximation of the Sin curve but does not peak exactly at 90deg Azimuth angle [5]. The value of AOA ranges between 14.477deg to -14.477deg. The result for this is represented by the following Figure 52.

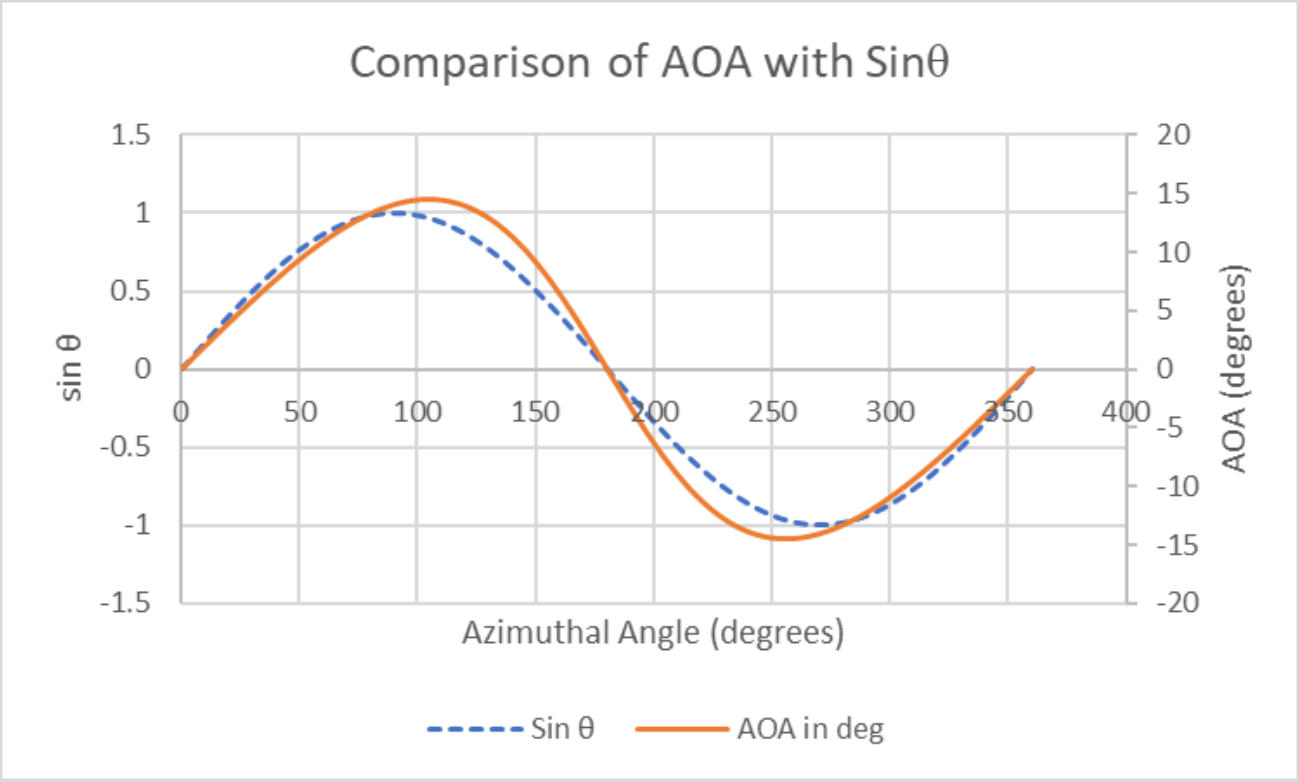

Figure 52 Angle of Attack and sinθ for Unpitched Rotor

6.2 Lift Force for NACA 0012 Airfoil- As it is mentioned earlier in the thesis that the Airfoil selected for the research is NACA 0012. In this graph, the results of the angle of attack on the Lift coefficient can be seen. This graph later helps in answering at which Azimuthal angle in a rotating frame of reference, will the Torque acquire a maximum value [17]. The value of torque is greatly influenced by Lift force. Therefore, a graph of Cl is developed by simulating the different AOA's for NACA 0012.

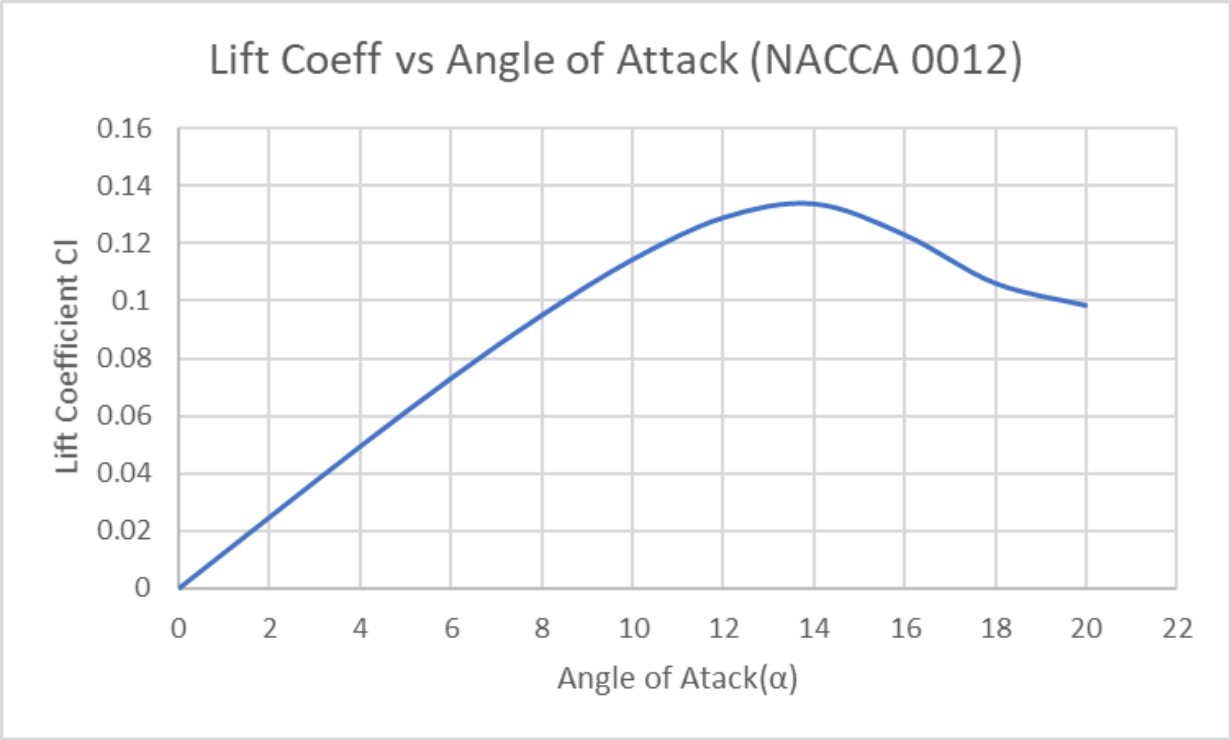

Figure 53 Lift Coefficient vs Angle of Attack

6.3 Torque/Cpr from Unpitched Transient Analysis of 1 Bladed System- The transient study yielded the most accurate results when compared to expectations and Literature. So, most credibility is awarded to studies with Transient Analysis method. In the following graph, the Torque and Cpr of a single bladed system is presented. The Cpr is the dimensionless quantity that is derived by dividing the Torque from rotor by Wind power [1]. From this graph, it is clear that the maximum Torque in one revolution occurs at 104deg Azimuthal Position. This is the location where the Local AOA is equal to 14.45deg and where the maximum Lift force occurs for a NACA 0012 airfoil [8].

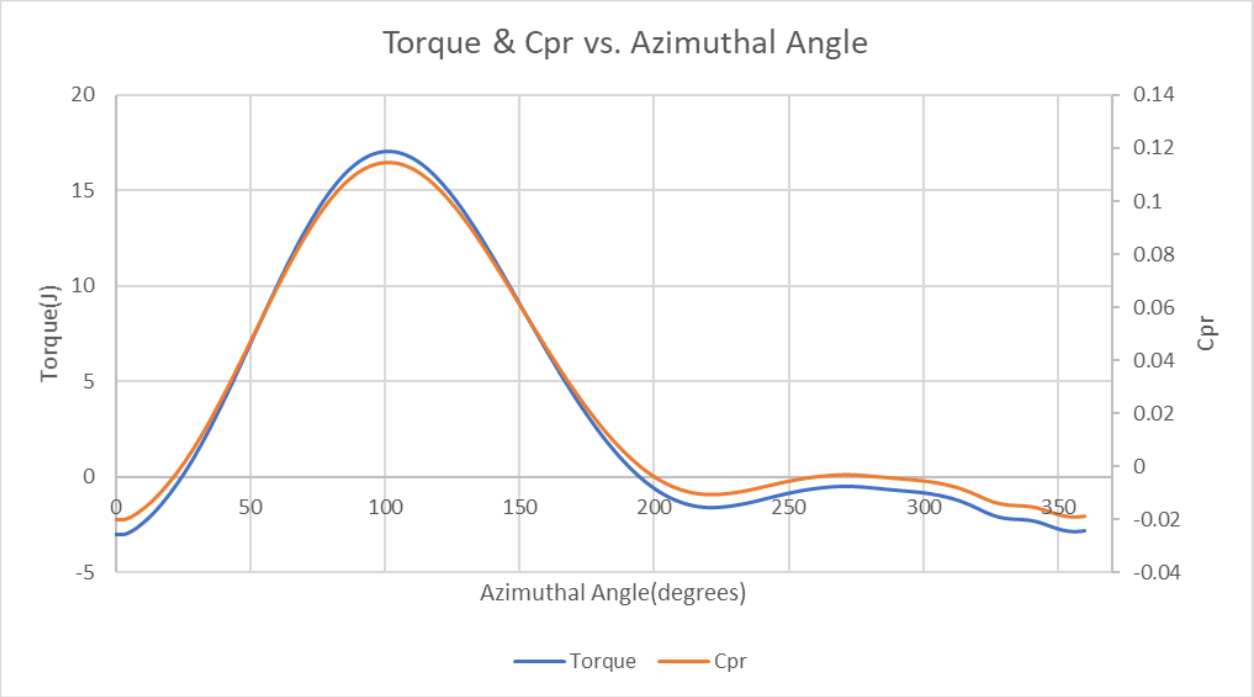

Figure 54 Torque and Rotor Power Coefficient vs Azimuthal Angle

6.4 Single Blade Constant Pitch- In order to figure out a variable Pitching equation that results in increased Torque when compared to an Unpitched system, constant pitch studies are completed, and the results of these studies are expressed in following figures 55 to 58. From these graphs, it is clear that not one constant Pitching angle can increase the Torque considerably and therefore an optimized approach is necessary. The constant Pitch angle varies from -6.477 deg to 22.477 deg. As all the values in one graph would be very chaotic, the curves are split up in different graphs. In order to make the comparisons easy and legible from graphs, only curves for Torque are considered. The total Torque available as a result of each constant Pitching is reported in the Table 3 below and the percentage increase or decrease compared to Unpitched condition [6].

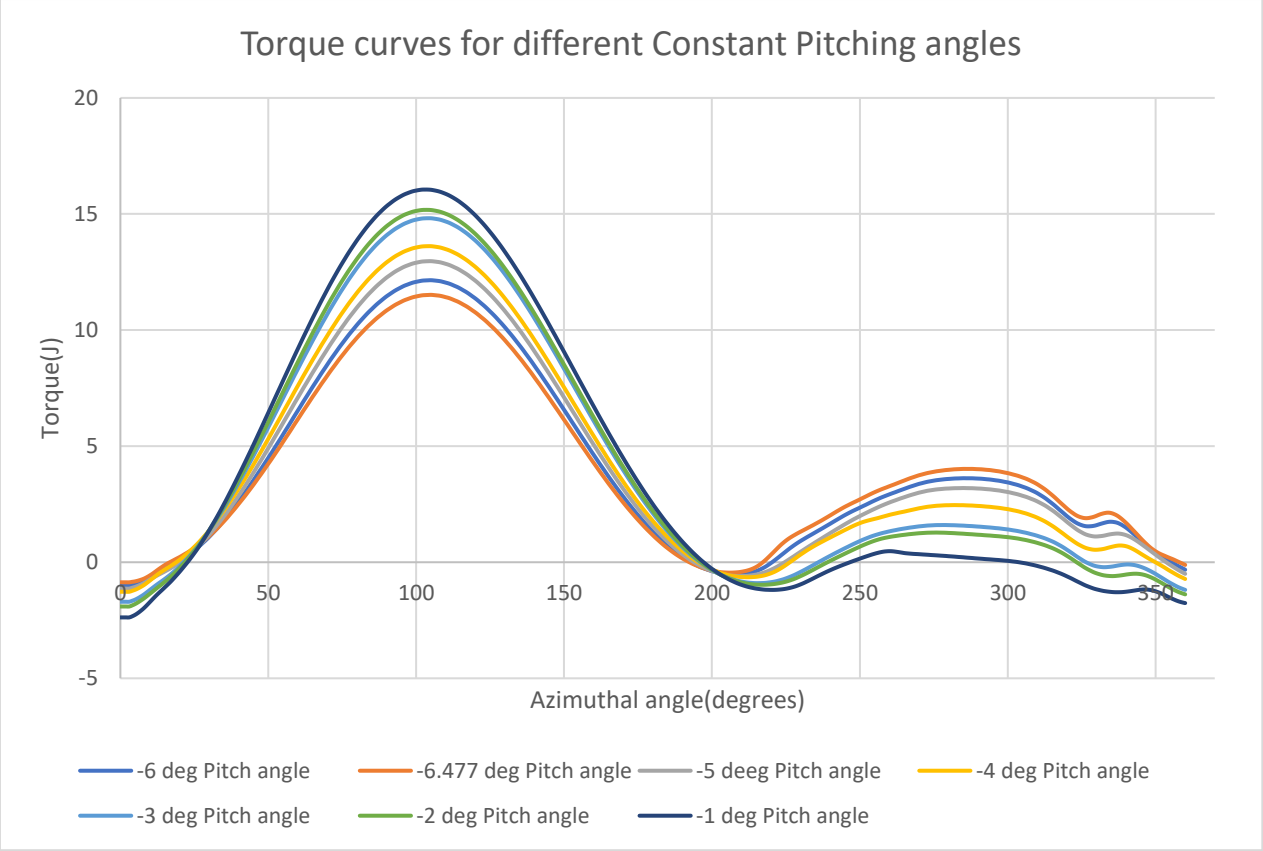

Figure 55 Torque curves for Constant Pitch angles from -6.477deg to -1deg

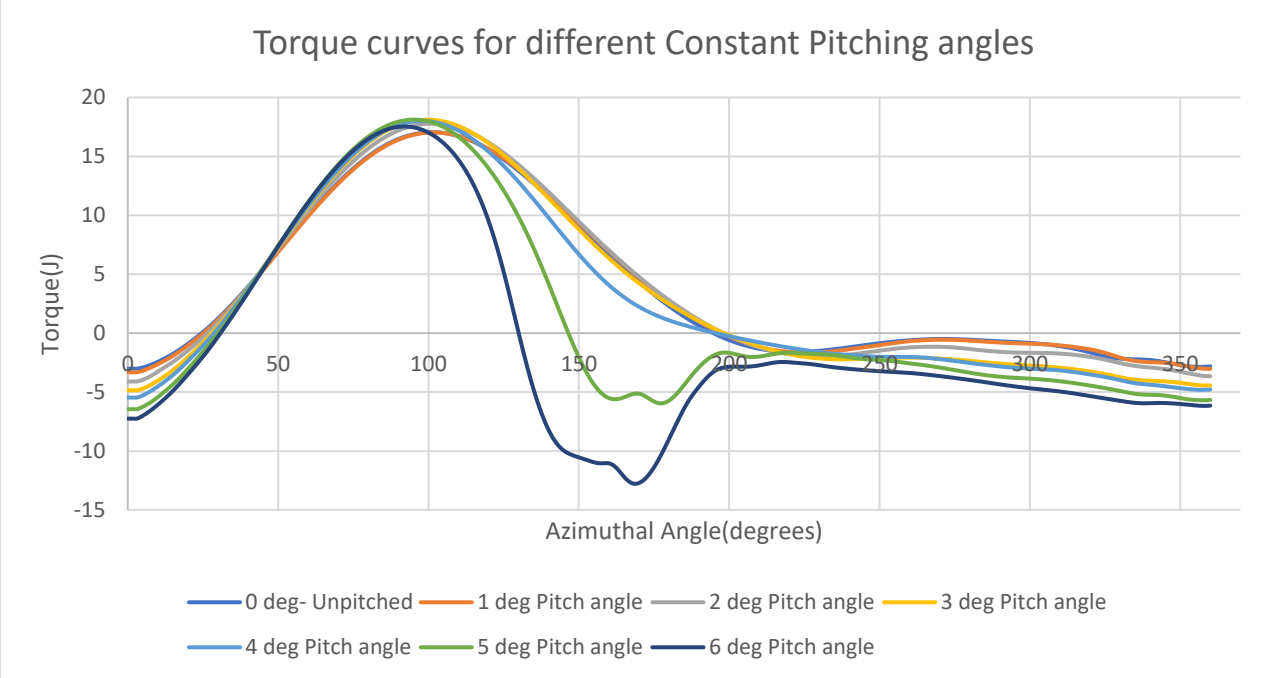

Figure 56 Torque curves for Constant Pitch angles from 0deg to 6deg

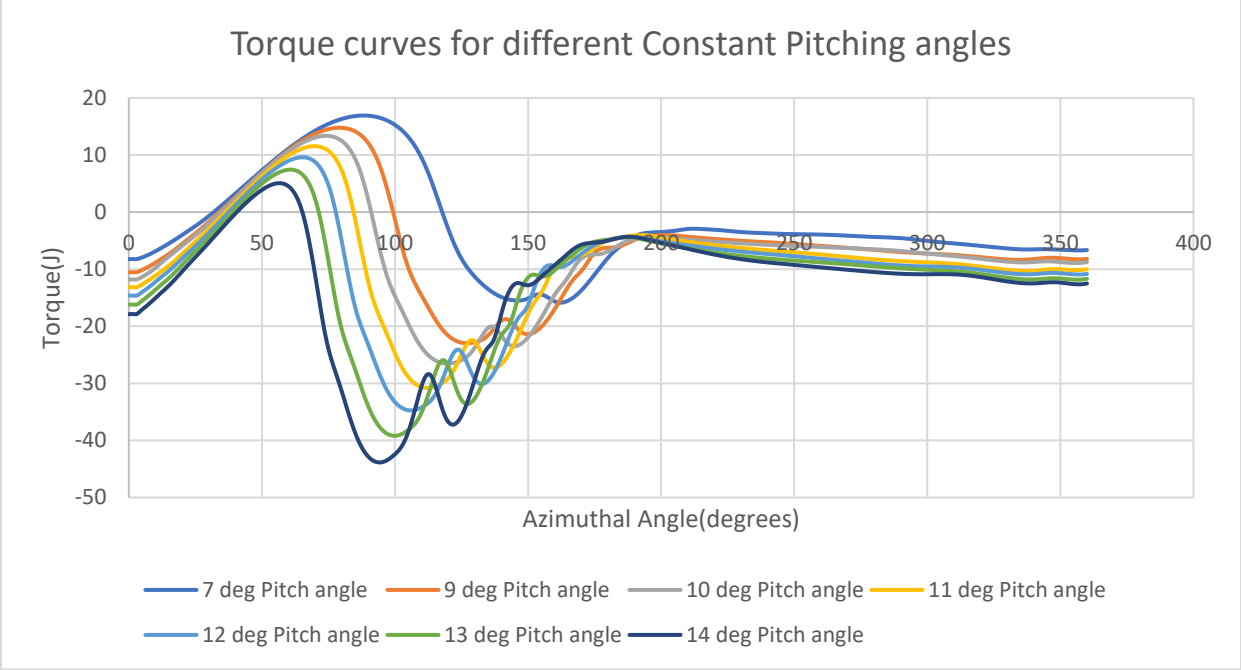

Figure 57 Torque curves for Constant Pitch angles from 7deg to 14deg

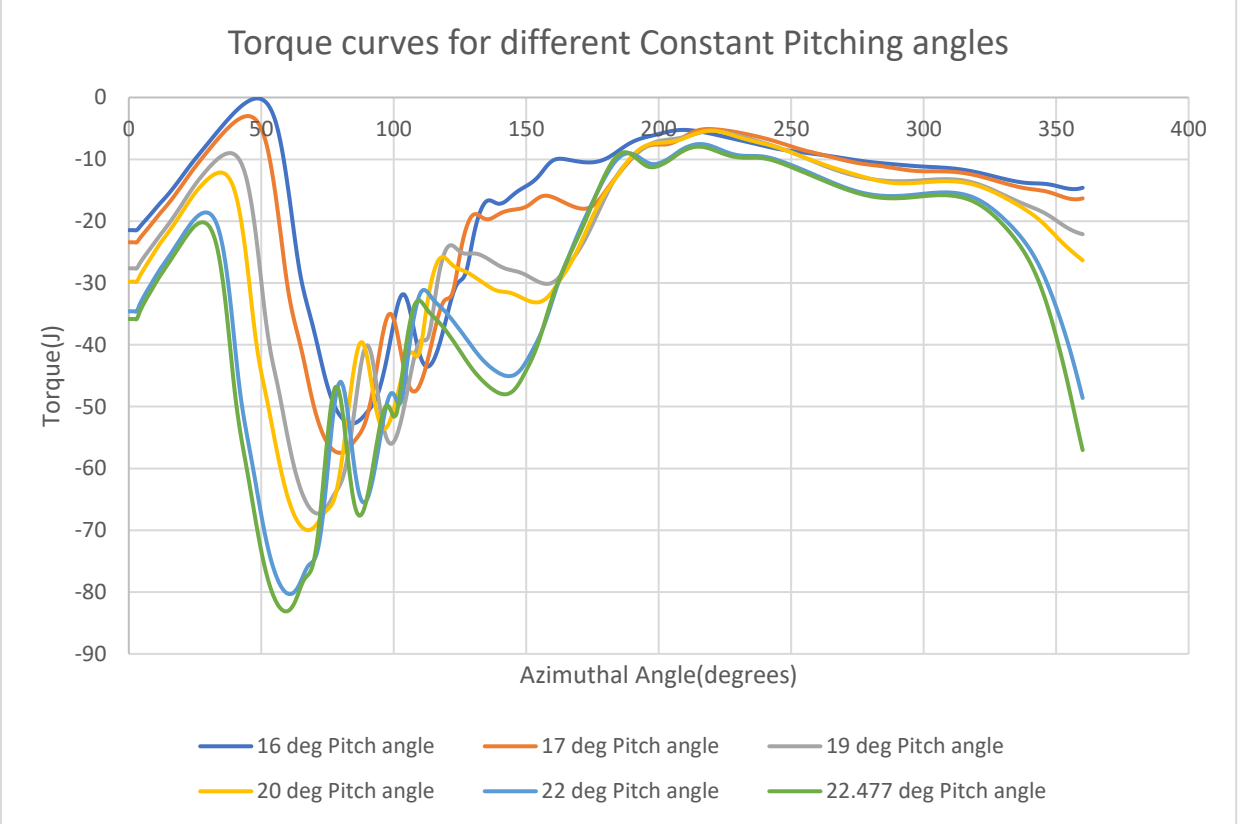

Figure 58 Torque curves for Constant Pitch angles from 16deg to 22.477deg

Table 3 Comparison of Total Torque and percentage change from Unpitched for different Constant Pitching Angles

Pitching Angle	Total Torque (J)	Percentage change than Unpitched
-6.477 deg	1415.79192	+3.1%
-6 deg	1421.697	+3.5%
-5 deg	1456.851	+6.1%
-4 deg	1464.525	+6.6%
-3 deg	1475.327	+7.4%
-2 deg	1472.224	+7.2%
-1 deg	1456.243	+6.0%
Unpitched	1373.3102	0%
1 deg	1381.59	+0.6%
2 deg	1345.772	-2.0%
3 deg	1194.634	-13.0%
4 deg	1055.978	-23.1%
5 deg	456.2805	-66.7%
6 deg	-265.079	-119.3%
7 deg	-846.499	-161.6%
9 deg	-2059.84	-249.9%
10 deg	-2539.29	-284.9%
11 deg	-3125.44	-327.6%
12 deg	-3668.6	-367.1%
13 deg	-4211.42	-406.7%
14 deg	-4743.74	-445.4%
16 deg	-5766.54	-519.9%
17 deg	-6522.78	-574.9%
19 deg	-8093.27	-689.3%
20 deg	-8580.14	-724.8%
22.477 deg	-10976	-899.2%

From the Table 3, it is clear that if a single Constant Pitch angle is required, the Best choice would be to select -3deg Pitch angle as this configuration provided the most increase, 7.4% increment of Torque when compared to an Unpitched configuration.

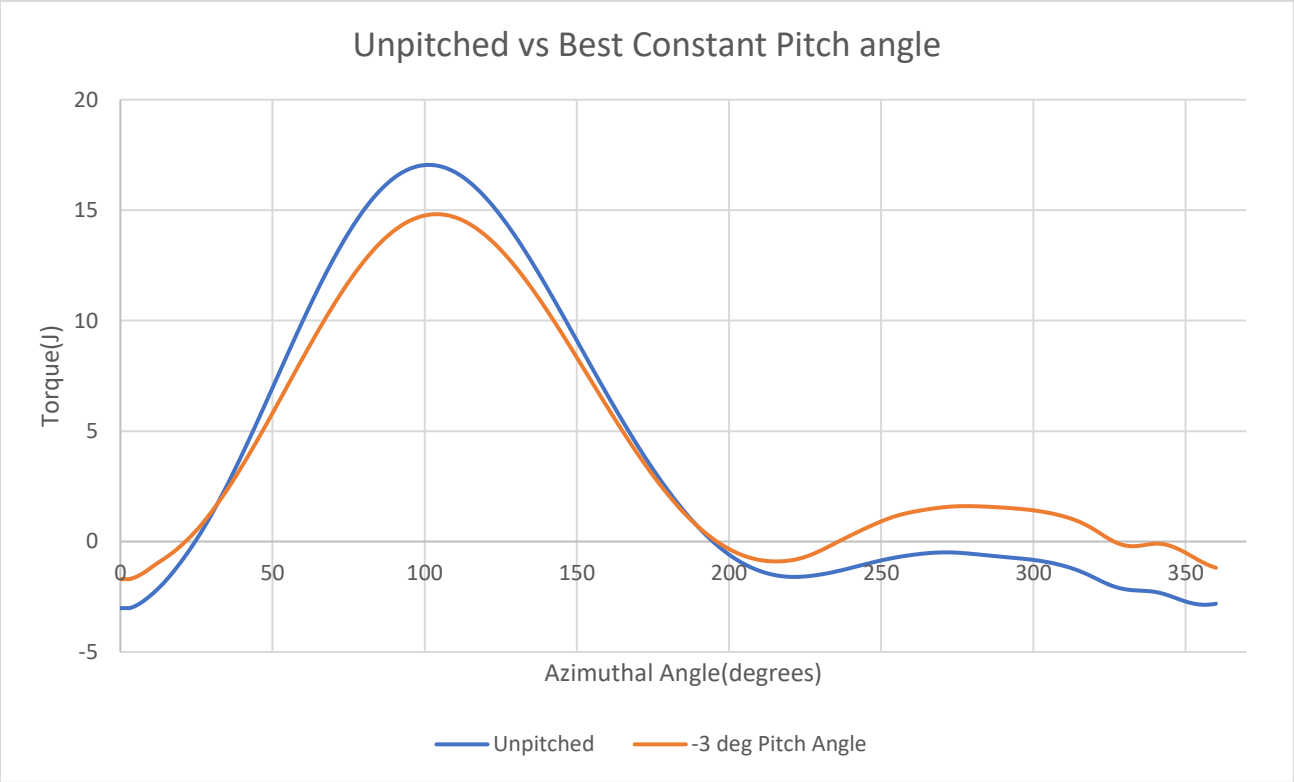

Figure 59 Torque Comparison for Best Constant Pitch angle(-3deg) and Unpitched Rotor

6.5 Single Blade Optimized Pitch- As the scope of this section is to figure out an equation, which when followed, should increase Torque more than any one of the constant Pitching configurations. To achieve this, the analysis of the Torque data is done and maximum Torque values corresponding to each Azimuthal position is noted and according to this analysis, the Torque curve for optimized pitching is given.

$$\boldsymbol{Optmised\ Pitching\ Angle} = [-6.477°]_{0°-23°} + [-4°]_{24°-29°} + [-1°]_{30°-33°} + [0°]_{34°-42°} + [2°]_{43°} + [4°]_{44°-46°} + [5°]_{47°-97°} + [3°]_{98°-117°} + [2°]_{118°-196°} + [3°]_{197°-201°} + [4°]_{202°-203°} + [-6.477°]_{204°-360°}$$

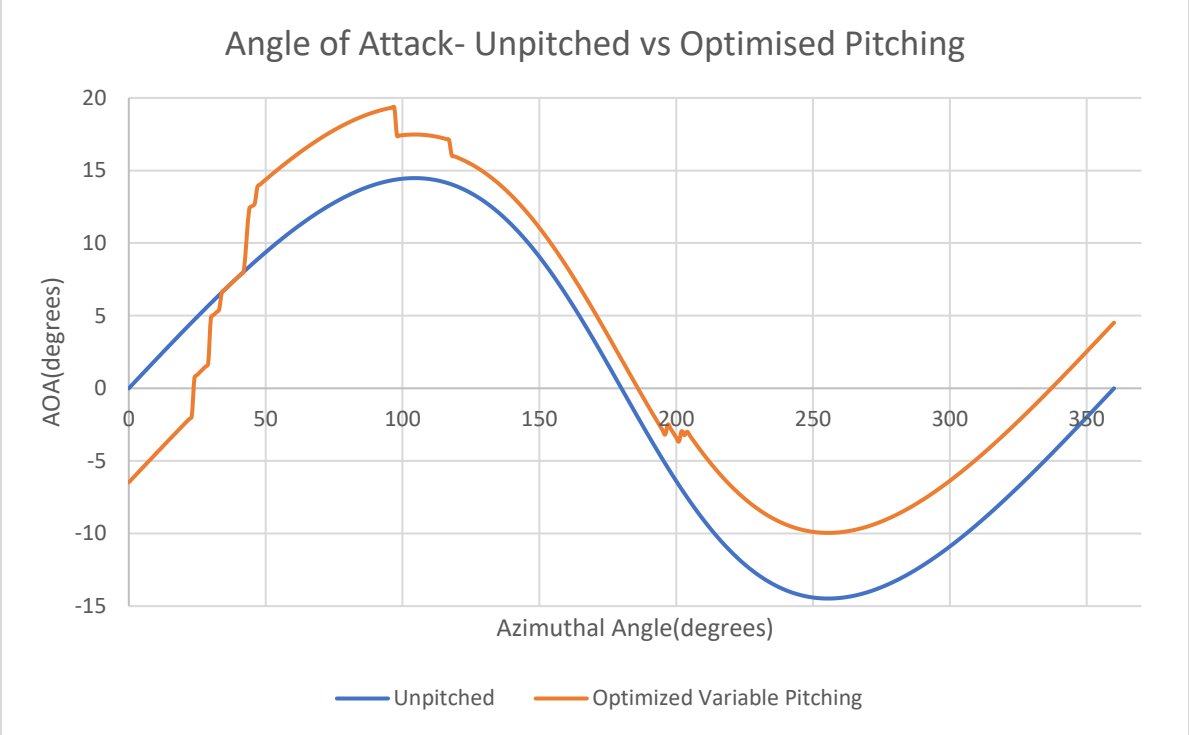

Figure 60 Angle of Attack (Unpitched) vs Optimized Angle of Attack (by Optimized Blade Pitching)

When this equation is followed for the specified Azimuthal angle ranges, the Torque is increased considerably, and Figure 61 represents that increase in Torque.

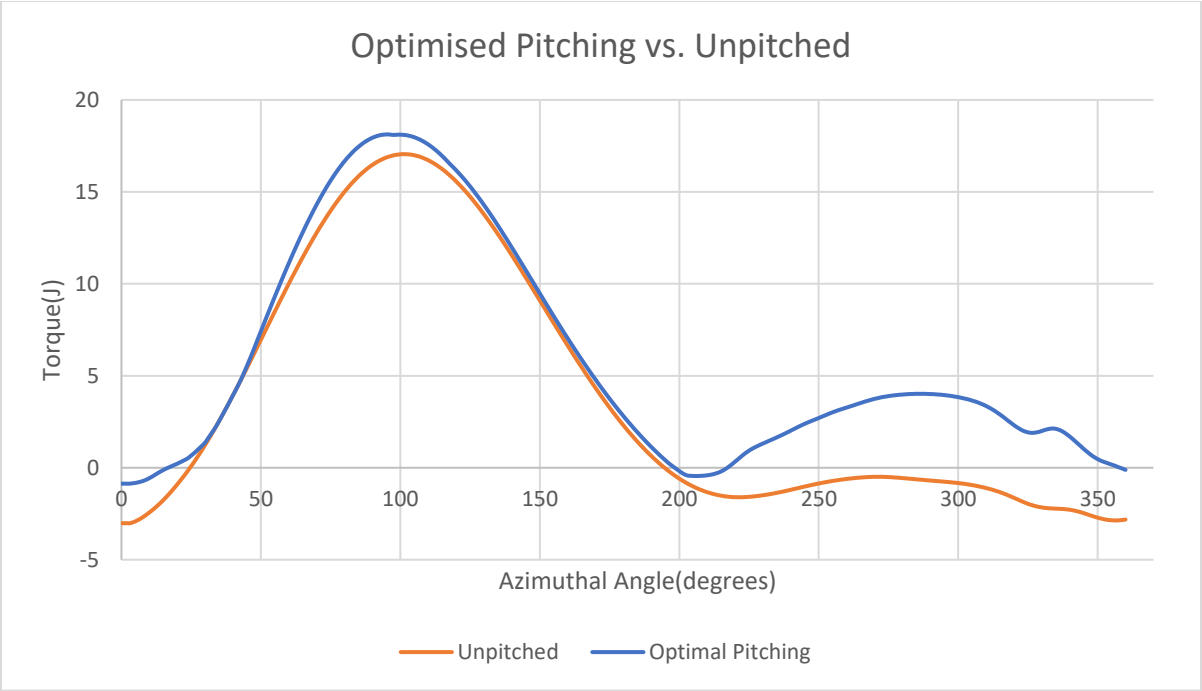

Figure 61 Comparison of Torque for Unpitched and Optimized Variable Pitching Approach

Table 4 Total Torque and percentage change by Optimized Variable Pitching Approach

Pitching Angle	Total Torque (J)	Total Unpitched Torque (J)	Percentage change than Unpitched
Optimized Pitching following the analyzed Equation	2097.9678	1373.3102	+52.8%

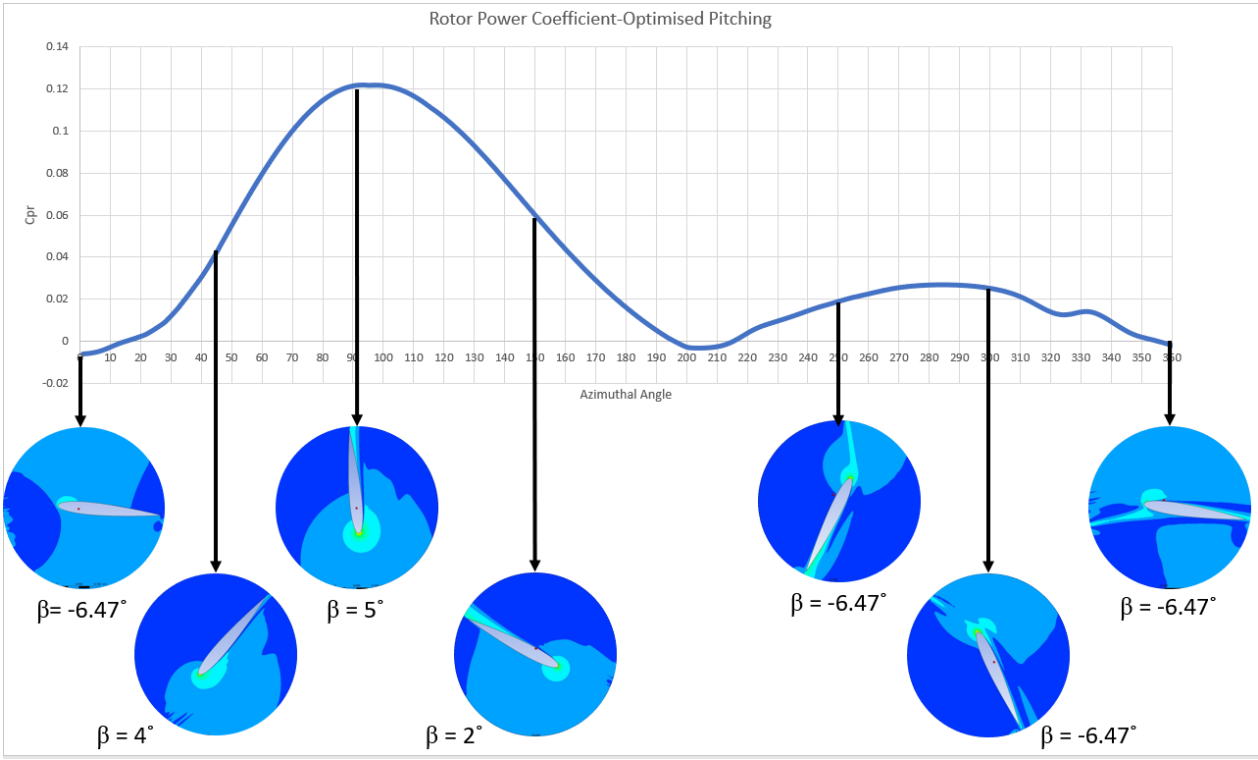

Figure 62 Rotor Power Coefficient along with Blade Pitch visualization for Optimized Variable Pitching

6.6 Two Blades Optimized Pitching- After the results from the Single blade Variable Pitching are analyzed, the equation so developed is deemed fit to be applied to a system of Two bladed rotor. In a way, this approach is also a verification of the Equation. In theory, the pitching approach when applied to 2-Bladed system should also increase the Torque output by considerable amount. As Two blades are introduced in the equation, care must be taken that each blade assumes its Optimized pitching angle for respective Azimuthal orientation. The Torque from each individual blade is recorded by Solver and these

can be added to give us the overall Torque by the Rotor system. The graph which emerges from this study is presented in Figure 63.

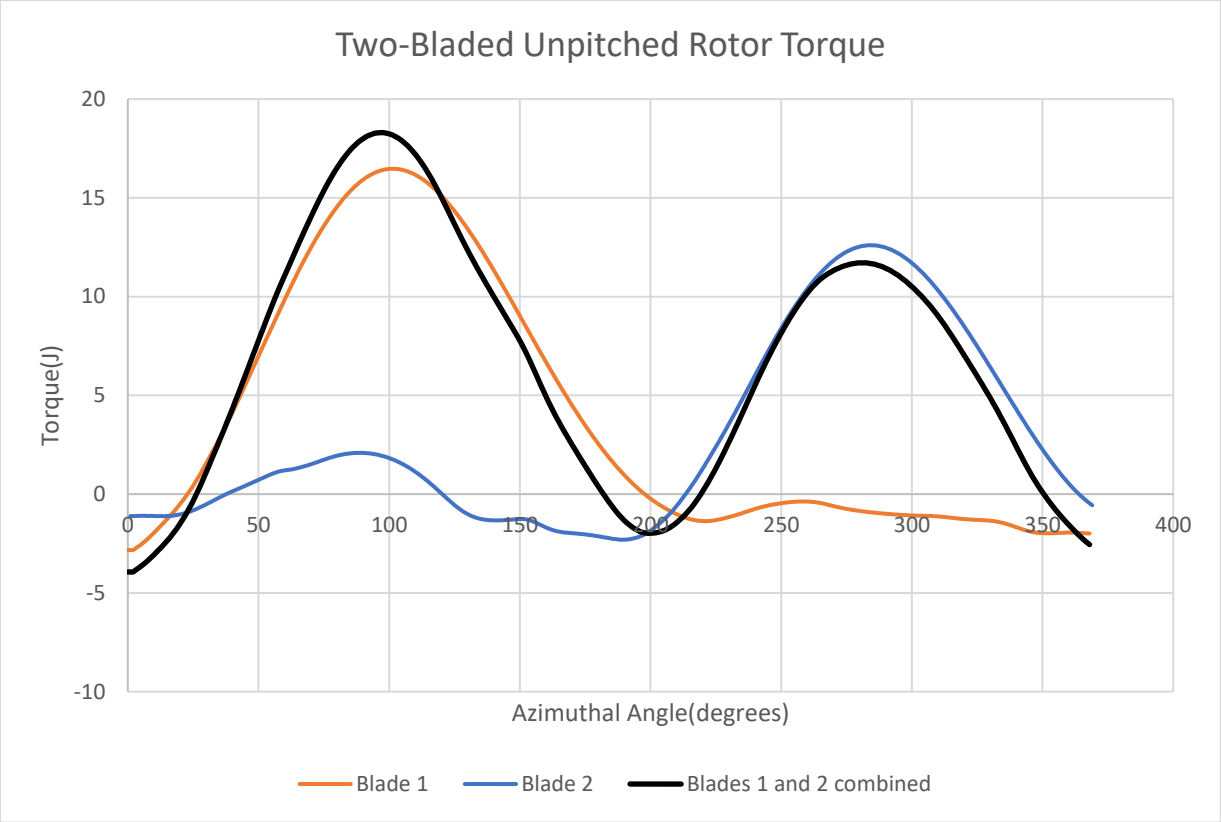

Figure 63 Torque Curves of Individual Blades and Combined Torque for 2-Bladed Rotor

In order to ensure the Optimized pitching, the following Table 5 helped in figuring out which sets of combinations must be performed to attain the highest value of Torque. As the two rotors are separated by 180deg physically, each experience different Local AOA at the same time. So, considering this, each Blade gets its optimized pitching angle according to the equation derived earlier.

Table 5 Mesh Combinations to ensure each Blade exists at Optimized Blade Pitching position

Blade 1		**Mesh Combination**	**Blade 2**	
Azimuthal Angle	*Optimized Pitch Angle*		*Azimuthal Angle*	*Optimized Pitch Angle*
0˚-16˚	-6.477˚	**-6.477˚ & 2˚**	180˚-196˚	2˚
17˚-21˚	-6.477˚	**-6.477˚ & 3˚**	197˚-201˚	3˚
22˚-23˚	-6.477˚	**-6.477˚ & 4˚**	202˚-203˚	4˚
24˚-29˚	-4˚	**-4˚ & -6.477˚**	204˚-209˚	-6.477˚
30˚-33˚	-1˚	**-1˚ & -6.477˚**	210˚-213˚	-6.477˚
34˚-42˚	0˚	**0˚ & -6.477˚**	214˚-222˚	-6.477˚
43˚	2˚	**2˚ & -6.477˚**	223˚	-6.477˚
44˚-46˚	4˚	**4˚ & -6.477˚**	224˚-226˚	-6.477˚
47˚-97˚	5˚	**5˚ & -6.477˚**	227˚-277˚	-6.477˚
98˚-117˚	3˚	**3˚ & -6.477˚**	278˚-297˚	-6.477˚
118˚-196˚	2˚	**2˚ & -6.477˚**	298˚-376˚ (16˚)	-6.477˚
197˚-201˚	3˚	**3˚ & -6.477˚**	17˚-21˚	-6.477˚
202˚-203˚	4˚	**4˚ & -6.477˚**	22˚-23˚	-6.477˚
204˚-209˚	-6.477˚	**-6.477˚ & -4˚**	24˚-29˚	-4˚
210˚-213˚	-6.477˚	**-6.477˚ & -1˚**	30˚-33˚	-1˚
214˚-222˚	-6.477˚	**-6.477˚ & 0˚**	34˚-42˚	0˚
223˚	-6.477˚	**-6.477˚ & 2˚**	43˚	2˚
224˚-226˚	-6.477˚	**-6.477˚ & 4˚**	44˚-46˚	4˚
227˚-277˚	-6.477˚	**-6.477˚ & 5˚**	47˚-97˚	5˚
278˚-297˚	-6.477˚	**-6.477˚ & 3˚**	98˚-117˚	3˚
298˚-360˚	-6.477˚	**-6.477˚ & 2˚**	118˚-180˚	2˚

As a result of applying the Pitching approach reported in Table 5, the Torque outcome of the 2 Bladed system is bound to increase. The results are expressed in Figure 64 and Table 6.

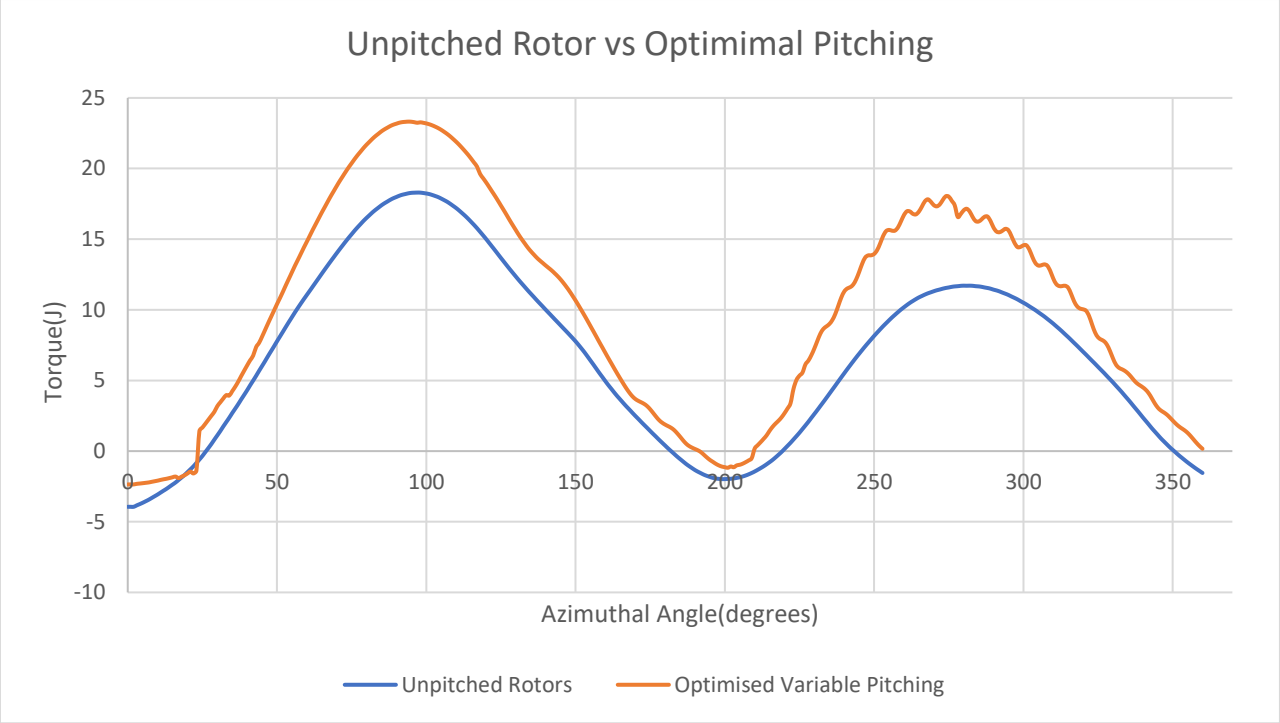

Figure 64 Torque Curves for Unpitched 2-Bladed Rotor vs Optimized Blade Pitch 2-Bladed Rotor

Table 6 Total Torque and percentage change than Unpitched 2-Bladed Rotor

Pitching Angle	Total Torque (J)	Total Unpitched Torque (J)	Percentage change than Unpitched
Optimized Pitching following the analyzed Equation	3613.7930	2439.3554	+48.2%

The increment of 48.2% is high enough to justify the application of the Optimized Variable Pitching approach to a 2-Bladed system. One thing to keep in mind in a system with multiple rotors is the TSR. In this research, the TSR is kept as 4 and as a result, the airfoils rotate faster than the Air mass can replenish and thus, the first airfoil travels through the turbulent Airflow which is left as wake by the second Airfoil [7]. In this case, this phenomenon can be seen when the first Airfoil travels through the Azimuthal positions of approximately 230deg and till the rotation completes i.e. 360deg. This effect can be seen clearly from the graph and this is the reason of the wavy nature of the Torque curve in downwind travel of the revolution. This can be seen from the figure 65 too and can be clearly visualized in a Simulation animation.

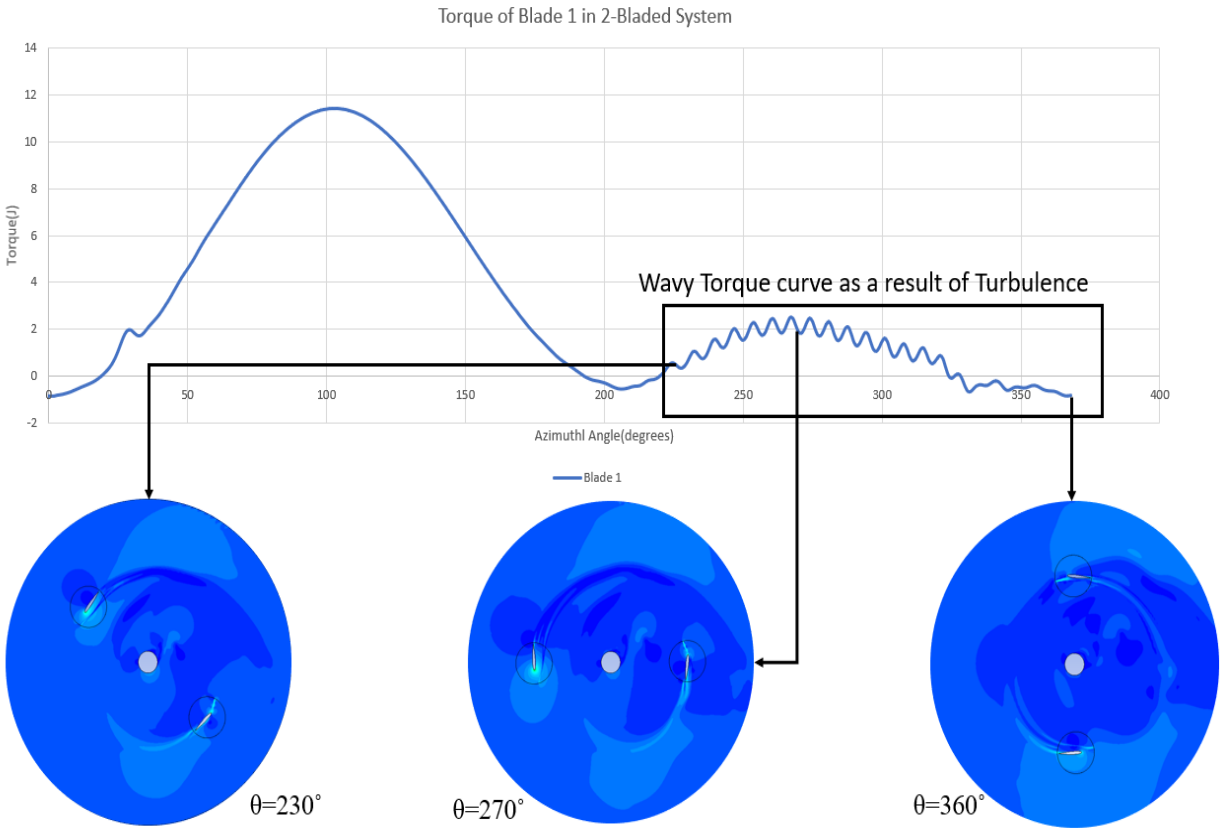

Figure 65 Turbulence due to Wake effects and Visualization at Azimuthal Positions

Another one of the observations made in the runs of two bladed system was a small streak of unexpected disturbance at the interface of domains containing the Airfoil and Fluid around it. Upon Investigation, the reason was concluded to be a minute overlap in the two meshes, due to a small deformity in the mesh which causes the overlap to be viewed as a ‘’Wall’’ in the Solver run. However, this does not and should not cause any effects on the quality of the results because this phenomenon is at a quite enough distance away from any part of the Airfoil and the resolution of mesh near the Airfoil ensure that the effects are not perpetrated. The prospective area of interest is near the surface of the Airfoil, where all the Expressions are defined and measured. As the location of disturbance is too far to cause any flow pattern changes, it is ruled out.

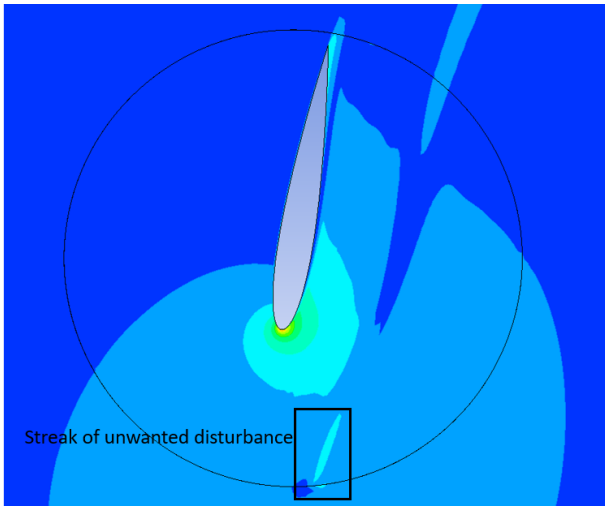

Figure 66 Small streak of flow disturbance at Mesh Interface

6.7 Quality of Mesh- One of the objectives is to investigate and report, if there is a drastic change in Torque Output by changing the quality and size of mesh elements. The two approaches were evaluated and the results in the form of Torque curves are presented in the Figure 67. It is clear from the graph that the quality of mesh has a pronounced effect on Torque. The Torque is visibly reduced, and the peak torque position is also off to the left and it does not corroborate with all the other findings and with Literature too [12]. So whenever making a decision about the mesh quality, it must be borne in mind that mesh quality may completely alter the expected outputs.

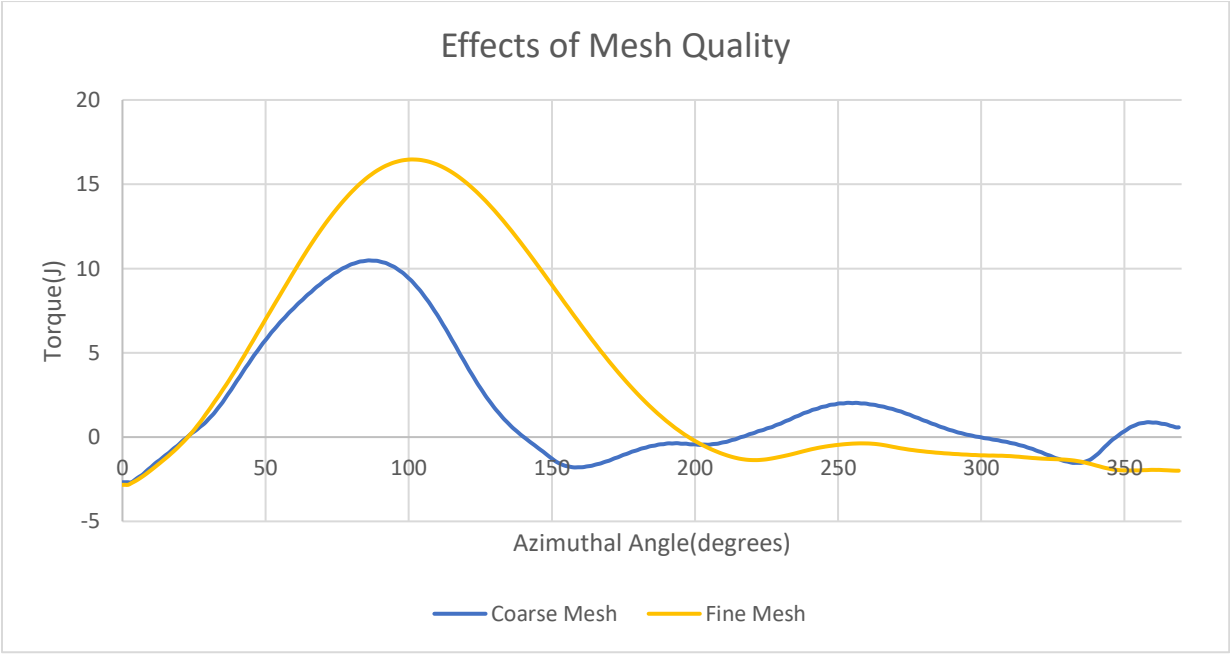

Figure 67 Torque Curves for Fine and Coarse mesh

6.8 Steady State Analysis and Transient State Analysis- One of the last objectives of the thesis is the discussion about the type of Analysis, which are preferred or suitable for the VAWTs. Although in theory, there must not be much difference between the results of the two studies. But in reality, the difference in results is so huge that it diminishes the outcomes of Steady State Analysis. The results from the Transient state analysis are in concurrence to theoretical expectations and also in conformity with Literature study. The results from the Steady State runs are unpredictable. There is also an absence of Steady State Analysis on VAWTs in the Literature too. Both of these factors contribute to Steady State Analysis being not the preferred type of Simulation analysis over Transient State analysis in the studies for VAWTs.

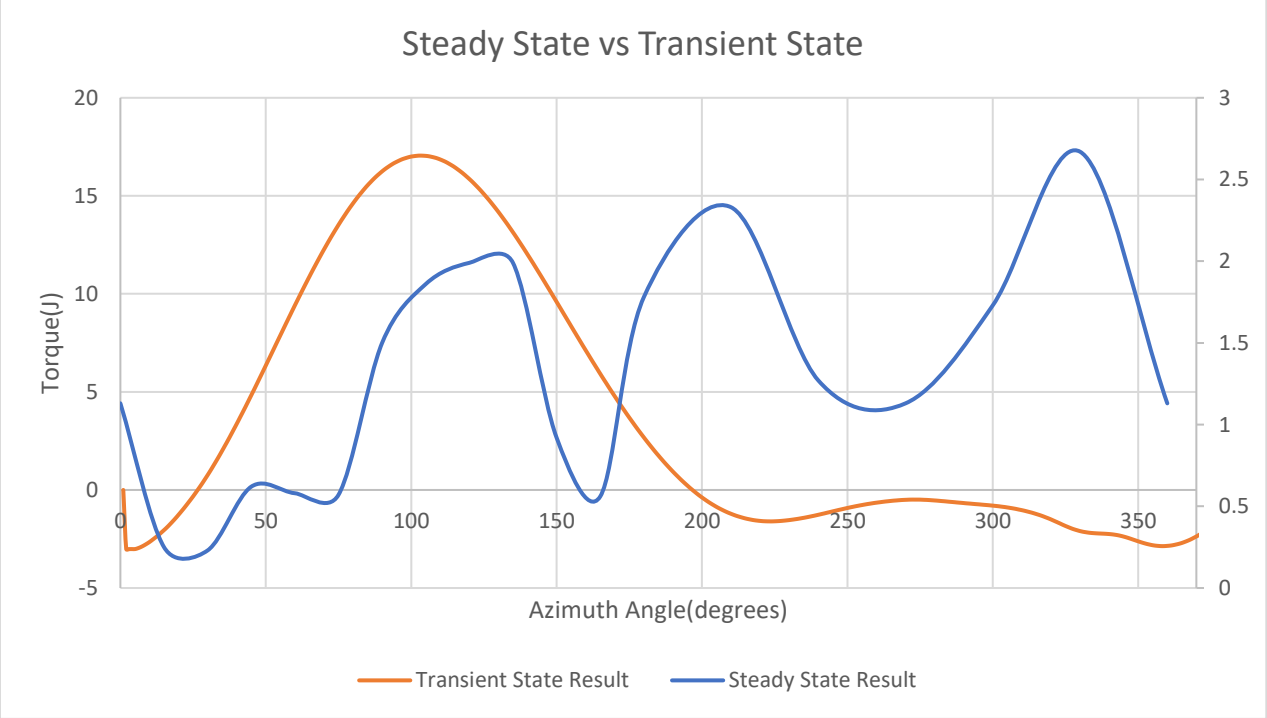

Figure 68 Torque Curves for Transient State and Steady State Analysis Type

Chapter 7

7. COMPARISON OF RESULTS WITH LITERATURE

The scope of this Master thesis is to perform an independent and stand-alone research. However, there are certain instances where the validation of the results proves useful and is necessary. The comparison of the results with published Literature provides a benchmark for progress and identification of errors. The results of various studies in this thesis, such as 2-Bladed Variable pitching are not available. Therefore, the inferences are drawn from personal judgements of results and validation of Simulation approach. Some of the comparisons which were found in Literature and are in conformance to derived results are presented in this chapter. The comparisons derived are limited to Qualitative resemblance as different variables which can vary the Quantity of compared in Literature are different from values in this research.

7.1 Localized Angle of Attack- The AOA for a VAWT varies constantly during a single rotation and the result from the Literature along with graph from this study are presented to show the comparison [18].

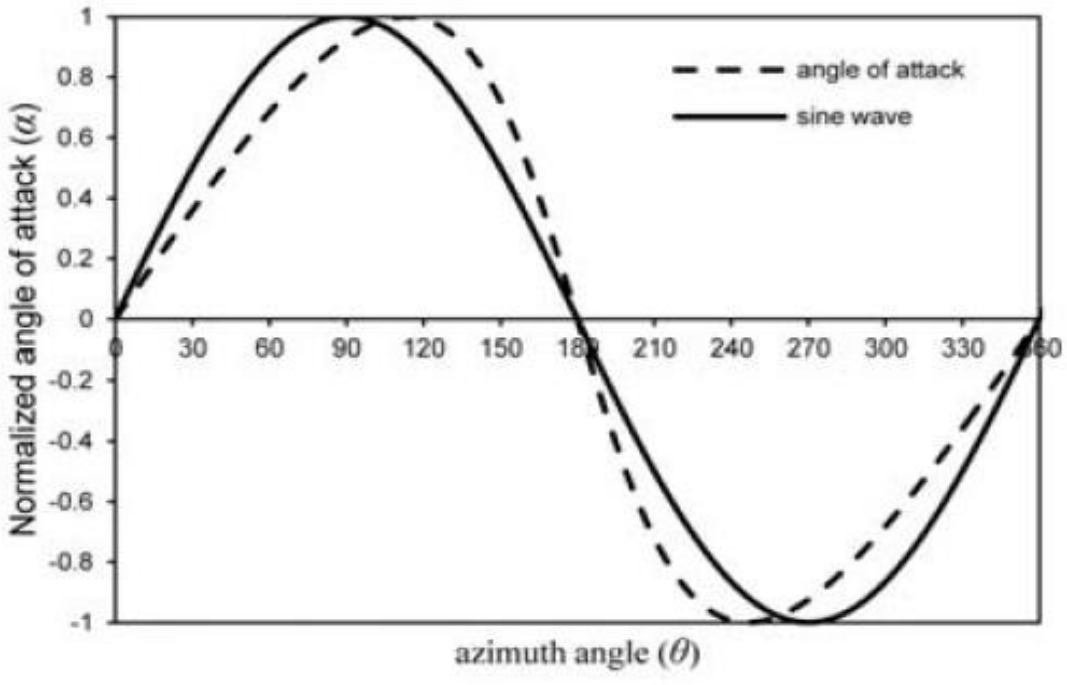

Figure 69 Angle of Attack vs Azimuthal Angle (Literature) [18]

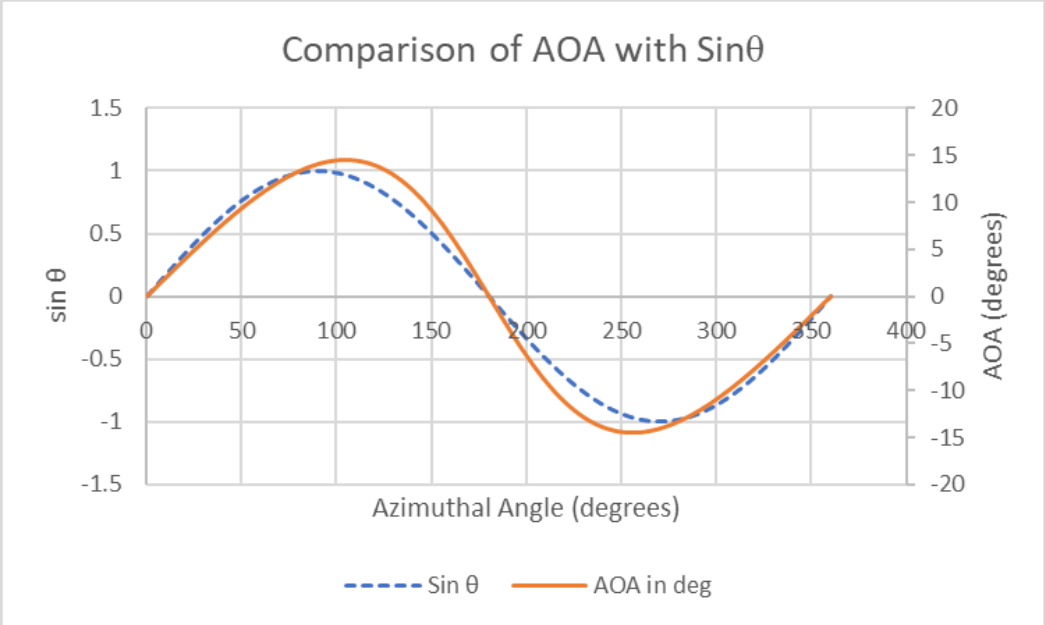

Figure 70 Angle of Attack vs Azimuthal Angle (Result of Study)

7.2 Coefficient of Lift Force vs Angle of Attack-The comparison of Cl with AOA for a NACA 0012 airfoil is obtained from a Lecture Script by Prof. Stank and comparison is made to one done in this study [8].

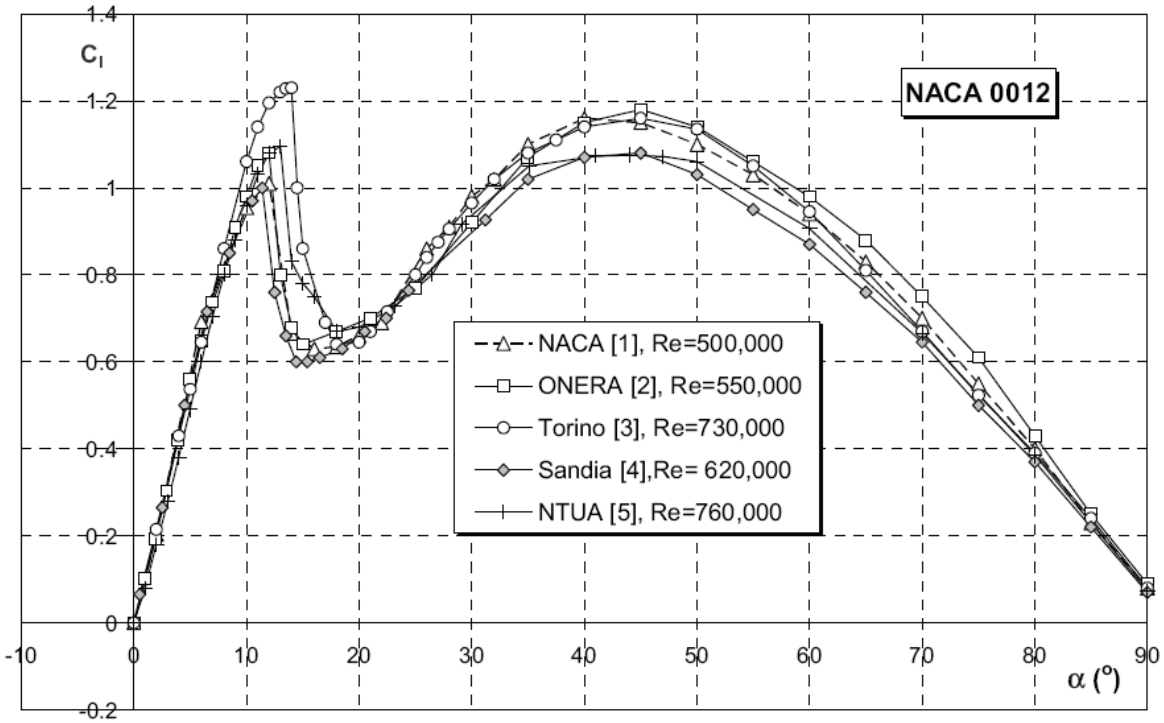

Figure 71 Lift Coefficient for NACA 0012 (Literature) [8]

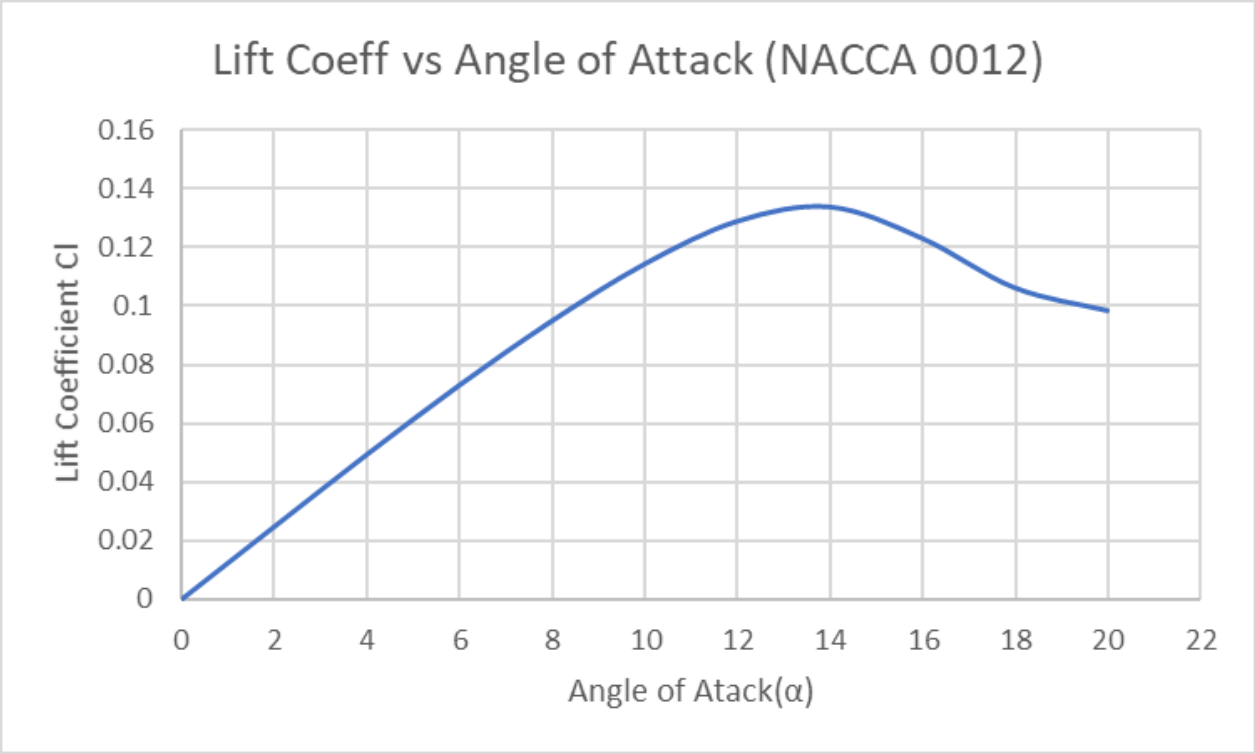

Figure 72 Lift Coefficient for NACA 0012 (Result of Study)

7.3 Torque of Single Blade vs Azimuthal angle- The qualitative Torque curve from this reference is in conformance with results from the research. The peak Torque occurs at similar Azimuthal position and the curve follows the similar trend [14].

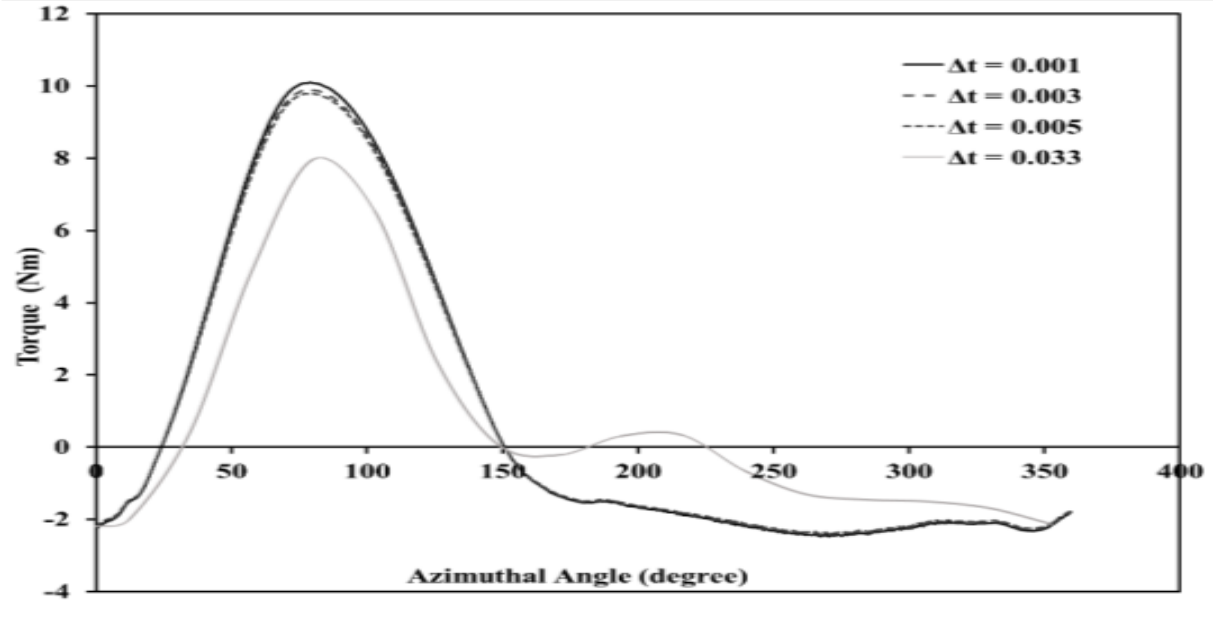

Figure 73 Torque Curve of Unpitched Single Blade Rotor (Literature) [14]

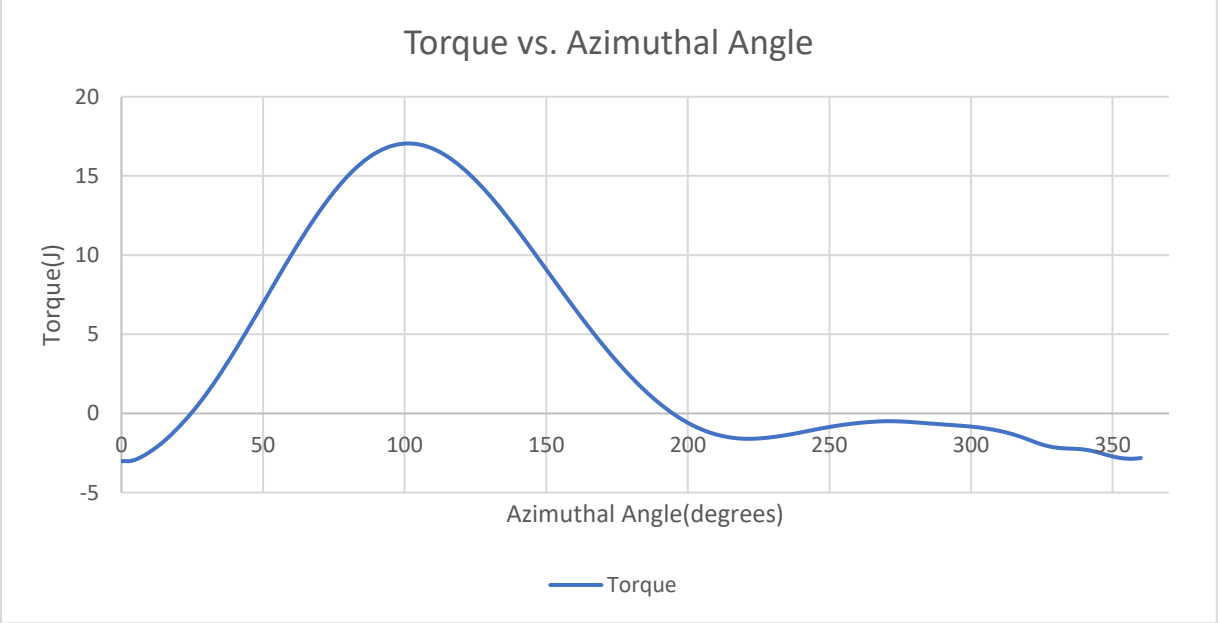

Figure 74 Torque Curve of Unpitched Single Blade Rotor (Result of Study)

7.4 Constant Pitching angle vs Torque- The research referred in this section also provides the different Torque Coefficient curves for some of the chosen Blade pitch angles. The comparison is not available for all the Blade pitch angles but similarity in operating trends between the Literature and research is relevant [6].

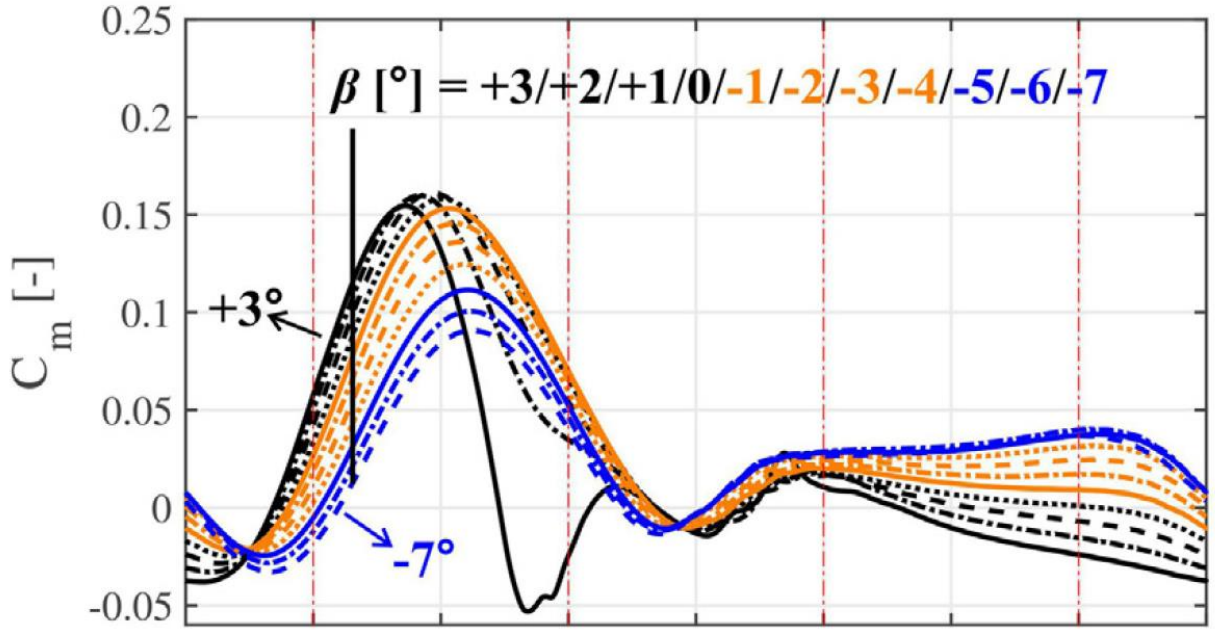

Figure 75 Torque curves for different Constant Pitch Angles (Literature) [6]

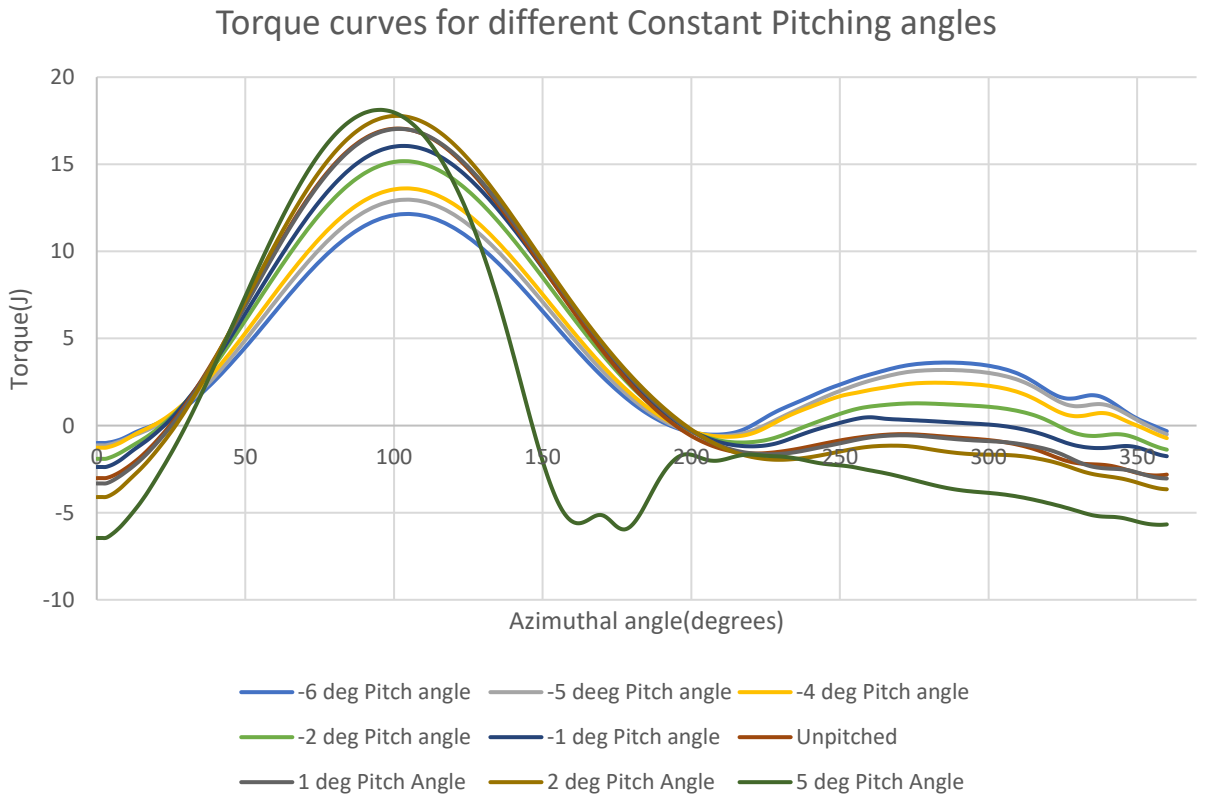

Figure 76 Torque curves for different Constant Pitch Angles (Result of Study)

7.5 Quality of Mesh-The comparison of mesh quality from results obtained from Literature and from the study are similar in the sense that the Peak Torque position shifts towards the left as a result of decreasing the Quality of the mesh and the Quantity of the torque is affected severely too [12].

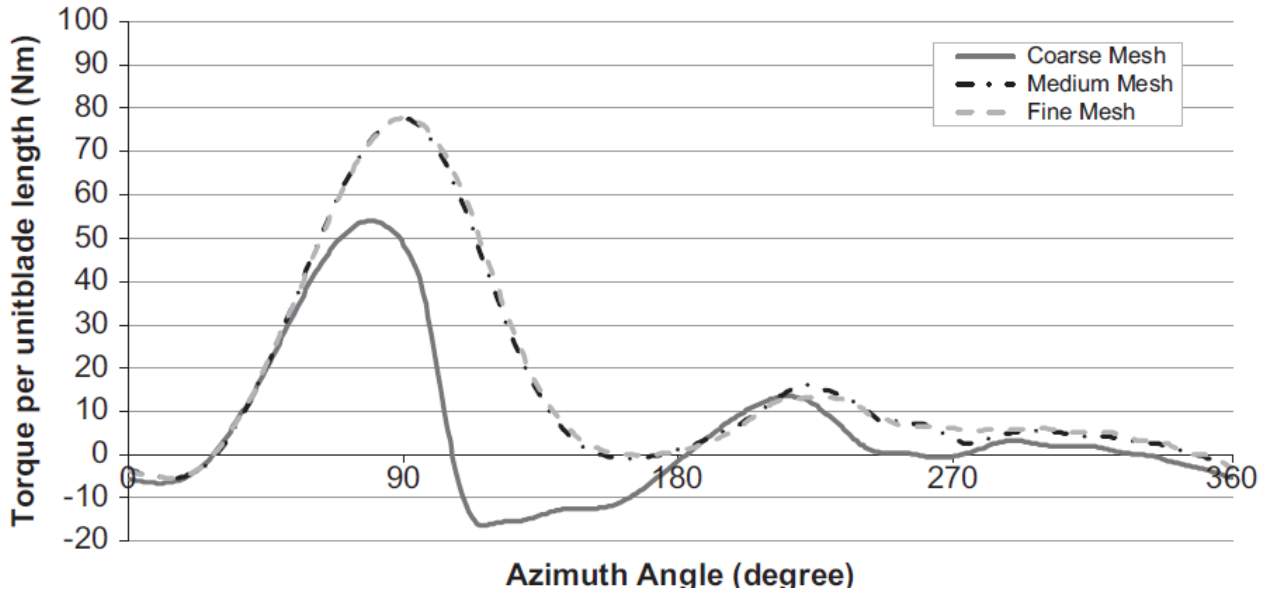

Figure 77 Torque Curves for different Qualities of Meshes (Literature) [12]

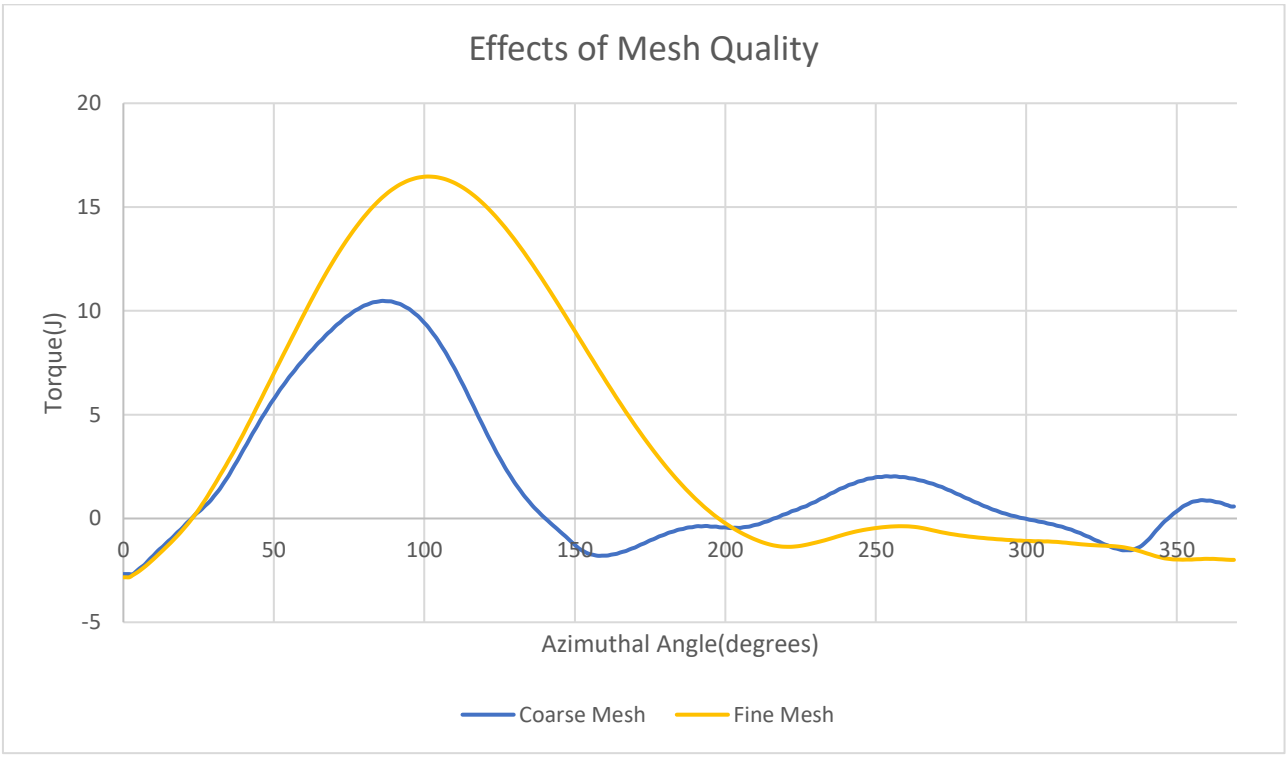

Figure 78 Torque Curves for different Qualities of Meshes (Result of Study)

Chapter 8

8. SUMMARY AND FUTURE SCOPE

The purpose of this graduation thesis is to perform and report the CFD investigations of a VAWT. There are various reasons why the research in the field of VAWTs is picking up the pace in recent times. Even though the history of VAWTs goes way back and past HAWTs, lesser efficiency is primarily the reason behind slow-paced research in field of VAWTs. Recently, the competition in viable Wind spots for HAWTs are attracting more researchers and companies to pick up the slack in research for VAWTs.

There are numerous Objectives outlined in this Thesis. The most crucial and important ones are, studying the effects of Constant Pitching, deriving an equation for Optimized Pitching and ultimately applying this Pitching approach to Multi-Blade Rotor System. The comparisons are drawn between Unpitched system and Literature, wherever similar research is found. Some of the other objectives of the thesis are, Understanding the operating principles and CFD approaches for Simulating VAWTs from Literature, comparing the effects of the Mesh Quality on Torque in CFD analysis and comparing the type of Analysis approach used for Simulation.

The above stated objectives are achieved in different stages with different Geometry, meshes, Boundary conditions. Each study is tailor made to achieve a specific objective. In order to understand the effects of different Pitching angles on Torque, numerous Solver Definition files are generated each with a specific Blade pitch angle in place. The results are then compared, and an Optimum pitching angle equation is created. The equation so created is utilized in next study, where the geometry is modified to include two blades instead of one and the results of the Optimized Pitching are reported. The mesh is varied in ICEM CFD to alter the number of elements and hence the quality of mesh and results are reported as well.

The results of this thesis are in accordance to what is expected from such an approach. There is an in increase in the amount of Torque generated by the rotor system when Variable Pitching is applied. There is an increase of 52.8% in case of Single blade system and an increase of 48.2% in case of two-bladed system. This increase validated the utility of the equation generated to optimize the pitching angle.

This research is a one of its kind with no complete resemblance to any other Literature and as with any other research, there is a lot of future scope in order to expand it. Some of the future research opportunities lie in the validation of the Pitching results by corroboration with experimental setup such as Wind tunnel studies on prototype or actual live-scale model. Another aspect of future research would be to perform the same approach on different number of Blades in a rotor system. As reported, the effect of increasing number of blades can cause Turbulent flow if TSR is not optimized. So, this would be an interesting research topic. Another valid and an important future extension of this research would be to complete a full-fledged 3-D study instead of a Quasi-2D approach and study the effects of constant and variable pitching. This would be highly time expensive and require a huge computational power. But such a study would be as close as possible to reality of an actual Wind Tunnel. Another suggestion for future scope would be to incorporate different Airfoil types, Symmetrical and Asymmetrical to study the effects of Variable pitching on different Airfoils.

Chapter 9

9. CITATIONS

[1] E. Hau, Wind Turbines- Fundamentals, Technologies, Application, Economics, Munich: Springer, 2005.

[2] M. K. Johari, M. A. A. Jalil and M. F. M. Shariff, "Comparison of horizontal axis wind turbine (HAWT) and vertical axis wind turbine (VAWT)," *International Journal of Engineering & Technology,* vol. 7, pp. 74-80, 2018.

[3] R. Stank, Interviewee, *Prototype of Agile VAWT at Zurich University of Applied Sciences.* [Interview]. 2018.

[4] A. Das and P. K. Talapatra, "Modelling and Analysis of a Mini Vertical Axis Wind Turbine," *International Journal of Emerging Technology and Advanced Engineering,* vol. 6, pp. 184-194, 2016.

[5] T. G. Abu-El-Yazied, A. . M. Ali, M. S. Al-Ajmi and I. M. Hassan, "Effect of Number of Blades and Blade Chord Length," *American Journal of Mechanical Engineering and Automation,* vol. 2, pp. 16-25, 2015.

[6] A. Rezaeiha, I. Kalkman and B. Blocken, "Effect of pitch angle on power performance and aerodynamics," *Applied Energy,* vol. 197, p. 132–150, 2017.

[7] F. Meng, H. Schwarze, F. Vorpahl and M. Strobel, "A free wake vortex lattice model for vertical axis wind turbines: Modeling, verification and validation," in *Journal of Physics: Conference Series 555*, Oldenburg, 2014.

[8] R. Stank, "Lecture on Computational Simulation Techniques for Analysis of Wind Turbines," HAW Hamburg, Hamburg, 2017.

[9] S. Brusca, R. Lanzafame and M. Messina, "Design of a vertical-axis wind turbine: how the aspect ratio affects," *International Journal of Energy and Environmental Engineering,* vol. 4, pp. 1-8, 2014.

[10] "World Weather and Climate Information," [Online]. Available: https://weather-and-climate.com/average-monthly-Wind-speed,Hamburg,Germany. [Accessed 16 October 2019].

[11] S. B. Qamar and I. Janajreh, "A comprehensive analysis of solidity for Cambered Darrieus VAWTs," *International Journal of Hydrogen Energy,* vol. 42, pp. 19420-19430, 2017.

[12] R. Nobile, M. Vahdati, J. F.Barlow and A. Mewburn-Crook, "Unsteady Flow Simulation of a Vertical Axis Augmented Wind Turbine: 2 Dimensional Study," *Journal of Wind Engineering,* vol. 125, p. 168–179, 2014.

[13] N. Qin, R. Howell, N. Durrani, K. Hamada and T. Smith, "Unsteady Flow Simulation and Dynamic Stall Behaviour of Vertical Axis Wind Turbine Blades," *Wind Engineering,* vol. 35, pp. 511-527, 2011.

[14] N. Mishra, P. Laws, R. V. Bethi and S. Mitra, "Two-Dimensional Unsteady Flow Calculations of a Five Bladed Vertical Axis Wind Turbine," in *The 8th International Conference on Computational Methods*, Guilin, 2017.

[15] Y. Yang, Z. Guo, Q. Song, Y. Zhang and Q. Li, "Effect of Blade Pitch Angle on the Aerodynamic Characteristics of a Straight-bladed Vertical Axis Wind Turbine Based on Experiments and Simulations," *Energies,* vol. 11, p. 1514, 2018.

[16] Z. Zhao, D. Su, T. Wang, B. Xu, H. Wu and Y. Zheng, "A blade pitching approach for vertical axis wind turbines based on the free vortex method," *Journal of Renewable Sustainable Energy,* vol. 11, pp. 1-16, 2019.

[17] M. Jakubowski, R. Starosta and P. Fritzkowski, "Kinematics of a vertical axis wind turbine with a variable pitch angle," in *AIP Conference Proceedings 1922*, Lublin, 2018.

[18] L. . A. Danao, N. Qin and R. Howell, "A numerical study of blade thickness and camber effects on vertical axis wind turbines," *Journal of Power and Energy,* vol. 226, p. 867–881, 2012.

[19] M. R. Castelli, A. Englaro and E. Benini, "The Darrieus wind turbine: Proposal for a new performance prediction model," *Energy,* vol. 36, pp. 4919-4934, 2011.

APPENDICES

APPENDIX 1: Figures of Initial 3-D Mesh Study with Tetrahedral mesh elements

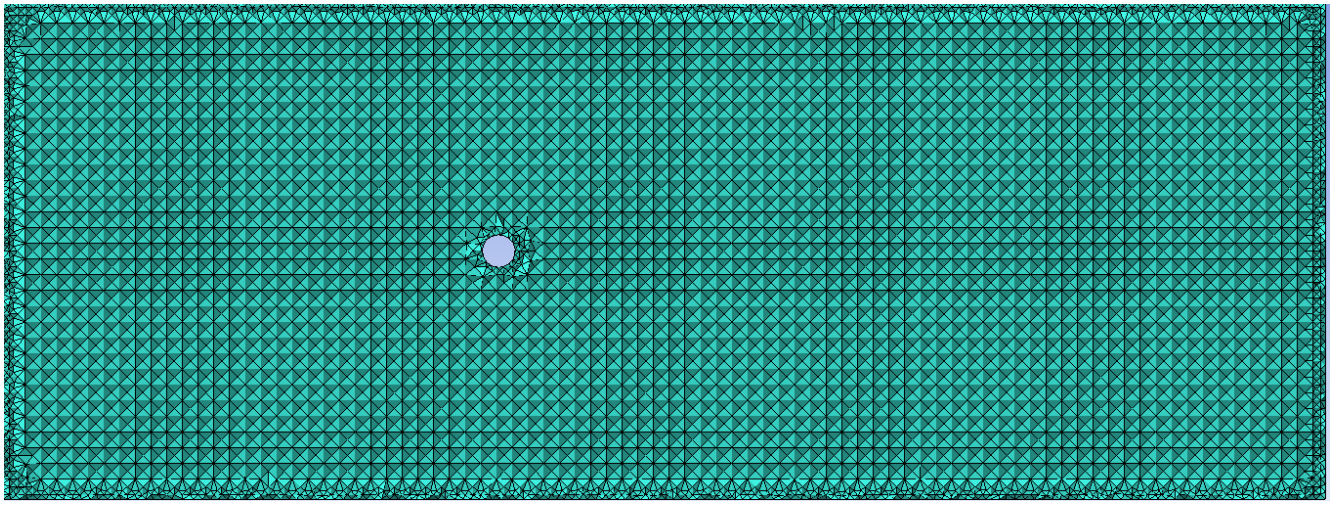

APPENDIX 2: Additional figures of AGILE VAWT with Pitching Mechanism

APPENDIX 3: Excel Worksheets of Selected Data

A small snippet of the Worksheet is referred here as the entire Worksheet could not be fitted in this Document. The thesis is accompanied by a CD, that contains the Digital version of the thesis and also acts as a Digital Appendix to Excel files as they are too large to be attached in entirety in this document. Refer to these files as to review the Data extraction and Analysis.

		Torque 1			Torque 2		
		Blade 1	Blade 2	Combined Torque	Blade 1	Blade 2	Combined Torque
	Rotation Applied	0 deg	0 deg	0 deg	(-6.477 deg)	2 deg	
Azimuth Angle ↓							
	0	-2.8309326	-1.1106718	-3.94160438	-0.8412461	-1.5163	-2.357548888
	1	-2.8309326	-1.1106718	-3.94160438	-0.8412461	-1.5163	-2.357548888
	2	-2.8309326	-1.1106718	-3.94160438	-0.8412461	-1.5163	-2.357548888
	3	-2.7418518	-1.1005086	-3.84236038	-0.8085557	-1.50914	-2.317698712
	4	-2.653228	-1.0991684	-3.75239646	-0.789722	-1.50632	-2.296043935
	5	-2.55989	-1.096889	-3.65677905	-0.7691047	-1.50251	-2.2716195
	6	-2.4509256	-1.1004267	-3.55135226	-0.7377779	-1.50669	-2.244463328
	7	-2.3378117	-1.1062561	-3.44406784	-0.7027756	-1.51489	-2.217670198
	8	-2.2178774	-1.1027491	-3.3206265	-0.6618266	-1.51315	-2.174975931
	9	-2.089185	-1.1070045	-3.19618952	-0.6113403	-1.5212	-2.132542134
	10	-1.9592511	-1.114776	-3.07402707	-0.5588087	-1.53349	-2.092295824
	11	-1.8238549	-1.1111617	-2.93501663	-0.50577	-1.53368	-2.039454398
	12	-1.6871152	-1.1128945	-2.80000973	-0.4531938	-1.541	-1.994196233
	13	-1.5504953	-1.1175889	-2.66808415	-0.4043819	-1.55221	-1.956592201
	14	-1.4093888	-1.1082733	-2.51766205	-0.3559286	-1.54911	-1.90503803
	15	-1.2705535	-1.099576	-2.37012947	-0.3030673	-1.54989	-1.852960647
	16	-1.1293259	-1.093537	-2.22286284	-0.2452299	-1.55528	-1.80051202
	17	-0.9764208	-1.0717957	-2.04821652	-0.1749324	-1.54561	-1.72053888
	18	-0.8258175	-1.0480541	-1.873871566	-0.0908067	-1.53681	-1.627618665
	19	-0.6687331	-1.0281661	-1.69689918	0.0058109	-1.53286	-1.527050211
	20	-0.4981685	-0.9938639	-1.492032408	0.11460205	-1.51356	-1.398960148
	21	-0.3317286	-0.9558528	-1.287581414	0.23519027	-1.49011	-1.254915838
	22	-0.1567364	-0.9210678	-1.077804208	0.37530106	-1.4679	-1.092596467
	23	0.03492891	-0.8723638	-0.837434896	0.55127555	-1.42738	-0.876106559
	24	0.22176048	-0.8181174	-0.596356958	0.77629602	-1.3776	-0.6013037
	25	0.4219884	-0.7681141	-0.346125692	1.05623758	-1.32778	-0.27154457
	26	0.64164835	-0.7063846	-0.064736247	1.37283838	-1.25854	0.11429775
	27	0.85632289	-0.6430447	0.213278234	1.67531705	-1.1802	0.49512184
	28	1.08261156	-0.5838042	0.49880737	1.8961699	-1.09803	0.79814434
	29	1.32822871	-0.5166869	0.811541794	1.98856425	-0.99459	0.993975815
	30	1.56241667	-0.4489686	1.113448081	1.94845796	-0.87167	1.076785389

APPENDIX 4: Figures depicting the manual Design Approach

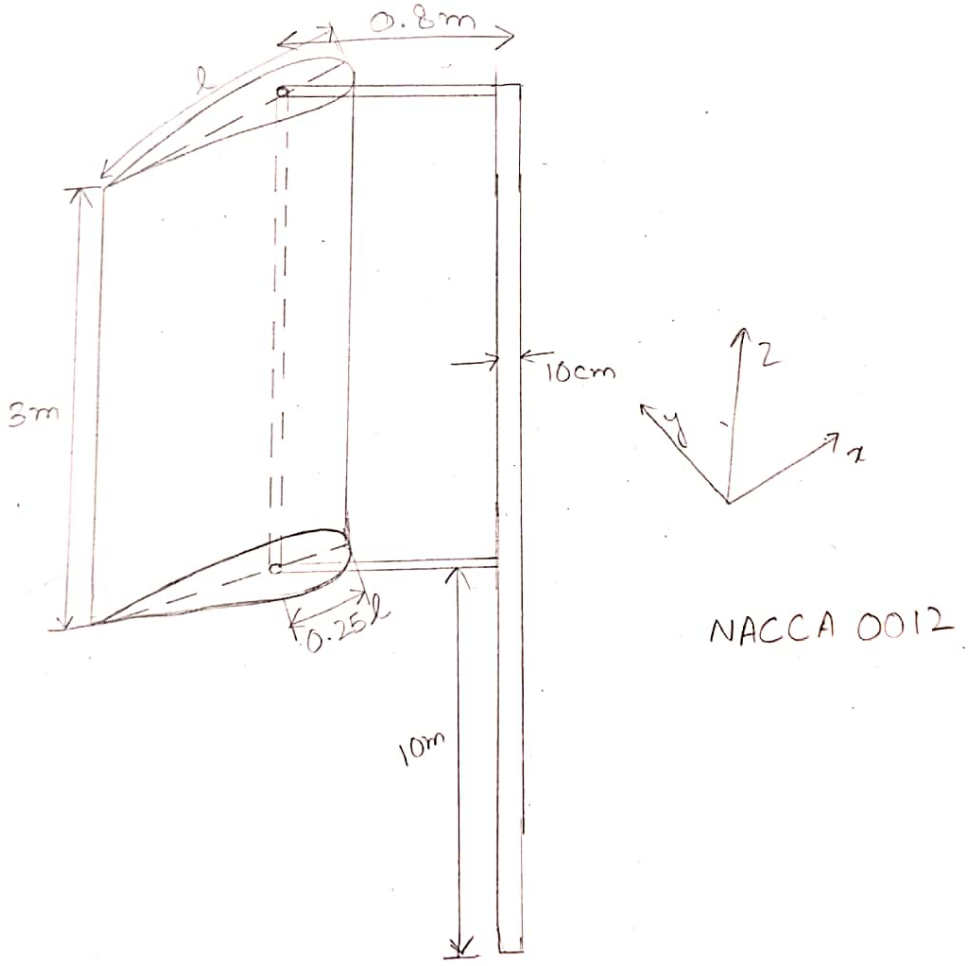

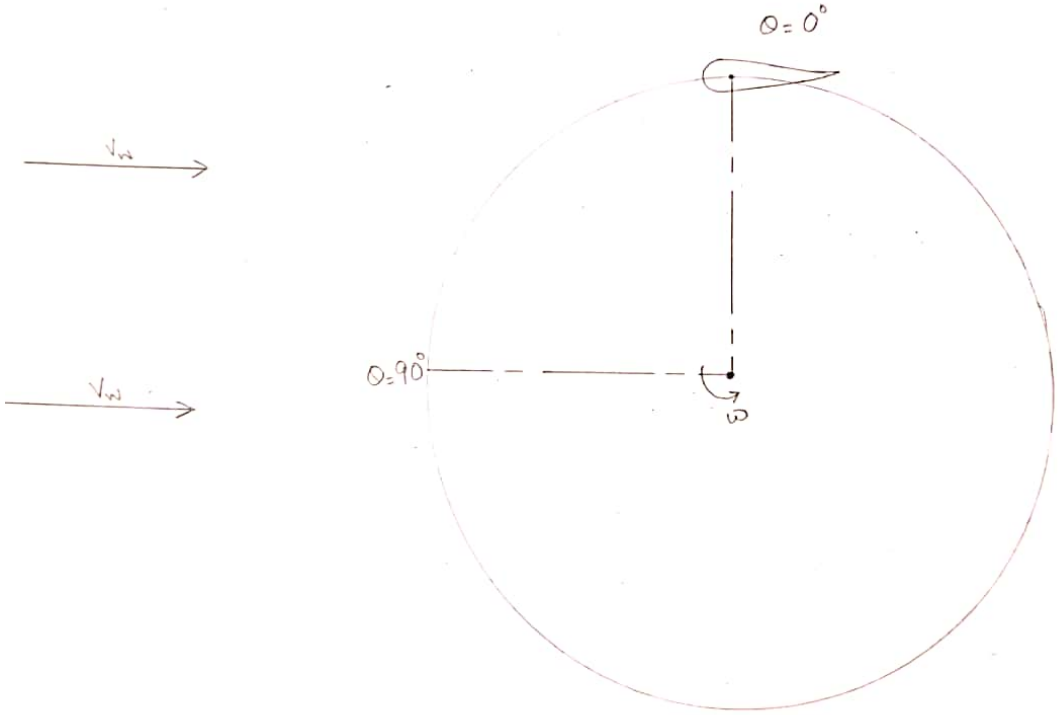
Θ = 0°
V_∞
V_∞
Θ = 90°
ω

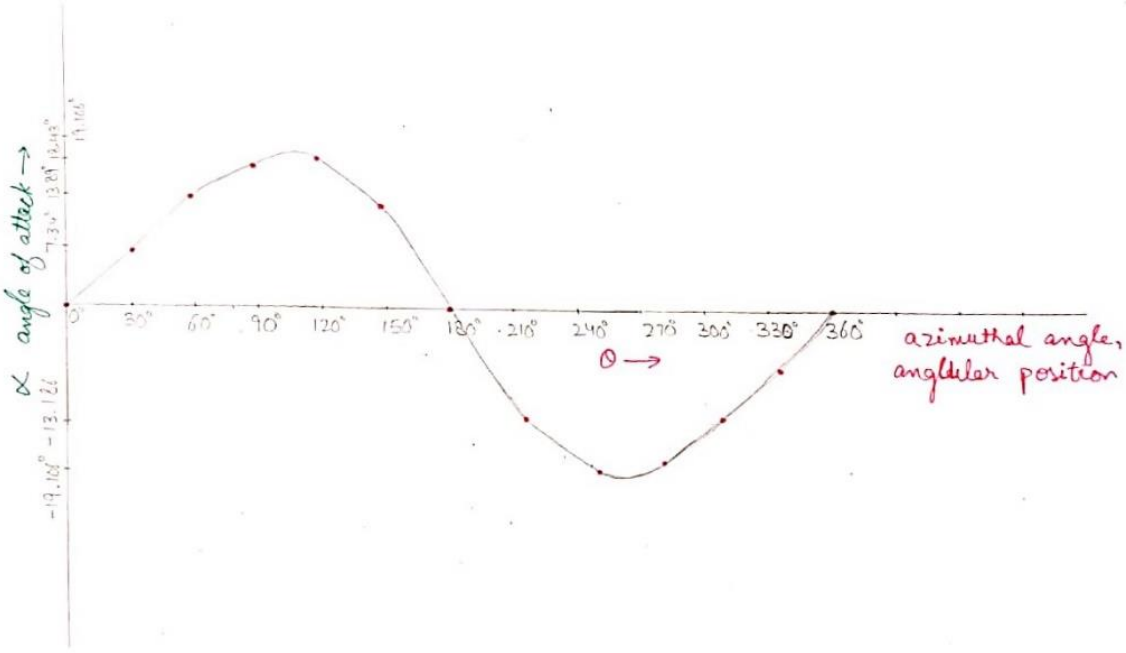
α angle of attack →
0°
30°
60°
90°
120°
150°
180°
210°
240°
270°
300°
330°
360°
Θ →
azimuthal angle,
angular position

APPENDIX 5: Forces acting on Airfoil in X and Y direction in Solver Monitors

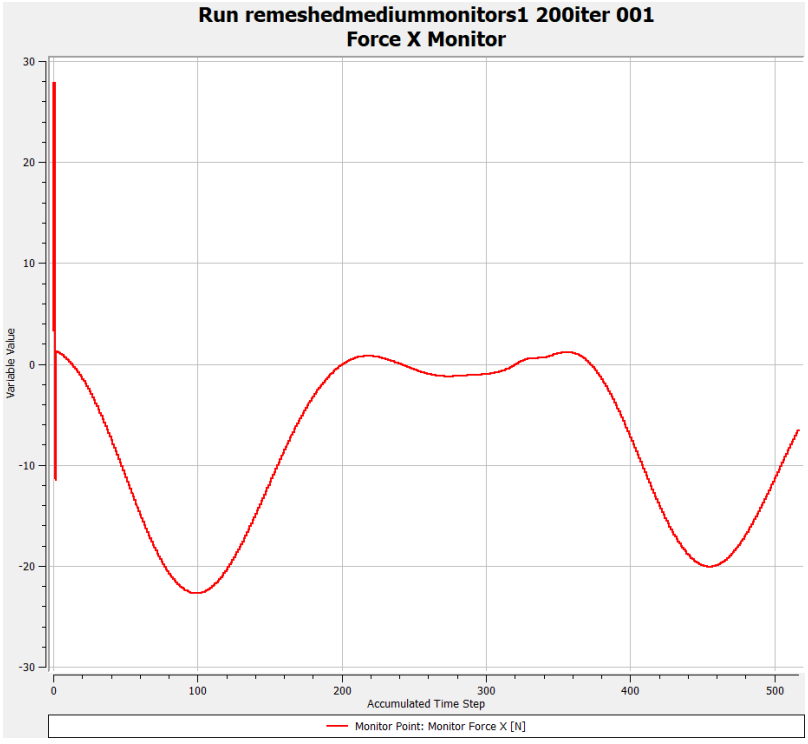

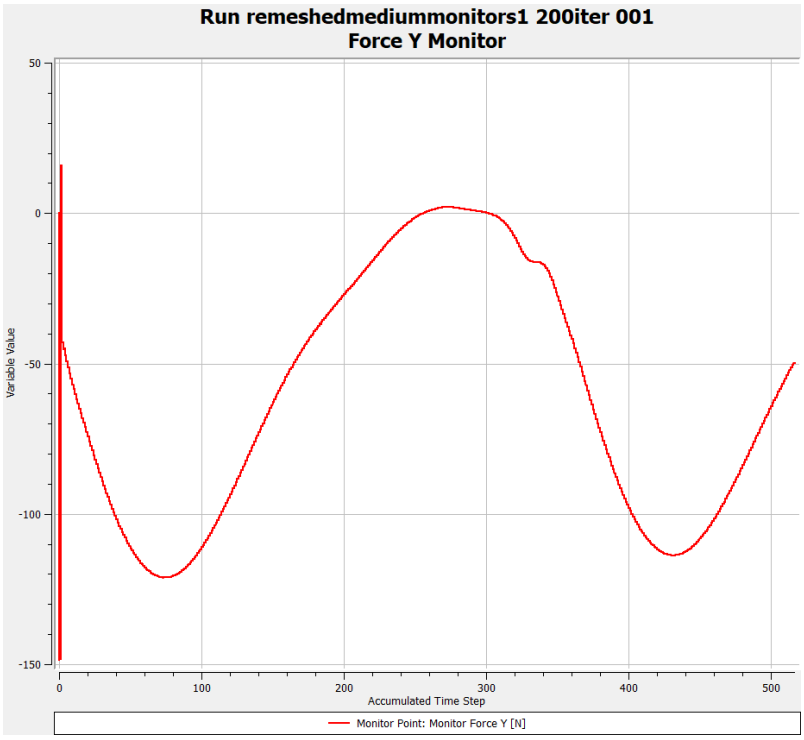

Declaration

The thesis entitled “CFD Investigations of Vertical Axis Wind Turbine” is conducted under the supervision of Prof. Dr. Ing-. Rainer Stank and Prof. Dr. Ing-. Holger Schwarze, Professors at HAW Hamburg.

I declare that the information reported in the current thesis is a result of my own work, except where relevant reference is made. I am the sole author of the work presented and the thesis is applied for completion of Masters degree in Renewable Energy Systems.

Hamburg, 21.10.2019 Prince Deep